THEORETICAL STUDIES ON THE NONLINEAR-OPTICAL PROPERTIES OF ORGANIC SUBSTANCES

MASAYOSHI NAKANO

Faculty of Engineering Science
Osaka University
1991

THEORETICAL STUDIES ON THE NONLINEAR-OPTICAL PROPERTIES OF ORGANIC SUBSTANCES

MASAYOSHI NAKANO

Faculty of Engineering Science
Osaka University
1991

Preface

One important theme of quantum theory is to explore new characteristics and physical phenomena of materials by the analysis of the interactions between materials and light. Particularly, studies on the nonlinear optical effects induced by the interactions between materials and strong electric fields have attracted considerable attention both theoretically and experimentally in recent years. The nonlinear optical effects originate from the microscopic polarization at the molecular level, which is characterized by the hyperpolarizability. In this thesis, methods of calculation and analysis of the molecular hyperpolarizability are first constructed quantum mechanically. Second, the mechanisms by which the nonlinear polarization is induced in organic molecular systems are analyzed and classified by theoretical computations of the hyperpolarizabilities. Finally, new models of organic nonlinear optical systems are proposed in the light of the classification of the mechanisms.

In part I of this thesis, the calculation method for hyperpolarizability is discussed on the basis of the time-dependent perturbation theory (TDPT). The method is useful when the external field is not strong. Semiempirical molecular orbital (MO) methods which can well reproduce the transition properties are mainly employed since several quantities relating to excited states are difficult to calculate quantitatively by the ab initio method. One advantage of this method lies in its ability to clarify the virtual excitation processes. Three types of approximation based on the TDPT are proposed in order to elucidate the characteristic details of the processes. The characteristics of the three types of virtual excitation processes are utilized to classify the representative nonlinear optical systems in part III.

In part II, the calculation methods which do not treat excited states directly are developed. Non- and semi-empirical MO methods are utilized to obtain the total energy of the ground state. First, the finite-field (FF) method by the use of the coupled-Hartree-Fock

(CHF) theory, in which the potentials by the external field are treated variationally, is explained. In order to include the correlation effects, the Møller-Plesset perturbation theory (MP) is employed. Second, the Rayleigh-Schrödinger perturbation theory (RSPT) is employed to include the external perturbation and electron correlation effects systematically and to explore the relations between CHF(+MP) and RSPT methods. Third, general equations giving the nth order response properties with respect to an external one-electron perturbation are derived on the basis of the coupled-cluster (CC) theory which can include higher order correlations effectively. These equations are useful for analytical calculations of the hyperpolarizabilities of any order. Moreover, in order to calculate the dynamic hyperpolarizability, the time-dependent CC (TDCC) theory is developed by analyzing the time-development of the phase factor. Finally, the γ density analysis method is proposed as an effective tool to clarify the spatial details of third-order hyperpolarizability (γ). It is possible to separate the γ density into different contributions, for example, the σ and π contributions.

In part III, various molecular, polymeric and CT complex systems are examined. For the polymeric systems, the characteristics of the longitudinal γ values are investigated with particular attention to the roles of several substituent groups. Dependences of the γ values on the chain lengths are also examined. Results for finite polymeric systems are extrapolated to an infinity of the chain length to predict the intrinsic γ values per unit cell of polymeric chains. For the CT complex systems, static third-order hyperpolarizabilities of alternate donor (D)-acceptor (A) stacks and of segregated molecular stacks in the column direction are compared. Dependences of γ on the size of the clusters are also investigated. In the TDPT, the CNDO/S approximation with the single-excitation configuration-interaction (SCI) method is employed for the calculations of several quantities relating to the excited states. On the other hand, in the CHF and CHF+MP theory, the INDO and ab initio MO methods are employed to obtain the perturbed ground state energy. From the results of these calculations, the representative

existing nonlinear optical systems are classified according to the mechanisms of operation of the third-order nonlinear effects. The criteria of the classification are the symmetry of charge distributions (centro- and noncentro-symmetric charge distributions) and the types of the interactions which induce the charge-transfer (CT) effects (through-bond and through-space interactions). Using the classification proposed here, polar-substituted polymer chains which involve both the CT interactions through space between the neighboring side chains and the intramolecular CT interactions through the main chain are proposed as a new model of the third-order nonlinear system.

Acknowledgments

The present thesis is a summary of the author's study from April 1986 to January 1991 at the Department of Chemical Engineering of the Faculty of Engineering Science of Osaka University.

The author wishes to express his sincere gratitude to Professor Takayuki Fueno for his warm encouragement, guidance and discussions throughout the course of his study. The author is deeply grateful to Dr. Kizashi Yamaguchi for his helpful suggestions and continuous severe discussions.

The author also thanks to Associate Professor Tadashi Okuyama and Dr. Kunihisa Yoshida for their continuous encouragement, to Messrs. Keiichi Yokoyama, Shin'ya Takane, Mitutaka Okumura, Junichi Kitagawa, Katuji Miyake, Tuyoshi Yorizane for their active collaboration and hot discussions, and to other members of the Fueno Laboratory for their encouragement.

The numerical calculations were carried out on the ACOS 2000 at the Computer Center of Osaka University, on the HITAC S820/10 computers at the Institute for Molecular Science, and on the Sun 3/60 and Macintosh II in the Fueno laboratory. The author also thanks to Dr. Koji Ohta in the Government Industrial Institute at Osaka for his interesting and helpful discussions.

Finally, the author thanks to his parents, Mr. Sigeru Nakano and Mrs. Hiroko Nakano for their understanding and encouragement of his study.

Masayoshi Nakano

February, 1991

Contents

Notes :

The number of equations, figures and tables are referred to as (the number of part . the number of chapter . the number of equations, figures and tables) when they are referred in other chapters.

ex.

Eq.(3) in chapter 2 of part III = Eq.(III.2.3)

PART I

CALCULATION METHOD OF THE HYPERPOLARIZABILITY BY THE TIME-DEPENDENT PERTURBATION THEORY (TDPT)

Introduction

The time-dependent perturbation theory (TDPT) is used for the calculation of the response property of the system in the presence of an external oscillating field. In this case, the required quantities relating to the ground and excited states are transition energies, dipole moment differences and transition moments. Therefore, the virtual excitation processes characterized by these quantities are able to be investigated and the explicit criteria designing the nonlinear optical systems are easily constructed. Moreover, the dispersion effects of the hyperpolarizability can be examined when the oscillating external fields are applied. However, a few ab initio calculations for the small-size systems are carried out due to the problem of the convergence of the hyperpolarizability including the sum over the excited states and to the difficulty of the calculations of precise quantities relating to the excited states. In general, the TDPT with the semiempirical molecular orbital (MO) methods which can well reproduce the quantities relating to the excited states is performed to analyze the virtual excitation processes qualitatively.

In chapter 1, first, it is shown that the macroscopic nonlinear optical effects are characterized by the hyperpolarizabilities at the molecular level through the nonlinear optical process. Next, the time-dependent perturbation theory (TDPT) is explained and is used to obtain the analytical formula of the dynamic polarizability (α) and hyperpolarizabilities (β, γ).

In chapter 2, in order to clarify the virtual excitation processes in the complicated expressions for β and γ, the diagonal and two-level approximations are applied to the expression of β, while the three type approximation is applied to the expression of γ. Moreover, the schematic diagrams of the transition matrices are introduced to obtain the spatial contributions of each dominant virtual excitation process.

Chapter 1

Nonlinear Optical Process and the Analytical Expressions for the Dynamic Hyperpolarizabilities by the Time-dependent Perturbation Theory (TDPT)

1. Nonlinear Optical Process

When the optical electric field $\boldsymbol{F}_O(\boldsymbol{r},t)$ is applied to the materials, the microscopic polarization $\boldsymbol{p}$ is induced in the molecules constructing the materials. The microscopic polarization induces the macroscopic polarization $\boldsymbol{P}$ whole over the crystal. As a result, new electric field $\boldsymbol{F}_N(\boldsymbol{r},t)$ is generated. This process is shown in Fig.1. When the angular frequency of $\boldsymbol{F}_O(\boldsymbol{r},t)$ does not equal that of $\boldsymbol{F}_N(\boldsymbol{r},t)$, the process is referred to as the nonlinear optical process. In this case, various nonlinear optical effects such as the second harmonic generation (SHG) and the third harmonic generation (THG) are observed. [1-8]

The macroscopic polarization $\boldsymbol{P}$ of the organic solid can be expanded as a function of an electric field $\boldsymbol{F}$:

$$\boldsymbol{P}^I(\omega)=\sum_J \chi^{(1)}_{IJ}\boldsymbol{F}^J(\omega_1)+\sum_{JK} \chi^{(2)}_{IJK}\boldsymbol{F}^J(\omega_1)\boldsymbol{F}^K(\omega_2)+\sum_{JKL} \chi^{(3)}_{IJKL}\boldsymbol{F}^J(\omega_1)\boldsymbol{F}^K(\omega_2)\boldsymbol{F}^L(\omega_3)+\cdots , \quad (1)$$

where $\boldsymbol{P}^I$ is the I component of the polarization in the laboratory reference frame and ω is the angular frequency of the polarization field. $\chi^{(1)}_{IJ}$ is the component of the linear susceptibility tensor of rank 2. $\chi^{(2)}_{IJK}$ and $\chi^{(3)}_{IJKL}$ are the components of the nonlinear susceptibility tensors of rank 3 and 4, respectively. $\boldsymbol{F}^I(\omega_k)$ is the I component of the external field oscillating at angular frequency ω_k.

The microscopic polarization $\boldsymbol{p}$ can be expanded in a similar manner :

$$p^i(\omega)= \mu^i_{tot} - \mu^i_0 = \sum_j \alpha_{ij}F'^j(\omega_1) + \sum_{jk} \beta_{ijk}F'^j(\omega_1)F'^k(\omega_2) + \sum_{jkl} \gamma_{ijkl}F'^j(\omega_1)F'^k(\omega_2)F'^l(\omega_3)+ \dots . \quad (2)$$

Here, $\boldsymbol{F}'$ represents the local electric field. Here, μ^i_{tot} is the molecule-fixed i component of the total electric dipole moment and μ^i_0 is the i component of the permanent dipole moment. In the case of the medium intense electric field $\boldsymbol{F}'$, the right-hand side of Eq.(2) can be approximated by the first-order term with respect to $\boldsymbol{F}'$. However, in the presence of the strong electric field such as the laser beam, the higher-order terms cannot be ignored. These higher-order terms give rise to various nonlinear optical properties. β_{ijk} and γ_{ijkl} are the tensor components of the second- and third-order hyperpolarizabilities, respectively. The magnitude and sign of the hyperpolarizability characterize the nonlinearity of the system.

When the coordinate system is inversed, the electric field $\boldsymbol{F}$ comes to be $-\boldsymbol{F}$ in Eq.(1). However, the even-order terms of the right-hand side of Eq.(1) are unchangeable. If the crystal is centrosymmetric, the polarization for the inversed system is expressed as [9]

$$-P^I(\omega)=-\sum_J \chi^{(1)}_{IJ}F^J(\omega_1)+ \sum_{JK} \chi^{(2)}_{IJK}F^J(\omega_1)F^K(\omega_2)-\sum_{JKL} \chi^{(3)}_{IJKL}F^J(\omega_1)F^K(\omega_2)F^L(\omega_3)+ \dots . \quad (3)$$

As can be seen from Eqs.(1) and (3), the even-order susceptibilities vanish in the centrosymmetric system, while the odd-order susceptibilities usually exist in any system. This relation is also correct in the microscopic polarization. Therefor, in order to exhibit the even-

order nonlinear effects, both the crystal and its elementary molecules must be possess noncentrosymmetric structures.

For most organic molecular crystals, their nonlinear susceptibilities can be expressed as a function of the number density of molecular units (N), local-field factor (L_n), the angle between the molecule-fixed and the laboratory coordinate axes (θ) and the nth-order molecular polarizability ($\alpha^{(n)}$) :

$$\chi^{(n)} = f\,(N, L_n, \theta, \alpha^{(n)}) \quad (n = 1,2,3,...). \tag{4}$$

For randomly oriented systems such as the gas or liquid phase, $\chi^{(n)}$ can be expressed as

$$\chi^{(n)} = NL_n\langle\alpha^{(n)}\rangle\,, \tag{5}$$

where L_n is a local-field factor determined by the refractive indices of the system. $\langle\alpha^{(n)}\rangle$ is the orientationally averaged molecular polarizability. For example, the third-order nonlinear susceptibility can be given by

$$\chi^{(3)}_{IJKL} = Nf(\omega)f(\omega_1)f(\omega_2)f(\omega_3)\langle\gamma\rangle_{IJKL}\,. \tag{6}$$

Here, $f(\omega_i)$ is the local-field factors for each of the electric fields. The subscripts I, J, K and L denote the components in the laboratory coordinate system.

The $\langle\gamma^{(n)}\rangle_{ZZZZ}$ is expressed as [9]

$$\gamma_s \equiv <\gamma>_{IJKL} = \frac{1}{5}(\gamma_{xxxx}+\gamma_{yyyy}+\gamma_{zzzz})+\frac{1}{15}(\gamma_{xxyy}+\gamma_{xyxy}+\gamma_{xyyx}+\gamma_{yyxx}+\gamma_{yxyx}+\gamma_{yxxy})$$
$$+\frac{1}{15}(\gamma_{xxzz}+\gamma_{xzxz}+\gamma_{xzzx}+\gamma_{zzxx}+\gamma_{zxzx}+\gamma_{zxxz})$$
$$+\frac{1}{15}(\gamma_{yyzz}+\gamma_{yzyz}+\gamma_{yzzy}+\gamma_{zzyy}+\gamma_{zyzy}+\gamma_{zyyz}) , \quad (7)$$

in which γ_{ijkl} is the component of γ and i, j, k and l represent the components in the molecular-fixed coordinate system.

Due to the symmetry of the electric fields along the molecular coordinate axes, γ_s for THG and SHG can be simplified as [9]

$$\gamma_s(-3\omega;\omega,\omega,\omega) = \frac{1}{5}(\gamma_{xxxx}+\gamma_{yyyy}+\gamma_{zzzz}+\gamma_{xxyy}+\gamma_{yyxx}+\gamma_{xxzz}$$
$$+\gamma_{zzxx}+\gamma_{yyzz}+\gamma_{zzyy}) , \quad (8)$$
$$\gamma_s(-2\omega;\omega,\omega,0) = \frac{1}{5}(\gamma_{xxxx}+\gamma_{yyyy}+\gamma_{zzzz})+\frac{1}{15}(2\gamma_{xxyy}+\gamma_{xyyx}+2\gamma_{yyxx}$$
$$+\gamma_{yxxy})+\frac{1}{15}(2\gamma_{yyzz}+\gamma_{yzzy}+2\gamma_{zzyy}+\gamma_{zyyz}) . \quad (9)$$

Further simplification of Eqs.(8) and (9) can be performed for the static or DC expression of γ by Kleinman's symmetry rule. The resultant expression for γ_s is given by

$$\gamma_s = \frac{1}{5}(\gamma_{xxxx}+\gamma_{yyyy}+\gamma_{zzzz}+2\gamma_{xxyy}+\gamma_{xxzz}+2\gamma_{yyzz}) . \quad (10)$$

In DC-SHG (=EFISH=electronic field induced second harmonic) method, the third-order susceptibility $\chi^{(3)}$ can be expressed as

$$\chi^{(3)}(-2\omega;\omega,\omega,0) = N f(2\omega)[f(2\omega)]^2 f(0)(\gamma_s+\frac{\mu_0\cdot\beta_v}{5kT}) , \quad (11)$$

where μ_0 is the permanent dipole moment; k is Boltzmann's constant and T is the absolute temperature. β_v is the vector given by

$$\beta_v = \begin{pmatrix} \beta_x \\ \beta_y \\ \beta_z \end{pmatrix} = \begin{pmatrix} \beta_{xxx}+1/3(\beta_{xyy}+\beta_{xzz}+\beta_{yyx}+\beta_{zzx}) \\ \beta_{yyy}+1/3(\beta_{yzz}+\beta_{yxx}+\beta_{zzy}+\beta_{xxy}) \\ \beta_{zzz}+1/3(\beta_{zxx}+\beta_{zyy}+\beta_{xxz}+\beta_{yyz}) \end{pmatrix}. \quad (12)$$

For the centrosymmetric systems, γ_s can be obtained from $\chi^{(3)}$ by Eq.(11) since μ_0 vanishes for the centrosymmetric systems. If γ_s is much smaller than $\mu_0 \cdot \beta_v / 5kT$, the projected β_v on to the direction of μ_0 can be obtained by Eq.(11). If γ_s is approximately as large as $\mu_0 \cdot \beta_v / 5kT$, both β_v and γ_s can be obtained using Eq.(11) by the DC-SHG method with varying the temperature.

2. Time-dependent Perturbation Theory (TDPT) [10,11]

Although macroscopic nonlinear effects are not expressed by the simple sum of microscopic polarization vectors, it is noted that macroscopic polarization mainly depend on the microscopic polarization [1-8]. Therefore, in this section, the analytical formula of hyperpolarizabilities are obtained quantum mechanically. The hyperpolarizability can be regarded as a response of the system with respect to the external field. If the electronic wavefunctions of the system in the presence of the external field are obtained, the response properties can be described completely by the calculation of the expected value of the one-electron dipole operator. The time-dependent perturbation theory (TDPT) is employed to calculate the wavefunctions in the presence of the electric field.

The Schrödinger equation for the unperturbed systems with Hamiltonian H_0 is expressed as

$$H_0 u_n = \varepsilon_n u_n . \tag{13}$$

Here, u_n and ε_n denote the nth electronic wavefunction and electronic energy, respectively. The time-dependent Schrödinger equation for the perturbed system in the presence of the oscillating field is expressed as

$$H \Psi = i\hbar \frac{\partial}{\partial t} \Psi , \tag{14}$$

in which

$$H = H_0 + H'(t) . \tag{15}$$

$H'(t)$ represents perturbed Hamiltonian involving the external oscillating field. The time-dependent Schrödinger equation with the unperturbed Hamiltonian H_0 is expressed as

$$H_0 \varphi = i\hbar \frac{\partial}{\partial t} \varphi , \tag{16}$$

where the eigenfunction φ is given by

$$\varphi = u_n e^{-i\omega_n t} , \quad \omega_n = \frac{\varepsilon_n}{\hbar} . \tag{17}$$

Here, $\hbar$ represents $h/2\pi$, in which h is Plank's constant. Using Eq.(17), Ψ in Eq.(14) can be expanded as

$$\Psi = \sum_{n=0} a_n(t)\, u_n e^{-i\omega_n t}, \tag{18}$$

where $a_n(t)$ is the expansion coefficients depending on time. If the expansion coefficients $a_n(t)$ are obtained, the wavefunction $\Psi(t)$ of the perturbed system on any time can be obtained by the use of the unperturbed wavefunction of the stationary state in Eq.(17). The TDPT is used for obtaining the expression of $a_n(t)$.

Substituting Eq.(18) into Eq.(14), we obtain

$$i\hbar[\sum_n (\dot{a}_n(t)u_n e^{-i\omega_n t} - i\omega_n a_n(t)u_n e^{-i\omega_n t})] = (H_0 + H'(t))\sum_n \dot{a}_n(t)u_n e^{-i\omega_n t},$$

$$i\hbar[\sum_n (\dot{a}_n(t) - i\omega_n a_n(t))u_n e^{-i\omega_n t}] = \sum_n (\varepsilon_n + H'(t))a_n(t)u_n e^{-i\omega_n t}.$$

Therefore,

$$\sum_n i\hbar\dot{a}_n(t)u_n e^{-i\omega_n t} = \sum_n a_n(t)H'(t)u_n e^{-i\omega_n t}. \tag{19}$$

Operating u_k^* on both sides of Eq.(19), the integration all over the space is carried out. Using the following orthonormal relation :

$$\int u_k^* u_n dv \equiv \langle u_k | u_n \rangle = \delta_{kn}, \tag{20}$$

we obtain

$$i\hbar\dot{a}_k(t)e^{-i\omega_k t} = \sum_n e^{-i\omega_k t}a_n(t)<k|H'(t)|n> . \tag{21}$$

Here,

$$<k|H'(t)|n> = \int u_k^* H'(t) u_n dv . \tag{22}$$

Now, using the notation :

$$\varepsilon_n - \varepsilon_k \equiv \hbar\omega_{nk} , \tag{23}$$

Eq.(21) is rewritten as

$$\dot{a}_k(t) = \frac{1}{i\hbar}\sum_n a_n(t)<k|H'(t)|n>e^{i\omega_{kn}t} . \tag{24}$$

The coefficient $a_n(t)$ is expanded as the power series of λ (order parameter) :

$$a_n(t) = a_n^{(0)}(t) + \lambda a_n^{(1)}(t) + \lambda^2 a_n^{(2)}(t) + \dots . \tag{25}$$

Substituting Eq.(25) into Eq.(24), we obtain

$$\dot{a}_k(t) = \frac{1}{i\hbar}\sum_n <k|\lambda H'(t)|n> a_n(t) e^{i\omega_{kn}t}$$
$$= \frac{1}{i\hbar}\sum_n <k|H'(t)|n> (\lambda a_n^{(0)}(t) + \lambda^2 a_n^{(1)}(t) + \lambda^3 a_n^{(2)}(t) + \dots) e^{i\omega_{kn}t} . \quad (26)$$

From each order term of Eq. (26), the following relations are obtained.

$$\dot{a}_k^{(0)}(t) = 0 , \quad (27)$$
$$\dot{a}_k^{(1)}(t) = \frac{1}{i\hbar}\sum_n <k|H'(t)|n> a_n^{(0)}(t) e^{i\omega_{kn}t} , \quad (28)$$
$$\dot{a}_k^{(2)}(t) = \frac{1}{i\hbar}\sum_n <k|H'(t)|n> a_n^{(1)}(t) e^{i\omega_{kn}t} , \quad (29)$$

The general expression for (l+1)th-order $\dot{a}_k^{(l+1)}(t)$ is expressed as

$$\dot{a}_k^{(l+1)}(t) = \frac{1}{i\hbar}\sum_n <k|H'(t)|n> a_n^{(l)}(t) e^{i\omega_{kn}t} . \quad (30)$$

In the first place, the result of the first-order perturbation theory is described. It is assumed that the system exists in the state u_0, which is one of the eigen states of H_0 :

$$a_k^{(0)}(0) = \delta_{k0} . \quad (31)$$

Using Eq.(31), Eq.(28) is rewritten as

$$\dot{a}_k^{(1)}(t) = \frac{1}{i\hbar} <k|H'(t)|0> e^{i\omega_{k0}t} .$$

Therefore, the first-order corrective coefficient $a_k^{(1)}(t)$ is given by

$$a_k^{(1)}(t) = \frac{1}{i\hbar}\int <k|H'(t')|0>e^{i\omega_{k0}t'}dt' . \tag{32}$$

In the second place, the result of the second-order perturbation theory is described. One state m except 0 and k is considered. From Eq.(28),

$$a_m^{(1)}(t) = \frac{1}{i\hbar}\int <m|H'(t')|0>e^{i\omega_{m0}t'}dt' . \tag{33}$$

Substituting Eq.(34) into Eq.(29), we obtain the third-order corrective coefficient $a_k^{(2)}(t)$:

$$\begin{aligned} a_k^{(2)}(t) &= \frac{1}{i\hbar}\int_0^t \sum_m a_m^{(1)}(t')<k|H'(t')|m>e^{i\omega_{km}t'}dt' \\ &= \frac{1}{i\hbar}\sum_m \int_0^t dt'<k|H'(t')|m>e^{i\omega_{km}t'}\int_0^{t'} dt''<m|H'(t'')|0>e^{i\omega_{m0}t''}. \end{aligned} \tag{34}$$

Finally, the third-order perturbation theory is applied. One state m' except 0, k and m is considered. In a similar manner, we obtain

$$a_{m'}^{(1)}(t'') = \frac{1}{i\hbar}\int_0^{t''} <m'|H'(t''')|0>e^{i\omega_{m'0}t'''}dt''' , \tag{35}$$

$$a_m^{(2)}(t') = \frac{1}{i\hbar}\int_0^{t'} \sum_{m'} a_{m'}^{(1)}(t'')<m|H'(t'')|m'>e^{i\omega_{mm'}t''}dt'' , \tag{36}$$

$$a_k^{(3)}(t) = \frac{1}{i\hbar}\int_0^t \sum_m a_m^{(2)}(t')\langle m|H'(t')|m\rangle e^{i\omega_{km}t'}dt' . \qquad (37)$$

As can be seen from the above expressions, the first-order perturbation is a process relating to the direct transition from 0 to k, the second-order perturbation is to the transition from 0 to k through m, the third-order perturbation is to the transition from 0 to k through m and m'.

3. Analytical Expressions for the Polarizability and the Second- and Third-order Hyperpolarizabilities [8,12,13]

The following external oscillating electric field is considered :

$$\begin{aligned} \boldsymbol{F}' &= \boldsymbol{F}_1 cos\omega_1 t + \boldsymbol{F}_2 cos\omega_2 t + \boldsymbol{F}_3 cos\omega_3 t \\ &= \boldsymbol{F}_1\left(\frac{e^{i\omega_1 t}+e^{-i\omega_1 t}}{2}\right) + \boldsymbol{F}_2\left(\frac{e^{i\omega_2 t}+e^{-i\omega_2 t}}{2}\right) + \boldsymbol{F}_3\left(\frac{e^{i\omega_3 t}+e^{-i\omega_3 t}}{2}\right). \end{aligned} \qquad (38)$$

The interactions between substance and electric field are assumed to be treated by the electric dipole approximation. The perturbed Hamiltonian is expressed as

$$H'(t) = -\boldsymbol{p}\cdot\boldsymbol{F}' = -\boldsymbol{p}\sum_{i=1}^{3}\boldsymbol{F}_i'\left(\frac{e^{i\omega_i t}+e^{-i\omega_i t}}{2}\right), \qquad (39)$$

where $\boldsymbol{p}$ represents the electric dipole operator $-e\boldsymbol{r}$, in which e is an elementary electric charge and $\boldsymbol{r}$ is the molecular coordinates.

First, the analytical expression of $a_k^{(1)}(t)$ is considered. Substituting Eq.(39) into Eq.(32), we obtain

$$a_k^{(1)}(t) = \frac{1}{i\hbar}\int_0^t <k|\sum_{a=1}^{3}\left(-\boldsymbol{p}\cdot\boldsymbol{F}_a'\left(\frac{e^{i\omega_a t'}+e^{-i\omega_a t'}}{2}\right)\right)|0>e^{i\omega_{k0}t'}dt'$$

$$= \frac{1}{2\hbar}\sum_{a=1}^{3}<k|\boldsymbol{p}\cdot\boldsymbol{F}_a'|0>\left[\frac{e^{i(\omega_a+\omega_{k0})t}-1}{\omega_{k0}+\omega_a}+\frac{e^{i(\omega_{k0}-\omega_a)t}-1}{\omega_{k0}-\omega_a}\right].$$

Therefor, the first-order corrective coefficient $a_k^{(1)}(t)$ is expressed as

$$a_k^{(1)}(t) = \frac{1}{2\hbar}\sum_{a=1}^{3}<k|\boldsymbol{p}\cdot\boldsymbol{F}_a'|0>\left[\frac{e^{i(\omega_a+\omega_{k0})t}}{\omega_{k0}+\omega_a}+\frac{e^{i(\omega_{k0}-\omega_a)t}}{\omega_{k0}-\omega_a}+\cdots\right]. \tag{40}$$

Second, the analytical expression of $a_k^{(2)}(t)$ is considered. Substituting Eq.(39) into Eq.(34), we obtain

$$a_k^{(2)}(t) = \frac{1}{i\hbar}\int_0^t \sum_m a_m^{(1)}(t')<k|H'(t')|m>e^{i\omega_{km}t'}dt'$$

$$= \frac{1}{2i\hbar^2}\int_0^t \sum_m\left[\sum_{a=1}^{3}<m|\boldsymbol{p}\cdot\boldsymbol{F}_a'|0>\left(\frac{e^{i(\omega_a+\omega_{m0})t'}}{\omega_{m0}+\omega_a}+\frac{e^{i(\omega_{m0}-\omega_a)t'}}{\omega_{m0}-\omega_a}+\cdots\right)\right.$$

$$\left.\times<k|\sum_{b=1}^{3}\left(-\boldsymbol{p}\cdot\boldsymbol{F}_b'\left(\frac{e^{i\omega_b t'}+e^{-i\omega_b t'}}{2}\right)\right)|m>e^{i\omega_{km}t'}\right]dt'$$

$$= -\frac{1}{4i\hbar^2}\sum_m\sum_{a=1}^{3}\sum_{b=1}^{3}\langle k|\boldsymbol{p}\cdot\boldsymbol{F}_b'|m\rangle\langle m|\boldsymbol{p}\cdot\boldsymbol{F}_a'|0\rangle$$

$$\times\int_0^t\left(\frac{e^{i(\omega_a+\omega_b+\omega_{k0})t'}}{\omega_{m0}+\omega_a}+\frac{e^{i(-\omega_a-\omega_b+\omega_{k0})t'}}{\omega_{m0}-\omega_a}+\cdots\right)dt'.$$

Therefore, the second-order corrective coefficient $a_k^{(2)}(t)$ is expressed as

$$a_k^{(2)}(t) = \frac{1}{4\hbar^2}\sum_m\sum_{a=1}^{3}\sum_{b=1}^{3}\langle k|\boldsymbol{p}\cdot\boldsymbol{F}_b'|m\rangle\langle m|\boldsymbol{p}\cdot\boldsymbol{F}_a'|0\rangle$$

$$\times\left[\frac{e^{i(\omega_a+\omega_b+\omega_{k0})t}}{(\omega_{m0}+\omega_a)(\omega_{k0}+\omega_a+\omega_b)}+\frac{e^{-i(\omega_a+\omega_b-\omega_{k0})t}}{(\omega_{m0}-\omega_a)(\omega_{k0}-\omega_a-\omega_b)}+\cdots\right]. \qquad (41)$$

Finally, the analytical expression of $a_k^{(3)}(t)$ is considered. Substituting Eq.(39) into Eqs.(35)-(37), we obtain

$$a_k^{(3)}(t) = \frac{1}{i\hbar}\int_0^t\sum_m a_m^{(2)}(t')\langle k|H'(t')|m\rangle e^{i\omega_{km}t'}dt'$$

$$= -\frac{1}{4i\hbar^3}\sum_m\sum_{m'}\sum_{a=1}^{3}\sum_{b=1}^{3}\langle m|\boldsymbol{p}\cdot\boldsymbol{F}_b'|m'\rangle\langle m'|\boldsymbol{p}\cdot\boldsymbol{F}_a'|0\rangle$$

$$\times\left[\frac{e^{i(\omega_a+\omega_b+\omega_{m0})t'}}{(\omega_{m'0}+\omega_a)(\omega_{m0}+\omega_a+\omega_b)}+\frac{e^{-i(\omega_a+\omega_b-\omega_{m0})t'}}{(\omega_{m'0}-\omega_a)(\omega_{m0}-\omega_a-\omega_b)}+\cdots\right]$$

$$\times\sum_c\langle k|\boldsymbol{p}\cdot\boldsymbol{F}_c'|m\rangle\left(\frac{e^{i\omega_c t'}+e^{-i\omega_c t'}}{2}\right)e^{i\omega_{km}t'}dt'$$

$$= -\frac{1}{8i\hbar^3}\sum_m\sum_{m'}\sum_{a=1}^{3}\sum_{b=1}^{3}\sum_{c=1}^{3}\langle k|\boldsymbol{p}\cdot\boldsymbol{F}_c'|m\rangle\langle m|\boldsymbol{p}\cdot\boldsymbol{F}_b'|m'\rangle\langle m'|\boldsymbol{p}\cdot\boldsymbol{F}_a'|0\rangle$$

$$\times\int_0^t\left[\frac{e^{i(\omega_a+\omega_b+\omega_c+\omega_{k0})t'}}{(\omega_{m'0}+\omega_a)(\omega_{m0}+\omega_a+\omega_b)}+\frac{e^{-i(\omega_a+\omega_b+\omega_c-\omega_{k0})t'}}{(\omega_{m'0}-\omega_a)(\omega_{m0}-\omega_a-\omega_b)}+\cdots\right]dt'.$$

Therefore, the second-order corrective coefficient $a_k^{(3)}(t)$ is expressed as

$$a_k^{(3)}(t) = \frac{1}{8\hbar^3}\sum_{m}\sum_{m'}\sum_{a=1}^{3}\sum_{b=1}^{3}\sum_{c=1}^{3}\langle k|p\cdot F_c|m\rangle\langle m|p\cdot F_b|m'\rangle\langle m'|p\cdot F_a|0\rangle$$
$$\times\left[\frac{e^{i(\omega_{k0}+\omega_a+\omega_b+\omega_c)t}}{(\omega_{k0}+\omega_a+\omega_b+\omega_c)(\omega_{m'0}+\omega_a)(\omega_{m0}+\omega_a+\omega_b)}\right.$$
$$\left.+\frac{e^{i(\omega_{k0}-\omega_a-\omega_b-\omega_c)t}}{(\omega_{k0}-\omega_a-\omega_b-\omega_c)(\omega_{m'0}-\omega_a)(\omega_{m0}-\omega_a-\omega_b)}+\ldots\right]. \qquad (42)$$

Substituting Eq.(25)(λ=1) into Eq.(18), the perturbed wavefunction Ψ is written as

$$\begin{aligned}\Psi &= \sum_n a_n(t)u_n e^{-i\omega_n t}\\ &= a_0(t)u_0e^{-i\omega_0 t} + a_1(t)u_1e^{-i\omega_1 t} + a_2(t)u_2e^{-i\omega_2 t} + \ldots\\ &= (a_0^{(0)}(t)+a_0^{(1)}(t)+\ldots)u_0e^{-i\omega_0 t}\\ &\quad + (a_1^{(0)}(t)+a_1^{(1)}(t)+\ldots)u_1e^{-i\omega_1 t}\\ &\quad + (a_2^{(0)}(t)+a_2^{(1)}(t)+\ldots)u_2e^{-i\omega_2 t}\\ &\quad + (a_3^{(0)}(t)+a_3^{(1)}(t)+\ldots)u_3e^{-i\omega_3 t} + \ldots\\ &= u_0e^{-i\omega_0 t} + \sum_n a_n^{(1)}(t)u_ne^{-i\omega_n t} + \sum_n a_n^{(2)}(t)u_ne^{-i\omega_n t} + \sum_n a_n^{(3)}(t)u_ne^{-i\omega_n t} + \ldots .\end{aligned} \qquad (43)$$

The expected value of p is expressed as

$$\begin{aligned}\langle\Psi|p|\Psi\rangle &= \langle u_0|p|u_0\rangle\\ &\quad + \sum_n a_n^{(1)*}(t)\langle n|p|0\rangle e^{i\omega_{n0}t} + \sum_n a_n^{(1)}(t)\langle 0|p|n\rangle e^{-i\omega_{n0}t} \quad \Big\}\ \text{(i)}\\ &\quad + \sum_n\sum_m a_m^{(1)*}(t)a_n^{(2)}(t)\langle m|p|n\rangle e^{i\omega_{mn}t} \quad \Big\}\\ &\quad + \sum_n \left\{a_n^{(2)*}(t)\langle n|p|0\rangle e^{i\omega_{n0}t} + a_n^{(2)}(t)\langle 0|p|n\rangle e^{-i\omega_{n0}t}\right\} \quad \Big\}\ \text{(ii)}\end{aligned}$$

$$
\left.
\begin{aligned}
&+\sum_n \sum_{m'} a_n^{(1)*}(t) a_{m'}^{(2)}(t) \langle n|p|m'\rangle e^{-i\omega_{m'n}t} \\
&+\sum_n \sum_{m'} a_n^{(1)}(t) a_{m'}^{(2)*}(t) \langle m'|p|n\rangle e^{i\omega_{m'n}t} \\
&+\sum_n \left\{ a_n^{(3)}(t) \langle 0|p|n\rangle e^{-i\omega_{n0}t} + a_n^{(3)*}(t) \langle n|p|0\rangle e^{i\omega_{n0}t} \right\}
\end{aligned}
\right\} \text{(iii)}
$$

$$
+ \dots \ . \tag{44}
$$

In comparison Eqs.(2) with (44), the analytical expression of each order polarizability is derived.

First, the analytical expression of polarizability α_{ij} is considered. Substituting Eq.(40) into the first-order corrective term (i) in Eq.(44), we can write

$$
\begin{aligned}
&\sum_n a_n^{(1)*}(t) \langle n|p|0\rangle e^{i\omega_{n0}t} + \sum_n a_n^{(1)}(t) \langle 0|p|n\rangle e^{-i\omega_{n0}t} \\
&= \frac{1}{2\hbar} \sum_n \sum_{a=1}^{3} \langle 0|p \cdot F_a'|n\rangle \left[\frac{e^{-i(\omega_a+\omega_{n0})t}}{\omega_{n0}+\omega_a} + \frac{e^{-i(\omega_{n0}-\omega_a)t}}{\omega_{n0}-\omega_a} + \dots \right] e^{i\omega_{n0}t} \langle n|p|0\rangle + c.c \\
&= \frac{1}{2\hbar} \sum_n \sum_{a=1}^{3} \langle 0|p \cdot F_a'|n\rangle \langle n|p|0\rangle \left(\frac{e^{-i\omega_a t}}{\omega_{n0}+\omega_a} + \frac{e^{i\omega_{n0}t}}{\omega_{n0}-\omega_a} + \dots \right) + c.c \ ,
\end{aligned} \tag{45}
$$

where $c.c$ means complex conjugate. Compared with Eq.(2), the coefficient of $F_1^j \cos\omega_1 t$ in Eq.(45) is equal to α_{ij}.

$$
\alpha_{ij} = \frac{1}{\hbar} \sum_n \langle 0|p^i|n\rangle \langle n|p^j|0\rangle \left(\frac{1}{\omega_{n0}+\omega_a} + \frac{1}{\omega_{n0}-\omega_a} \right) .
$$

Using the definition for transition moment μ_{n0} and transition energy E_{n0} :

$$
\mu_{n0}^i = \langle n|p^i|0\rangle = -e\langle n|r^i|0\rangle \ , \tag{46}
$$

$$
E_{n0} = \hbar\omega_{n0} \ , \tag{47}
$$

the analytical expression of α_{ij} is given by

$$\alpha_{ij}(-\omega_1;\omega_1) = 2\sum_n \mu^i_{0n}\mu^j_{n0}\frac{E_{n0}}{E^2_{n0} - (\hbar\omega_1)^2}. \tag{48}$$

Second, the analytical expression of the second-order hyperpolarizability β_{ijk} is considered. Substituting Eq.(40) into the first term (ii-1) of the second-order corrective term (ii) in Eq.(44), we obtain

$$\begin{aligned}(\text{ii-1}) = \sum_n\sum_m \Bigg\{ &\sum_{a=1}^{3}\frac{1}{2\hbar}\langle 0|\boldsymbol{p}\cdot\boldsymbol{F}_a'|m\rangle\left[\frac{e^{-i(\omega_a+\omega_{m0})t}}{\omega_{m0}+\omega_a} + \frac{e^{-i(\omega_{m0}-\omega_a)t}}{\omega_{m0}-\omega_a} + \ldots\right]e^{i\omega_{m0}t} \\ &\times\frac{1}{2\hbar}\sum_{b=1}^{3}\langle n|\boldsymbol{p}\cdot\boldsymbol{F}_b'|0\rangle\left[\frac{e^{i(\omega_b+\omega_{n0})t}}{\omega_{n0}+\omega_b} + \frac{e^{i(\omega_{n0}-\omega_b)t}}{\omega_{n0}-\omega_b} + \ldots\right]e^{-i\omega_{n0}t}\langle m|p|n\rangle\Bigg\} \\ = \sum_n\sum_m &\frac{1}{4\hbar^2}\sum_{a=1}^{3}\sum_{b=1}^{3}\langle 0|\boldsymbol{p}\cdot\boldsymbol{F}_a'|m\rangle\langle m|p|n\rangle\langle n|\boldsymbol{p}\cdot\boldsymbol{F}_b'|0\rangle \\ &\times\left[\frac{e^{-i(\omega_a+\omega_b)t}}{(\omega_{m0}+\omega_a)(\omega_{n0}-\omega_b)} + \frac{e^{i(\omega_a+\omega_b)t}}{(\omega_{m0}-\omega_a)(\omega_{n0}+\omega_b)} + \ldots\right].\end{aligned} \tag{49}$$

The coefficient of $F_1^j F_2^k \cos(\omega_1+\omega_2)t$ in Eq.(49) is

$$\begin{aligned}&\frac{1}{2\hbar^2}\sum_n\sum_m\langle 0|p^j|m\rangle\langle m|p^i|n\rangle\langle n|p^k|0\rangle \\ &\qquad\times\left[\frac{1}{(\omega_{m0}+\omega_1)(\omega_{n0}-\omega_2)} + \frac{1}{(\omega_{m0}-\omega_1)(\omega_{n0}+\omega_2)}\right].\end{aligned} \tag{50}$$

Substituting Eq.(41) into the second and third terms (ii-2) of the second-order corrective term (ii) in Eq.(44), we obtain

$$
\begin{aligned}
\text{(ii-2)} = & \sum_n \sum_m \frac{1}{4\hbar^2} \sum_{a=1}^{3} \sum_{b=1}^{3} \langle 0 | p \cdot F_b' | m \rangle \langle m | p \cdot F_a' | n \rangle \\
& \times \left[\frac{e^{-i(\omega_a+\omega_b+\omega_{n0})t}}{(\omega_{m0}+\omega_a)(\omega_{n0}+\omega_a+\omega_b)} + \frac{e^{i(\omega_a+\omega_b-\omega_{n0})t}}{(\omega_{m0}-\omega_a)(\omega_{n0}-\omega_a-\omega_b)} \right] \langle n | p | 0 \rangle e^{i\omega_{n0}t} + c.c \\
= & \frac{1}{4\hbar^2} \sum_n \sum_m \sum_{a=1}^{3} \sum_{b=1}^{3} \langle 0 | p \cdot F_a' | m \rangle \langle m | p \cdot F_b' | n \rangle \langle n | p | 0 \rangle \\
& \times \left[\frac{e^{-i(\omega_a+\omega_b)t}}{(\omega_{m0}+\omega_a)(\omega_{n0}+\omega_a+\omega_b)} + \frac{e^{i(\omega_a+\omega_b)t}}{(\omega_{m0}-\omega_a)(\omega_{n0}-\omega_a-\omega_b)} \right] + c.c \ . \qquad (51)
\end{aligned}
$$

The coefficient of $F_1^j F_2^k \cos(\omega_1+\omega_2)t$ in Eq.(51) is

$$
\begin{aligned}
& \frac{1}{2\hbar^2} \sum_n \sum_m \left\{ \langle 0 | p^j | m \rangle \langle m | p^k | n \rangle \langle n | p^i | 0 \rangle \left[\frac{1}{(\omega_{m0}+\omega_1)(\omega_{n0}+\omega_1+\omega_2)} + \frac{1}{(\omega_{m0}-\omega_1)(\omega_{n0}-\omega_1-\omega_2)} \right] \right. \\
& \left. + \langle 0 | p^k | m \rangle \langle m | p^j | n \rangle \langle n | p^i | 0 \rangle \left[\frac{1}{(\omega_{m0}+\omega_2)(\omega_{n0}+\omega_1+\omega_2)} + \frac{1}{(\omega_{m0}-\omega_2)(\omega_{n0}-\omega_1-\omega_2)} \right] \right\} \qquad (52)
\end{aligned}
$$

Now, the coefficient of $F_1^j F_2^k \cos(\omega_1+\omega_2)t$ in the second-order corrective terms equal to $\beta_{ijk}(-(\omega_1+\omega_2);\omega_1,\omega_2)+\beta_{ikj}(-(\omega_1+\omega_2);\omega_2,\omega_1)$. Therefore, from Eqs.(50) and (52), the second-order hyperpolarizability β_{ijk} is expressed as

$$
\begin{aligned}
\beta_{ijk}(-(\omega_1+\omega_2);\omega_1,\omega_2) = & \frac{1}{4} \sum_n \sum_{n'} \\
& \left[\mu_{0n}^j \mu_{n'n}^i \mu_{n0}^k \left(\frac{1}{(E_{n'0}+\hbar\omega_1)(E_{n0}-\hbar\omega_2)} + \frac{1}{(E_{n'0}-\hbar\omega_1)(E_{n0}+\hbar\omega_2)} \right) \right. \\
& \mu_{0n}^j \mu_{n'n}^k \mu_{n0}^i \left(\frac{1}{(E_{n'0}+\hbar\omega_1)(E_{n0}+\hbar(\omega_1+\omega_2))} + \frac{1}{(E_{n'0}-\hbar\omega_1)(E_{n0}-\hbar(\omega_1+\omega_2))} \right) \\
& \left. \mu_{0n}^k \mu_{n'n}^j \mu_{n0}^i \left(\frac{1}{(E_{n'0}+\hbar\omega_2)(E_{n0}+\hbar(\omega_1+\omega_2))} + \frac{1}{(E_{n'0}-\hbar\omega_2)(E_{n0}-\hbar(\omega_1+\omega_2))} \right) \right] \cdot \qquad (53)
\end{aligned}
$$

Here, the replacement of variable m with n' was carried out and Eqs.(46) and (47) were used.

Finally, the analytical expression of the third-order hyperpolarizability γ_{ijkl} is considered. Substituting Eqs.(40) and (41) into the first term (iii-1) of the third-order corrective term (iii) in Eq.(44), we obtain

$$
\begin{aligned}
\text{(iii-1)} = \sum_{n}\sum_{m'}\Bigg\{ & \frac{1}{2\hbar}\sum_{a=1}^{3}\langle 0|\boldsymbol{p}\cdot\boldsymbol{F}_a'|n\rangle\left(\frac{e^{-i(\omega_a+\omega_{n0})t}}{\omega_{n0}+\omega_a}+\frac{e^{-i(\omega_{n0}-\omega_a)t}}{\omega_{n0}-\omega_a}+\cdots\right)\Bigg\} \\
& \times\Bigg\{\frac{1}{4\hbar^2}\sum_{b=1}^{3}\sum_{c=1}^{3}\sum_{m}\langle m'|\boldsymbol{p}\cdot\boldsymbol{F}_c'|m\rangle\langle m|\boldsymbol{p}\cdot\boldsymbol{F}_b'|0\rangle \\
& \times\left(\frac{e^{i(\omega_b+\omega_c+\omega_{m'0})t}}{(\omega_{m0}+\omega_b)(\omega_{m'0}+\omega_b+\omega_c)}+\frac{e^{-i(\omega_b+\omega_c-\omega_{m'0})t}}{(\omega_{m0}-\omega_b)(\omega_{m'0}-\omega_b-\omega_c)}+\cdots\right)\Bigg\} \\
& \times e^{-i\omega_{m'n}t}\langle n|\boldsymbol{p}|m'\rangle \\
= & \frac{1}{8\hbar^3}\sum_{n}\sum_{m'}\sum_{m}\sum_{a=1}^{3}\sum_{b=1}^{3}\sum_{c=1}^{3}\langle 0|\boldsymbol{p}\cdot\boldsymbol{F}_a'|n\rangle\langle n|\boldsymbol{p}|m'\rangle\langle m'|\boldsymbol{p}\cdot\boldsymbol{F}_c'|m\rangle\langle m|\boldsymbol{p}\cdot\boldsymbol{F}_b'|0\rangle \\
& \times\left(\frac{e^{-i\omega_a t}}{\omega_{n0}+\omega_a}+\frac{e^{i\omega_a t}}{\omega_{n0}-\omega_a}+\cdots\right)\left(\frac{e^{i(\omega_b+\omega_c)t}}{(\omega_{m0}+\omega_b)(\omega_{m'0}+\omega_b+\omega_c)}+\frac{e^{-i(\omega_b+\omega_c)t}}{(\omega_{m0}-\omega_b)(\omega_{m'0}-\omega_b-\omega_c)}+\cdots\right) \\
= & \frac{1}{8\hbar^3}\sum_{n}\sum_{m'}\sum_{m}\sum_{a=1}^{3}\sum_{b=1}^{3}\sum_{c=1}^{3}\langle 0|\boldsymbol{p}\cdot\boldsymbol{F}_a'|n\rangle\langle n|\boldsymbol{p}|m'\rangle\langle m'|\boldsymbol{p}\cdot\boldsymbol{F}_c'|m\rangle\langle m|\boldsymbol{p}\cdot\boldsymbol{F}_b'|0\rangle \\
& \left(\frac{e^{-i(\omega_a+\omega_b+\omega_c)t}}{(\omega_{n0}+\omega_a)(\omega_{m0}-\omega_b)(\omega_{m'0}-\omega_b-\omega_c)}\right. \\
& \left.+\frac{e^{i(\omega_a+\omega_b+\omega_c)t}}{(\omega_{n0}-\omega_a)(\omega_{m0}+\omega_b)(\omega_{m'0}+\omega_b+\omega_c)}+\cdots\right). \qquad (54)
\end{aligned}
$$

The coefficient of $F_1^j F_2^k F_3^l \cos(\omega_1+\omega_2+\omega_3)t$ in Eq.(54) in which variables n, m' and m are replaced with n', m and n, respectively, is given by

$$
\begin{aligned}
& \frac{1}{8\hbar^3}\sum_{n}\sum_{m}\sum_{n'} \\
& \Bigg\{\mu_{0n'}^{j}\mu_{n'm}^{i}\mu_{mn}^{l}\mu_{n0}^{k}\left(\frac{1}{(\omega_{n'0}+\omega_1)(\omega_{n0}-\omega_2)(\omega_{m0}-\omega_2-\omega_3)}+\frac{1}{(\omega_{n'0}-\omega_1)(\omega_{n0}+\omega_2)(\omega_{m0}+\omega_2+\omega_3)}\right) \\
& +\mu_{0n'}^{j}\mu_{n'm}^{i}\mu_{mn}^{k}\mu_{n0}^{l}\left(\frac{1}{(\omega_{n'0}+\omega_1)(\omega_{n0}-\omega_3)(\omega_{m0}-\omega_2-\omega_3)}+\frac{1}{(\omega_{n'0}-\omega_1)(\omega_{n0}+\omega_3)(\omega_{m0}+\omega_2+\omega_3)}\right)
\end{aligned}
$$

$$+\mu^{k}_{0n'}\mu^{i}_{n'm}\mu^{l}_{mn}\mu^{j}_{n0}\left(\frac{1}{(\omega_{n'0}+\omega_2)(\omega_{n\,0}-\omega_1)(\omega_{m0}-\omega_1-\omega_3)}+\frac{1}{(\omega_{n'0}-\omega_2)(\omega_{n\,0}+\omega_1)(\omega_{m0}+\omega_1+\omega_3)}\right)$$
$$+\mu^{k}_{0n'}\mu^{i}_{n'm}\mu^{j}_{mn}\mu^{l}_{n0}\left(\frac{1}{(\omega_{n'0}+\omega_2)(\omega_{n\,0}-\omega_3)(\omega_{m0}-\omega_1-\omega_3)}+\frac{1}{(\omega_{n'0}-\omega_2)(\omega_{n\,0}+\omega_3)(\omega_{m0}+\omega_1+\omega_3)}\right)$$
$$+\mu^{l}_{0n'}\mu^{i}_{n'm}\mu^{k}_{mn}\mu^{j}_{n0}\left(\frac{1}{(\omega_{n'0}+\omega_3)(\omega_{n\,0}-\omega_1)(\omega_{m0}-\omega_1-\omega_2)}+\frac{1}{(\omega_{n'0}-\omega_3)(\omega_{n\,0}+\omega_1)(\omega_{m0}+\omega_1+\omega_2)}\right)$$
$$+\mu^{l}_{0n'}\mu^{i}_{n'm}\mu^{j}_{mn}\mu^{k}_{n0}\left(\frac{1}{(\omega_{n'0}+\omega_3)(\omega_{n\,0}-\omega_2)(\omega_{m0}-\omega_1-\omega_2)}+\frac{1}{(\omega_{n'0}-\omega_3)(\omega_{n\,0}+\omega_2)(\omega_{m0}+\omega_1+\omega_2)}\right)\Bigg\}. \quad (55)$$

The coefficient of $F^{j}_{1}F^{k}_{2}F^{l}_{3}cos\,(\omega_1+\omega_2+\omega_3)t$ in the second term (iii-2) of the third-order corrective terms (iii) in Eq.(44) becomes the same type of Eq.(55) since (iii-1) is the complex conjugated term of (iii-2). Substituting Eq.(42) into the third and fourth terms (iii-3) of the third-order corrective terms (iii) in Eq.(44), we obtain

$$(\text{iii-3}) = \frac{1}{8\hbar^3}\sum_{n}\sum_{m'}\sum_{m}\sum_{a=1}^{3}\sum_{b=1}^{3}\sum_{c=1}^{3}\langle 0|p|n\rangle\langle n|p\cdot F_c'|m\rangle\langle m|p\cdot F_b'|m'\rangle\langle m'|p\cdot F_a'|0\rangle$$
$$\times\left(\frac{e^{-i(\omega_a+\omega_b+\omega_c)t}}{(\omega_{n0}+\omega_a+\omega_b+\omega_c)(\omega_{m'0}+\omega_a)(\omega_{m0}+\omega_a+\omega_b)}\right.$$
$$\left.+\frac{e^{i(\omega_a+\omega_b+\omega_c)t}}{(\omega_{n0}-\omega_a-\omega_b-\omega_c)(\omega_{m'0}-\omega_a)(\omega_{m0}-\omega_a-\omega_b)}\right)+c.c\ . \quad (56)$$

The coefficient of $F^{j}_{1}F^{k}_{2}F^{l}_{3}cos\,(\omega_1+\omega_2+\omega_3)t$ in Eq.(56) in which variables n and m' are replaced with n' and n, respectively, is expressed as

$$\frac{1}{4\hbar^3}\sum_{n}\sum_{m}\sum_{n'}$$
$$\left\{\mu^{i}_{0n'}\mu^{l}_{n'm}\mu^{k}_{mn}\mu^{j}_{n0}\times\right.$$
$$\left.\left(\frac{1}{(\omega_{n'0}+\omega_1+\omega_2+\omega_3)(\omega_{n\,0}+\omega_1)(\omega_{m0}+\omega_1+\omega_2)}+\frac{1}{(\omega_{n'0}-\omega_1-\omega_2-\omega_3)(\omega_{n\,0}-\omega_1)(\omega_{m0}-\omega_1-\omega_2)}\right)\right.$$

$$
\begin{aligned}
&+\mu^{i}_{0n'}\mu^{k}_{n'm}\mu^{l}_{mn}\mu^{j}_{n0} \times \\
&\left(\frac{1}{(\omega_{n'0}+\omega_1+\omega_2+\omega_3)(\omega_{n\,0}+\omega_1)(\omega_{m0}+\omega_1+\omega_3)}+\frac{1}{(\omega_{n'0}-\omega_1-\omega_2-\omega_3)(\omega_{n\,0}-\omega_1)(\omega_{m0}-\omega_1-\omega_3)}\right) \\
&+\mu^{i}_{0n'}\mu^{l}_{n'm}\mu^{j}_{mn}\mu^{k}_{n0} \times \\
&\left(\frac{1}{(\omega_{n'0}+\omega_1+\omega_2+\omega_3)(\omega_{n\,0}+\omega_2)(\omega_{m0}+\omega_1+\omega_2)}+\frac{1}{(\omega_{n'0}-\omega_1-\omega_2-\omega_3)(\omega_{n\,0}-\omega_2)(\omega_{m0}-\omega_1-\omega_2)}\right) \\
&+\mu^{i}_{0n'}\mu^{j}_{n'm}\mu^{l}_{mn}\mu^{k}_{n0} \times \\
&\left(\frac{1}{(\omega_{n'0}+\omega_1+\omega_2+\omega_3)(\omega_{n\,0}+\omega_2)(\omega_{m0}+\omega_2+\omega_3)}+\frac{1}{(\omega_{n'0}-\omega_1-\omega_2-\omega_3)(\omega_{n\,0}-\omega_2)(\omega_{m0}-\omega_2-\omega_3)}\right) \\
&+\mu^{i}_{0n'}\mu^{k}_{n'm}\mu^{j}_{mn}\mu^{l}_{n0} \times \\
&\left(\frac{1}{(\omega_{n'0}+\omega_1+\omega_2+\omega_3)(\omega_{n\,0}+\omega_3)(\omega_{m0}+\omega_1+\omega_3)}+\frac{1}{(\omega_{n'0}-\omega_1-\omega_2-\omega_3)(\omega_{n\,0}-\omega_3)(\omega_{m0}-\omega_1-\omega_3)}\right) \\
&+\mu^{i}_{0n'}\mu^{j}_{n'm}\mu^{k}_{mn}\mu^{l}_{n0} \times \\
&\left(\frac{1}{(\omega_{n'0}+\omega_1+\omega_2+\omega_3)(\omega_{n\,0}+\omega_3)(\omega_{m0}+\omega_2+\omega_3)}+\frac{1}{(\omega_{n'0}-\omega_1-\omega_2-\omega_3)(\omega_{n\,0}-\omega_3)(\omega_{m0}-\omega_2-\omega_3)}\right).
\end{aligned}
\tag{57}
$$

The coefficient of $F_1^j F_2^k F_3^l \cos(\omega_1+\omega_2+\omega_3)t$ in the third-order corrective terms (iii) in Eq.(44) are equal to

$$
\begin{aligned}
&\gamma_{ijkl}(-\omega_4;\omega_1,\omega_2,\omega_3)+\gamma_{ijlk}(-\omega_4;\omega_1,\omega_3,\omega_2)+\gamma_{ikjl}(-\omega_4;\omega_2,\omega_1,\omega_3) \\
&+\gamma_{iklj}(-\omega_4;\omega_2,\omega_3,\omega_1)+\gamma_{iljk}(-\omega_4;\omega_3,\omega_1,\omega_2)+\gamma_{ilkj}(-\omega_4;\omega_3,\omega_2,\omega_1).
\end{aligned}
$$

Here, $\omega_4 = \omega_1 + \omega_2 + \omega_3$. Consequently, from (iii-1)-(iii-3), we obtain

$$
\begin{aligned}
&\gamma_{ijkl}(-\omega_4;\omega_1,\omega_2,\omega_3) = \frac{1}{24}\sum_{n}\sum_{m}\sum_{n'} \\
&\left\{\mu^{i}_{0n'}\mu^{l}_{n'm}\mu^{k}_{mn}\mu^{j}_{n0} \times \right. \\
&\left(\frac{1}{(E_{n'0}+\hbar\omega_4)(E_{n\,0}+\hbar\omega_1)(E_{m0}+\hbar(\omega_1+\omega_2))}+\frac{1}{(E_{n'0}-\hbar\omega_4)(E_{n\,0}-\hbar\omega_1)(E_{m0}-\hbar(\omega_1+\omega_2))}\right) \\
&+\mu^{i}_{0n'}\mu^{k}_{n'm}\mu^{l}_{mn}\mu^{j}_{n0} \times \\
&\left(\frac{1}{(E_{n'0}+\hbar\omega_4)(E_{n\,0}+\hbar\omega_1)(E_{m0}+\hbar(\omega_1+\omega_3))}+\frac{1}{(E_{n'0}-\hbar\omega_4)(E_{n\,0}-\hbar\omega_1)(E_{m0}-\hbar(\omega_1+\omega_3))}\right)
\end{aligned}
$$

$$
\begin{aligned}
&+ \mu^{i}_{0n'}\mu^{l}_{n'm}\mu^{j}_{mn}\mu^{k}_{n0} \times \\
&\left(\frac{1}{(E_{n'0}+\hbar\omega_4)(E_{n\,0}+\hbar\omega_2)(E_{m0}+\hbar(\omega_1+\omega_3))} + \frac{1}{(E_{n'0}-\hbar\omega_4)(E_{n\,0}-\hbar\omega_2)(E_{m0}-\hbar(\omega_1+\omega_2))}\right) \\
&+ \mu^{i}_{0n'}\mu^{j}_{n'm}\mu^{l}_{mn}\mu^{k}_{n0} \times \\
&\left(\frac{1}{(E_{n'0}+\hbar\omega_4)(E_{n\,0}+\hbar\omega_2)(E_{m0}+\hbar(\omega_2+\omega_3))} + \frac{1}{(E_{n'0}-\hbar\omega_4)(E_{n\,0}-\hbar\omega_2)(E_{m0}-\hbar(\omega_2+\omega_3))}\right) \\
&+ \mu^{i}_{0n'}\mu^{k}_{n'm}\mu^{j}_{mn}\mu^{l}_{n0} \times \\
&\left(\frac{1}{(E_{n'0}+\hbar\omega_4)(E_{n\,0}+\hbar\omega_3)(E_{m0}+\hbar(\omega_1+\omega_3))} + \frac{1}{(E_{n'0}-\hbar\omega_4)(E_{n\,0}-\hbar\omega_3)(E_{m0}-\hbar(\omega_1+\omega_3))}\right) \\
&+ \mu^{i}_{0n'}\mu^{j}_{n'm}\mu^{k}_{mn}\mu^{l}_{n0} \times \\
&\left(\frac{1}{(E_{n'0}+\hbar\omega_4)(E_{n\,0}+\hbar\omega_3)(E_{m0}+\hbar(\omega_2+\omega_3))} + \frac{1}{(E_{n'0}-\hbar\omega_4)(E_{n\,0}-\hbar\omega_3)(E_{m0}-\hbar(\omega_2+\omega_3))}\right) \\
&+ \mu^{j}_{0n'}\mu^{i}_{n'm}\mu^{l}_{mn}\mu^{k}_{n0} \times \\
&\left(\frac{1}{(E_{n'0}+\hbar\omega_1)(E_{n\,0}-\hbar\omega_2)(E_{m0}-\hbar(\omega_2+\omega_3))} + \frac{1}{(E_{n'0}-\hbar\omega_1)(E_{n\,0}+\hbar\omega_2)(E_{m0}-\hbar(\omega_2+\omega_3))}\right) \\
&+ \mu^{j}_{0n'}\mu^{i}_{n'm}\mu^{k}_{mn}\mu^{l}_{n0} \times \\
&\left(\frac{1}{(E_{n'0}+\hbar\omega_1)(E_{n\,0}-\hbar\omega_3)(E_{m0}+\hbar(\omega_2+\omega_3))} + \frac{1}{(E_{n'0}-\hbar\omega_1)(E_{n\,0}+\hbar\omega_3)(E_{m0}+\hbar(\omega_2+\omega_3))}\right) \\
&+ \mu^{k}_{0n'}\mu^{i}_{n'm}\mu^{l}_{mn}\mu^{j}_{n0} \times \\
&\left(\frac{1}{(E_{n'0}+\hbar\omega_2)(E_{n\,0}-\hbar\omega_1)(E_{m0}-\hbar(\omega_1+\omega_3))} + \frac{1}{(E_{n'0}-\hbar\omega_2)(E_{n\,0}-\hbar\omega_1)(E_{m0}+\hbar(\omega_1+\omega_3))}\right) \\
&+ \mu^{k}_{0n'}\mu^{i}_{n'm}\mu^{j}_{mn}\mu^{l}_{n0} \times \\
&\left(\frac{1}{(E_{n'0}+\hbar\omega_2)(E_{n\,0}-\hbar\omega_3)(E_{m0}-\hbar(\omega_1+\omega_3))} + \frac{1}{(E_{n'0}-\hbar\omega_2)(E_{n\,0}+\hbar\omega_3)(E_{m0}+\hbar(\omega_1+\omega_3))}\right) \\
&+ \mu^{l}_{0n'}\mu^{i}_{n'm}\mu^{k}_{mn}\mu^{j}_{n0} \times \\
&\left(\frac{1}{(E_{n'0}+\hbar\omega_3)(E_{n\,0}-\hbar\omega_1)(E_{m0}-\hbar(\omega_1+\omega_2))} + \frac{1}{(E_{n'0}-\hbar\omega_3)(E_{n\,0}+\hbar\omega_1)(E_{m0}+\hbar(\omega_1+\omega_2))}\right) \\
&+ \mu^{l}_{0n'}\mu^{i}_{n'm}\mu^{j}_{mn}\mu^{k}_{n0} \times \\
&\left.\left(\frac{1}{(E_{n'0}+\hbar\omega_3)(E_{n\,0}-\hbar\omega_2)(E_{m0}-\hbar(\omega_1+\omega_2))} + \frac{1}{(E_{n'0}-\hbar\omega_3)(E_{n\,0}+\hbar\omega_2)(E_{m0}+\hbar(\omega_1+\omega_2))}\right)\right|. \qquad (58)
\end{aligned}
$$

Here, the indices n' and n run only over excited states excluding the ground state.

References

[1] *Nonlinear Optical Properties of Organic and Polymeric Materials*, edited by D. J. Williams (Am. Chem. Soc., Washington, D. C. , 1983).

[2] D. J. Williams, Angew. Chem. Int. Ed. **23** (1984) 690.

[3] *Nonlinear Optical Properties of Polymers*, edited by A. J. Heeger, J. Orenstein and D. R. Ulrich, Vol. **109** (Material Research Society Publication, Pittsburgh, 1988).

[4] *Nonlinear Optical and Electroactive Polymers*, edited by D. Ulrich and P. Prasad (Plenum, New York, 1987).

[5] *Nonlinear Optical Properties of Organic Molecules and Crystals*, edited by D. S. Chemla and J. Zyss, Vols. **I** and **II** (Academic, Orlando, 1987).

[6] *Nonlinear Optics of Organics and Semiconductors*, edited by T. Kobayashi, Springer Proceedings in Physics **36** (1989). 98.

[7] *Organic Materials for Nonlinear Optics*, edited by R. A. Hann and D. Bloor, Special Publication No. 69 (Royal Society of Chemistry, London, 1988).

[8] N. Bloembergen, *Nonlinear Optics* (Benjamin, New York, 1965).

[9] B. M. Pierce, J. Chem. Phys. **91** (1989) 791.

[10] P. A. M. Dirac, Proc. Roy. Soc. (London) **A112** (1927) 661 ; **A114** (1927) 243 .

[11] L. I. Schiff, Quantum Mechanics, (McGraw-Hill, 1982).

[12] J. A. Armstrong, N. Bloembergen, J. Ducuing and P. S. Pershan, Phys. Rev. **127** (1962) 1918.

[13] J. F. Ward and B. J. Orr, Mol. Phys. **20** (1971) 513.

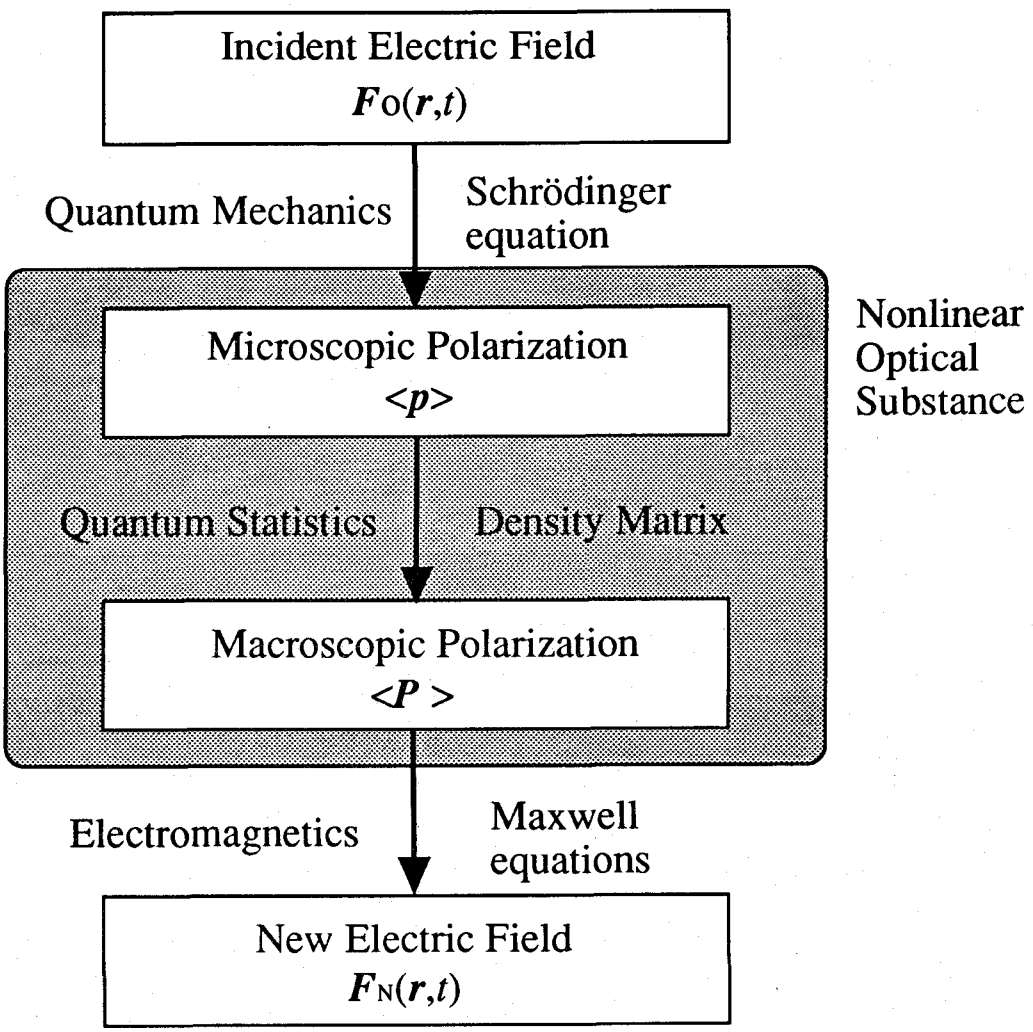

Frequency of $\boldsymbol{F}o(\boldsymbol{r},t)$ $\neq$ Frequency of $\boldsymbol{F}_N(\boldsymbol{r},t)$

Frequency Mixing
Harmonic Generation
...

Fig.1. Nonlinear optical process

Chapter 2

Approximate Expressions for the Second- and Third-order Hyperpolarizabilities and the Schematic Diagrams of Transition Matrix Elements

1. Approximate Expressions for the Second-order Hyperpolarizability β_{ijk}

For DC-SHG method which is usually used for measuring $\beta_{ijk}(-2\omega;\omega,\omega)$, Eq.(I.1.53) is rewritten as [1-14]

$$\beta_{ijk}(-2\omega;\omega,\omega) = \frac{1}{4}\sum_{n}\sum_{n'} \left[\mu^{j}_{0n'}\mu^{i}_{n'n}\mu^{k}_{n0}\left(\frac{1}{(E_{n'0}+\hbar\omega)(E_{n0}-\hbar\omega)}+\frac{1}{(E_{n'0}-\hbar\omega)(E_{n0}+\hbar\omega)}\right) + (\mu^{j}_{0n'}\mu^{k}_{n'n}\mu^{i}_{n0}+\mu^{k}_{0n'}\mu^{j}_{n'n}\mu^{i}_{n0})\times \left(\frac{1}{(E_{n'0}+\hbar\omega)(E_{n0}+2\hbar\omega))}+\frac{1}{(E_{n'0}-\hbar\omega)(E_{n0}-2\hbar\omega)}\right)\right]. \quad (1)$$

The virtual excitation process [15-18] represented by the subscript of transition matrices in Eq.(1) can be illustrated in Fig.1 (a). There are two types of processes : - type (I) involving one excited state and type (II) involving two excited states.

For most strong intramolecular charge-transfer (CT) systems, the transitions from the ground to CT excited states are found to be most contribute to β_{ijk} [19]. Therefore, total β_{ijk} can be well approximated by the contributions of type (I) which represents the interactions between the ground and the CT excited states. This is referred to as the diagonal approximation [2]. Under the diagonal approximation, the expression of β_{ijk} is given as

$$\beta_{ijk}(-2\omega\ ;\omega,\omega) = \frac{1}{2}\sum_{n}$$

$$\left[\mu_{0n}^{j}\mu_{nn}^{i}\mu_{n0}^{k}\frac{1}{(E_{n0}^{2}-(\hbar\omega)^{2})} + \mu_{0n}^{i}(\mu_{nn}^{k}\mu_{n0}^{j}+\mu_{nn}^{j}\mu_{n0}^{k})\frac{E_{n0}^{2}+2(\hbar\omega)^{2}}{(E_{n0}^{2}-(\hbar\omega)^{2})(E_{n0}^{2}-(2\hbar\omega)^{2})}\right]. \quad (2)$$

In this case, the i component of β is expressed as

$$\beta_{iii}(-2\omega\ ;\omega,\omega) = \frac{3}{2}\sum_{n}(\mu_{0n}^{i})\mu_{nn}^{i}\ \frac{E_{n0}^{2}}{(E_{n0}^{2}-(\hbar\omega)^{2})(E_{n0}^{2}-(2\hbar\omega)^{2})}. \quad (3)$$

Using the electronic-charge-centroid coordinate system (see Appendix 1), Eq.(3) is written as

$$\beta_{iii}(-2\omega\ ;\omega,\omega) = \frac{3}{2}\sum_{n}(\Delta\mu_{0n}^{i})(\mu_{0n}^{i})^{2}\ \frac{E_{n0}^{2}}{(E_{n0}^{2}-(\hbar\omega)^{2})(E_{n0}^{2}-(2\hbar\omega)^{2})}, \quad (4)$$

where $\Delta\mu_{0n}^{i}$ denotes the differences between excited and ground state dipole moments. The index n runs over excited states.

When one excited state n and ground state 0 mainly contribute to total β, the two level approximation [19] can be applied. In this case, Eq.(4) is approximated as

$$\beta_{iii}(-2\omega\ ;\omega,\omega) = \frac{3}{2}(\Delta\mu_{0n}^{i})(\mu_{0n}^{i})^{2}\ \frac{E_{n0}^{2}}{(E_{n0}^{2}-(\hbar\omega)^{2})(E_{n0}^{2}-(2\hbar\omega)^{2})}. \quad (5)$$

Using the oscillator strength :

$$f = \frac{2\mu E_{n0}}{\hbar^{2}e^{2}}|\mu_{0n}^{i}|^{2}, \quad (6)$$

Eq.(5) is written as

$$\beta_{iii}(-2\omega;\omega,\omega) = \frac{3e^2\hbar^2}{4m} f(\Delta\mu^i_{0n}) \frac{E_{n0}}{(E_{n0}^2-(\hbar\omega)^2)(E_{n0}^2-(2\hbar\omega)^2)} . \quad (7)$$

In the case of the static electric field, Eq.(5) is represented as follows.

$$\beta_{iii}(0;0,0) = \frac{3}{2} \frac{(\Delta\mu^i_{0n})(\mu^i_{0n})^2}{E_{n0}^2} . \quad (8)$$

2. Approximate Expressions for the Third-order Hyperpolarizability γ_{ijkl}

In the case of THG($\omega_1=\omega_2=\omega_3\equiv\omega$) [14-22], Eq.(I.1.58) is considered here. The virtual excitation processes can be divided into three types shown in Fig.2 (a) [15-18,22]. Type (I) represents the process (0,*n*-*n*,*n*-*n*,*n*-*n*,0)($n\neq0$) which is concerned with the excitation energies (E_{n0}), transition moments (μ_{0n}) and dipole moment differences between excited state *n* and ground state 0 (μ_{nn}). Type (II) represents the process (0,*n*'-*n*',0-0,*n*-*n*,0) (*n*,*n*'$\neq$0) with the ground state in the middle of the process. This process is concerned with the excitation energies ($E_{n'0}$, E_{n0}) and transition moments ($\mu_{0n'}$, μ_{0n}). Type (III) represents the process (0,*n*'-*n*',*m*-*m*,*n*-*n*,0) in which another higher or lower excited state *m* than the excited states (*n*, *n*') in the former two processes are included. The process is concerned with the excitation energies ($E_{n'0}$,E_{n0},E_{m0}), transition moments associated with the ground state ($\mu_{0n'}$, μ_{0n}) and ones between excited states ($\mu_{n'm}$, μ_{nm}).

In order to more clarify the characteristics of the virtual excitation processes, we propose the three type approximation [15] as follows. For type (I), all terms are considered. For type (II), the most contributable process (0,*n*-*n*,0-0,*n*-*n*,0) illustrated by the type (II) equalized *n* to *n*' are considered. This process is refereed to as type (II)' . This approximation is identical to the diagonal approximation used for the second-order hyperpolarizability. Type

(III) is reduced to the process (0,*n*-*n*,*m*-*m*,*n*-*n*,0) by eliminating the terms with $n \neq n'$ from the process (0,*n*'-*n*',*m*-*m*,*n*-*n*,0). This is refereed to as type (III)'. Under three type approximation, the analytic formula for $\gamma_{iiii}(-3\omega;\omega,\omega,\omega)$ is expressed as

$$\gamma_{iiii}(-3\omega;\omega,\omega,\omega) =$$

$$\left.\sum_{n=1} (\mu^i_{n0})^2(\Delta\mu^i_{n0})^2 \frac{E_{n0}(E_{n0}^2+(\hbar\omega)^2)}{(E_{n0}^2-(3\hbar\omega)^2)(E_{n0}^2-(2\hbar\omega)^2)(E_{n0}^2-(\hbar\omega)^2)}\right\} \text{(I)}$$

$$\left. - \sum_{n=1} (\mu^i_{n0})^4 \frac{E_{n0}}{(E_{n0}^2-(3\hbar\omega)^2)(E_{n0}^2-(\hbar\omega)^2)}\right\} \text{(II)'}$$

$$\left. + \sum_{\substack{m,n=1 \\ m\neq n}} (\mu^i_{n0})^2(\mu^i_{mn})^2 \frac{E_{n0}^2E_{m0}+4E_{n0}(\hbar\omega)^2-3E_{n0}(\hbar\omega)^2}{(E_{n0}^2-(3\hbar\omega)^2)(E_{n0}^2-(\hbar\omega)^2)(E_{m0}^2-(2\hbar\omega)^2)}.\right\} \text{(III)'} \quad (9)$$

In the case of a static electric field, Eq. (9) is reduced to Eq.(11).

$$\gamma_{iiii}(-0;0,0,0) = \sum_{n=1} \frac{(\mu^i_{n0})^2(\Delta\mu^i_{n0})^2}{E_{n0}^3} - \sum_{n=1} \frac{(\mu^i_{n0})^4}{E_{n0}^3} + \sum_{\substack{m,n=1 \\ m\neq n}} \frac{(\mu^i_{n0})^2(\mu^i_{mn})^2}{E_{n0}^2E_{m0}}. \quad (10)$$

Here, the first, second and third terms correspond to the type (I), type (II)' and type (III)' contributions, respectively. From Eq.(10), the terms expressed by type (I) and type (III)' contributions are positive in sign, while the type (II)' contribution is a negative. Therefore, the overall sign of γ_{iiii} is determined by the detailed balance between the (I+III')- and (II')- terms. Particularly, for the centrosymmetric system, it is noted that the type (I) values come to be zero since $\Delta\mu_{n0}$ disappears because of the centrosymmetric charge distribution.

3. Schematic Diagrams of the Transition Matrix Elements [15-18,22]

The analysis method of the TDPT three type contributions is described. We schematically represent the characteristic of the transition matrix μ_{nm} which is one of the quantities related to the excited states much contributing to γ value. The transition moment μ_{nm} is defined by $-\langle\Psi_n|r|\Psi_m\rangle$, in which Ψ_n and Ψ_m are wavefunctions of state n and m, respectively. The direction and the tendency of the transition moment can be investigated by the schematic diagram in which the phases for $\Psi_n \times \Psi_m$ are drawn on each atomic site. For the molecule constructed of atoms A and B including one π orbital respectively, if the phase of $\Psi_n \times \Psi_m$ is plus on atom A and minus on atom B, it shows that the seeming polarization is induced in the molecule. The atom A has a minus charge and atom B has a plus one, so that, in an intact, the dipole moment directed from A to B is effected by the electronic excitation from the state n to m. In this case, the transition moment is directed from atom A (positive phase of $\Psi_n \times \Psi_m$) to atom B (negative phase of $\Psi_n \times \Psi_m$). In general, the transition moment is directed from the site with the plus phase of $\Psi_n \times \Psi_m$ to the site with minus phase. Differences between the excited and ground state dipole moments ($\Delta\mu_{n0}$) is illustrated by the way that the phase of $\Psi_n \times \Psi_n$ is drawn on each atomic site. In this representation, the plus phase of $\Psi_n \times \Psi_n$ indicates the increase of the charge, while the minus phase indicates the decrease of the charge. In this paper, the TDPT three type approximation is performed by the use of the CNDO/S (see Appendix 2) [23] molecular orbital (MO) method including the single-excitation configuration interaction (SCI). In the SCI procedure, the transition matrix and the dipole moment differences are expressed as follows.

$$\mu^{i}_{0n} = -e\sqrt{2}\sum_{ij} C_{n\,i\to j}\, m^{i}_{ij}, \tag{11}$$

$$\mu^{i}_{nm} = -e\sum_{ij}\sum_{kl} C_{n\,i\to j}\, C_{m\,k\to l}(\delta_{ik}\, m^{i}_{jl} - \delta_{jl}\, m^{i}_{jk}), \tag{12}$$

$$\mu^i_{nn} = -e \sum_{ij}{}' \sum_{kl}{}' C_{n\, i\to j}\, C_{n\, k\to l}(\, \delta_{ik}\, m^i_{jl} - \delta_{jl}\, m^i_{ik}) + \sum_{ij} |C_{n\, i\to j}|^2 (m^i_{jj} - m^i_{ii}) \,, \tag{13}$$

$$m^i_{ij} = \int \psi_i\, r^i\, \psi_j\, dv \,. \tag{14}$$

Here, $C_{n\, i\to j}$ is the CI coefficient of the one electron excited determinant exchanged between orbitals i and j. The symbol Σ' signifies the summation except the case satisfying both $i=k$ and $j=l$ at the same time. For the transition moment μ_{n0}, since the low-lying excited states are mainly constructed of one dominant one electron excited determinant $|\Psi_{i\to j}>$, the corresponding coefficient $|C_{n\, i\to j}|$ is approximated to 1. Therefore, the phases of (the sign of $C_{n\, i\to j}$) x ψ_i x ψ_j are used for illustrating the transition moment μ_{n0}. Other transition matrices are illustrated in a similar manner.

4. Characteristics of Each Order Polarizability

From the analytical expressions for each order of the polarizability and hyperpolarizabilities within the limits of wavelengths where the dispersion effects can be ignored, the following relations can be approximately obtained :

$$\alpha \propto \frac{|\mu_{n0}|^2}{E_{n0}}, \tag{15}$$

$$\beta \propto \frac{|\mu_{n0}|^2 \Delta\mu_{n0}}{E^2_{n0}}, \tag{16}$$

$$\gamma \propto \frac{|\mu_{n0}|^2 |\Delta\mu_{n0}|^2}{E^3_{n0}} - \frac{|\mu_{n0}|^4}{E^3_{n0}} + \frac{|\mu_{n0}|^2 |\mu_{mn}|^2}{E_{m0} E^2_{n0}}, \tag{17}$$

where the proportional coefficients are positive in sign. From Eq.(15), it is found that polarizability α is always positive in sign. The sign of the second-order hyperpolarizability β can be varied with the coordinate system since the $\Delta\mu_{n0}$ is included in Eq.(16). As can be seen from Eqs.(15) and (16), the magnitudes of α and β become large when $|\Delta\mu_{n0}|$and $|\mu_{n0}|$ are large and E_{n0} is small. For the third-order hyperpolarizability γ, the sign of type (II) contribution (the second term in Eq.(17)) is contrary to others. Therefore, the total $\gamma$is characterized by the three types of virtual excitation processes.

Appendix

1. Electronic-charge-centroid coordinate system [9]

In the electronic-charge-centroid coordinate system ($\boldsymbol{r}'$), the following relation is satisfied :

$$<0|\boldsymbol{r}'|0> = 0\,, \tag{A.1}$$

where $|0>$ denotes the ground state wavefunction. Here $\boldsymbol{r}'$ is represented as

$$\boldsymbol{r}' = \boldsymbol{r} + \boldsymbol{r}_0\,, \tag{A.2}$$

in which $\boldsymbol{r}_0$ signifies the displacement of some other system ($\boldsymbol{r}$) from the charge-centroid coordinate system. Using (A.2),

$$\begin{aligned} \mu_{00}' &= <0|-e\,\boldsymbol{r}'|0> = 0 = -e(<0|\boldsymbol{r}\,|0> + <0|\boldsymbol{r}_0\,|0>) \\ &= \mu_{00} + (-e\boldsymbol{r}_0), \end{aligned} \tag{A.3}$$

$$\begin{aligned} \mu_{nn}' &= <n|-e\,\boldsymbol{r}'|n> = <n|-e\boldsymbol{r}\,|n> - <n|-e\boldsymbol{r}_0\,|n> \\ &= \mu_{nn} + (-e\boldsymbol{r}_0) \\ &= \mu_{nn} + \mu_{00}) \equiv \Delta\mu_{n0}\,, \end{aligned} \tag{A.4}$$

$$\mu_{0n}' = <0|-e\,\boldsymbol{r}'|n> = <0|-e\boldsymbol{r}\,|n> - <0|-e\boldsymbol{r}_0\,|n> = \mu_{0n}\,. \tag{A.5}$$

Here, μ_{00}', μ_{nn}' and μ_{0n}' are ground state dipole moment, excited state dipole moment and transition moment in the charge-centroid coordinate system, respectively. Therefore, μ_{0n} in Eq. (3) signifies the change in dipole moment between the ground and excited states.

2. CNDO/S method [23]

Under the CNDO (complete neglect of differential overlap) approximation [24], the Fock matrix elements are expressed as follows.

$$F_{rr} = H_{rr} + \frac{1}{2}P_{rr}(rr|rr) + \sum_{t \neq r} P_{tt}(rr|tt), \tag{A.6}$$

$$F_{rs} = H_{rs} - \frac{1}{2}P_{rs}(rr|ss) \qquad (r \neq s), \tag{A.7}$$

where Hrs is the core integral and the bond order matrix element P_{rs} is expressed as

$$P_{rs} = 2\sum_{j}^{n} C_r^j C_s^j . \tag{A.8}$$

Here, C_r^i is the linear coefficient of the atomic orbital r in molecular orbital i. The total electronic energy is represented by

$$E_{elec} = \sum_{i=1}^{n} \varepsilon_i + \frac{1}{2}\sum_{r,s} P_{rs}H_{rs} , \tag{A.9}$$

where ε_i is the energy of the molecular orbital i.

Two electron integrals of atomic orbitals are approximated by

$$(rr|rr) = \gamma_{AA} = I_r - A_r , \tag{A.10}$$

$$(rr|ss) = \gamma_{AB} = \frac{14.395}{R_{rs} + \frac{28.79}{\gamma_{AA}+\gamma_{BB}}} \quad \text{(Mataga-Nishimoto equation)}, \tag{A.11}$$

where the atomic orbitals r and s belong to atoms A and B, respectively. The parameters I_r and A_r signify the ionization potential and electron affinity, respectively.

The diagonal and non-diagonal terms of core integrals are approximated by

$$H_{rr} = -\frac{1}{2}(I_r + A_r) - (Z_A - \frac{1}{2})\gamma_{AA} - \sum_{B(\neq A)} Z_B \gamma_{AB}, \quad \text{(A.12)}$$

$$H_{rs} = \frac{\kappa S_{rs}}{2}(\beta_A + \beta_B), \quad \text{(A.13)}$$

where Z_A denotes the effective nuclear charge of atom A ; S_{rs} is the element of the overlap integral matrix ; κ is a parameter which is defined as 1.0 for σ bonding and 0.585 for π bonding and β is a specific parameter given for exch atom. These parameters used for the CNDO/S method are listed in Table 1.

References

[1] M. Nakano, K. Yamaguchi and T. Fueno, ' *CNDO/S-CI Calculations of Hyperpolarizabilities I., II.* ' : in *Nonlinear Optics of Organics and Semiconductors*, edited by T. Kobayashi, Springer Proceedings in Physics **36** (1989) 98 ; 103.

[2] S. J. Lalama and A. F. Garito, Phys. Rev. **A20** (1979) 1179.

[3] C. C. Teng and A. F. Garito, Phys. Rev. Lett. **50** (1983) 350.

[4] C. C. Teng and A. F. Garito, Phys. Rev. **B28** (1983) 6766.

[5] J. A. Morrell, A. C. Albrecht, K. H. Levine and C. L. Tang, J. Chem. Phys. **71** (1979) 5063.

[6] J. A. Morrell and A. C. Albrecht, Chem. Phys. Lett. **64** (1979) 46.

[7] J. Zyss, J. Chem. Phys. **70** (1979) 3333, 3341 ; **71** (1979) 909.

[8] J. Zyss and G. Berthier, J. Chem. Phys. **77** (1982) 3635.

[9] V. J. Docherty, D. Pugh and J. O. Morley, J. Chem. Soc. Faraday Trans. II. **81** (1985) 1179.

[10] D. N. Beratan, J. N. Onuchic and J. W. Perry, J. Phys. Chem. **91** (1987) 2696.

[11] D. Li, M. A. Ratner and T. J. Marks, J. Am. Chem. Soc. **110** (1988) 1707.

[12] W. Dirk, R. J. Twieg and G. Wagniere, J. Am. Chem. Soc. **108** (1986) 5387.

[13] D. M. Bishop and B. Lam, J. Chem. Phys. **89** (1988) 1571 ; **91** (1989) 3549.

[14] G. H. Wagniere and J. B. Hutter, J. Opt. Soc. Am. **B6** (1989) 693.

[15] M. Nakano, M. Okumura, K. Yamaguchi and T. Fueno, Mol. Cryst. Liq. Cryst **182A** (1990) 1.

[16] A. F. Garito and J. R. Heflin, K. Y. Wong and O. Zamani-Khamiri, in : *Organic Materials for Nonlinear Optics*, edited by R. A. Hann and D. Bloor, Special Publication No. **69** (Royal Society of Chemistry, London, 1988).

[17] J. R. Heflin, K. Y. Wong, O. Zamani-Khamiri and A. F. Garito, Phys. Rev. **B38** (1988) 1573.

[18] A. F. Garito, J. R. Heflin, K. Y. Wong and O. Zamani-Khamiri, in *Nonlinear Optical Properties of Polymers*, edited by A. J. Heeger, J. Orenstein and D. R. Ulrich (Material Research Society, Pittsburgh, 1988), MRS Symp. Proc. No.109 , 91.

[19] D. J. Williams, Angew. Chem. Int. Ed. **23** (1984) 690.

[20] B. M. Pierce, in *Nonlinear Optical Properties of Polymers*, edited by A. J. Heeger, J. Orenstein and D. R. Ulrich (Material Research Society, Pittsburgh, 1988), MRS Symp. Proc. No.109 , 109.

[21] B. M. Pierce, J. Chem. Phys. **91** (1989) 791.

[22] J. W. Wu, J. R. Heflin, R. A. Norwood, K. Y. Wong, O. Zamani-Khamiri and A. F. Garito J. Opt. Soc. Am. **B6** (1989) 707.

[23] J. Del Bene and H. H. Jaffe, J. Chem. Phys. **48** (1968) 1807.

[24] J. A. Pople and D. L. Beveridge, *Approximate Molecular Orbital Theory* (McGraw-Hill, New York, 1970).

Table 1. Parameters for atoms H, C, N, O and F used for CNDO/S method.

	H	C	N	O	F
$I_s + A_s$	14.35	29.92	40.97	54.51	56.96
$I_p + A_p$	0.0	11.61	16.96	21.93	24.36
γ_{AA}	12.85	10.93	11.88	15.13	17.36
β	-12.0	-17.5	-26.0	-45.0	-50.0

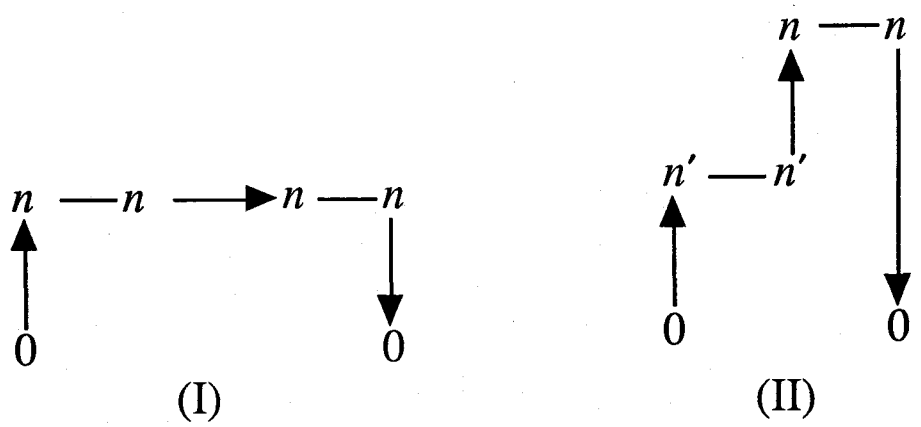

(a) Virtual excitation process

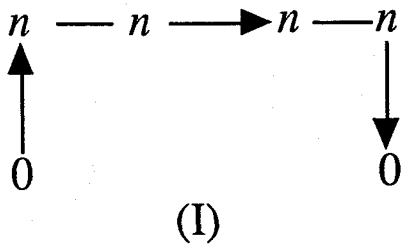

(b) Diagonal approximation

Fig.1. Virtual excitation process involving in the analytical formula of β and its diagonal approximation.

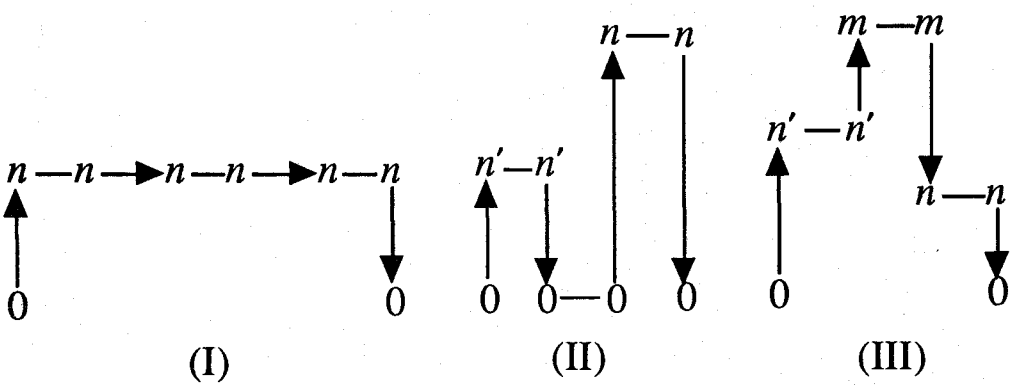

(a) Three types of contributing terms to γ

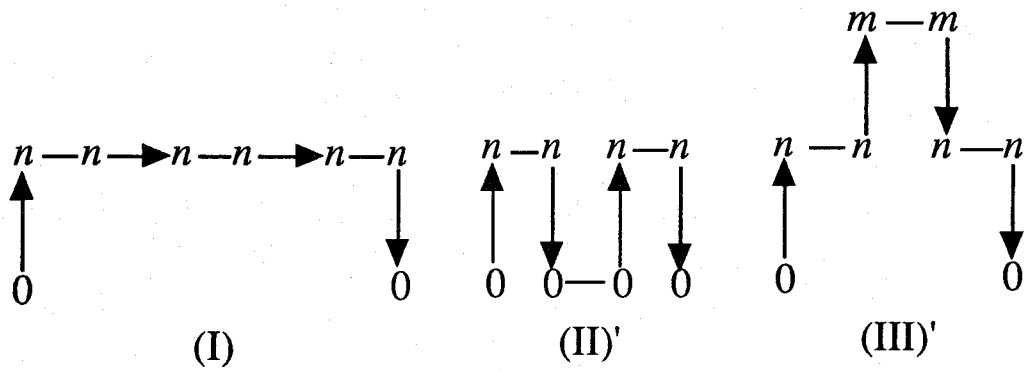

(b) Approximation of terms illustrated by types (II) and (III) contributions in Fig.1.

Fig.2. Virtual excitation process in analytical formula of γ and three type approximation.

PART II

CALCULATION METHODS OF HYPERPOLARIZABILITY BY THE RAYLEIGH-SCHRÖDINGER PERTURBATION THEORY (RSPT), COUPLED-HARTREE-FOCK (CHF) AND COUPLED-CLUSTER (CC) THEORY

Introduction

For the methods based on the time-dependent perturbation theory (TDPT) mentioned in part I, the analysis of the virtual excitation process can be performed and the dispersion effects are able to be considered. However, the TDPT approach entails calculations of several quantities relating to excited states. In general, it is very difficult to obtain the quantities relating to excited states precisely. Therefore, in this part, the variational and perturbational methods dealing with only the ground state are applied to the calculation of the hyperpolarizability. The total energy in the presence of the external field can be expanded as the power series of the field $\boldsymbol{F}$. The first-order coefficient of the field $\boldsymbol{F}$ represents the dipole moment μ, and the second-, third- and fourth-order coefficients are α, β and γ, respectively.

In chapter 1, the calculation method of hyperpolarizability based on the coupled-Hartree-Fock (CHF) theory is described. The total energy in the presence of the field calculated variationally is differentiated with respect to the field. This procedure is referred to as the finite-field (FF) method. For the semiempirical (INDO) molecular orbital (MO) method, the CHF method is explained. In order to examine the contributions of the electron correlation effects, Møller-Plesset (MP) perturbation theory is applied. Moreover, the γ density analysis method is proposed for analyzing the spatial contributions of γ.

In chapter 2, the double perturbation theory based on the Rayleigh-Schrödinger perturbation theory (RSPT) is adopted for the analysis of the inclusion of the correlation effects. The analytical expressions of the hyperpolarizabilities without correlation effects (RSPT0 approximation) are obtained. Moreover, the coupled-cluster (CC) theory which can include higher-order correlation effects systematically is employed to obtain the general equations for the nth-order response properties with respect to an external field.

Chapter 1

Calculation methods of the Hyperpolarizability by the Coupled-Hartree-Fock (CHF) and CHF with the Møller-Plesset (MP) Perturbation Theory

1. Coupled-Hartree-Fock (CHF) Theory [1-9]

The total Hamiltonian in the presence of a uniform electric field $\boldsymbol{F}$ is expressed as

$$H = H_0 + \sum_i \boldsymbol{F}\cdot\boldsymbol{r}_i - \sum_I Z_I \boldsymbol{F}\cdot\boldsymbol{R}_I \quad , \tag{1}$$

where indices i and I signify electrons and nuclei, respectively. Z_I is the atomic number of the Ith nucleus and H_0 is the field-free Hamiltonian. The total energy can be obtained as the expectation values for the wavefunctions Ψ in the presence of the field.

$$E = \langle \Psi | H | \Psi \rangle . \tag{2}$$

Similarly, the dipole moment is expressed as

$$\mu = \langle \Psi | \sum_I Z_I \boldsymbol{R}_I - \sum_i \boldsymbol{r}_i | \Psi \rangle . \tag{3}$$

In the coupled-Hartree-Fock (CHF) method, Ψ is approximated by a single Slater determinant whose orbitals are reoptimized for each field $\boldsymbol{F}$. Differentiation of Eq.(2) with respect to $\boldsymbol{F}$ gives

$$\frac{\partial E}{\partial F^i} = <\frac{\partial \Psi}{\partial F^i}|H|\Psi> + <\Psi|\frac{\partial H}{\partial F^i}|\Psi> + <\Psi|H|\frac{\partial \Psi}{\partial F^i}> . \qquad (4)$$

If Ψ is the true wavefunction, the first and third terms on the right-hand side of Eq.(4) is equal to zero by the Hellmann-Feynman theorem [10]. The CHF method satisfy the theorem. If the Hellmann-Feynman theorem is satisfied, the dipole moment defined by Eq.(3) can be expressed as

$$\mu^i = -\frac{\partial E}{\partial F^i} . \qquad (5)$$

In general, the total energy and dipole moment can be expanded as the power series of the applied field.

$$E = E_0 - \sum_i \mu_0^i F^i - \frac{1}{2}\sum_{ij} \alpha_{ij} F^i F^j - \frac{1}{3}\sum_{ijk} \beta_{ijk} F^i F^j F^k - \frac{1}{4}\sum_{ijkl} \gamma_{ijkl} F^i F^j F^k F^l - \cdots , \qquad (6)$$

$$\mu^i = \mu_0^i + \sum_j \alpha_{ij} F^j + \sum_{jk} \beta_{ijk} F^j F^k + \sum_{jkl} \gamma_{ijkl} F^j F^k F^l + \cdots , \qquad (7)$$

where μ_0 is the permanent dipole moment. The Hellmann-Feynman theorem asserts that Eqs.(6) and (7) are compatible. For the Møller-Plesset (MP) theory [11] or limited excitation configuration interaction (CI), the Hellmann-Feynman theorem is not satisfied. Practically, however, there is little computational differences between the hyperpolarizabilities in these two expansions [12].

The γ values are evaluated by the numerical differentiation of the self-consistent-field (SCF) energy of molecules in the presence of an electric field as a function of field. This method

based on the finite-field (FF) treatment [13-15] (see Appendix 1) is here referred to as the CHF method. In contrast, the coupled-perturbed-Hartree-Fock (CPHF) method [16-24], which is an analytical differentiation method, requires no calculations of the ground states in the presence of the field. Indeed, the γ_{ijkl} value by the CHF method are liable to involve some numerical errors. However, when precise calculation of the total energy and appropriate numerical differentiation are carried out under careful selection of field strength, the numerical errors between the CHF and CPHF can be minimized [6]. One advantage of the CHF method is that it can be applied to almost any quantum chemical formalism, for example, MP theory, in which the analytical method is not available at the present time. The CHF method based on the INDO approximation [25] is explained in Appendix 2.

2. Møller-Plesset (MP) Perturbation Theory [11]

When the zeroth-order Hamiltonian is chosen as the Fock operator in the Rayleigh-Schrödinger perturbation theory (RSPT), the electron correlation (the error of the Hartree-Fock approach) can be included by the perturbation calculation. This is referred to as the Møller-Plesset (MP) perturbation theory. If the system can be well described by a single determinant, the MP theory suitable for the evaluation of the electron correlation effects.

In most cases, the second-order MP contribution for the correlation energy is larger than others. The second-order MP (MP2) formula for the correlation energy in terms of spinorbitals is expressed as

$$E^{(2)}=\left(\frac{1}{2}\right)^2\sum_{abrs}\frac{<ab||rs><rs||ab>}{\varepsilon_a+\varepsilon_b-\varepsilon_r-\varepsilon_s}. \qquad (8)$$

where $a, b, c,$ and $r, s, t,$ label the occupied and virtual spin orbitals, respectively ; ε_i signifies the energy of orbital i. The antisymmetrized two electron integral is defined by

$$\langle ij||kl\rangle \equiv \langle ij|kl\rangle - \langle ij|lk\rangle. \tag{9}$$

In the case of the MP theory based on the unrestricted Hartree-Fock (UHF) reference state (unrestricted MP (UMP)), Eq.(8) is rewritten in terms of the spatial orbitals by

$$\begin{aligned} E^{(2)} = & \frac{1}{2}\sum_{abrs}\frac{(ar|bs)(ra|sb)}{\varepsilon_a+\varepsilon_b-\varepsilon_r-\varepsilon_s} + \frac{1}{2}\sum_{\bar{a}\bar{b}\bar{r}\bar{s}}\frac{(\bar{a}\bar{r}|\bar{b}\bar{s})(\bar{r}\bar{a}|\bar{s}\bar{b})}{\varepsilon_{\bar{a}}+\varepsilon_{\bar{b}}-\varepsilon_{\bar{r}}-\varepsilon_{\bar{s}}} \\ & + \frac{1}{2}\sum_{\bar{a}b\bar{r}s}\frac{(\bar{a}\bar{r}|bs)(\bar{r}\bar{a}|sb)}{\varepsilon_{\bar{a}}+\varepsilon_b-\varepsilon_{\bar{r}}-\varepsilon_s} + \frac{1}{2}\sum_{abrs}\frac{(ar|\bar{b}\bar{s})(\bar{r}\bar{a}|s\bar{b})}{\varepsilon_{\bar{a}}+\varepsilon_{\bar{b}}-\varepsilon_{\bar{r}}-\varepsilon_{\bar{s}}} \\ & - \frac{1}{2}\sum_{abrs}\frac{(ar|bs)(rb|sa)}{\varepsilon_a+\varepsilon_b-\varepsilon_r-\varepsilon_s} - \frac{1}{2}\sum_{abrs}\frac{(\bar{a}\bar{r}|\bar{b}\bar{s})(\bar{r}\bar{b}|\bar{s}\bar{a})}{\varepsilon_{\bar{a}}+\varepsilon_{\bar{b}}-\varepsilon_{\bar{r}}-\varepsilon_{\bar{s}}}. \end{aligned} \tag{10}$$

Here, i and $\bar{i}$ signify the spatial orbitals of α and β spins, respectively. In the case of the restricted MP (RMP) theory, Eq.(10) is reduced to the expression :

$$E^{(2)} = \sum_{abrs}^{N/2}\frac{(ar|bs)(2(ra|sb)-(rb|sa))}{\varepsilon_a+\varepsilon_b-\varepsilon_r-\varepsilon_s}. \tag{11}$$

In order to evaluate the hyperpolarizability, the CHF (instead of the HF) orbitals and orbital energies are used in Eqs.(10) and (11). In this case, the effects of the external field can be included variationally by the CHF calculation at first and then the electron correlation effects can be included based on the MP theory.

3. γ density Analysis in the Variational Approach

The analysis of the virtual excitation processes is impossible in the variational approach since the variational approach only deals with the ground state directly. Therefore, the derivatives of charge densities with respect to the applied field are employed in order to interpret the spatial characteristics of the γ value. The charge density function $\rho(\boldsymbol{r},\boldsymbol{F})$ can be expanded in powers of the field $\boldsymbol{F}$ in the same as the expansions of energy and dipole moment in Eqs.(6) and (7) [6]. To simplify the notation, the field is fixed in the direction i. The charge density function $\rho(\boldsymbol{r},\boldsymbol{F})$ are expressed as

$$\rho(\boldsymbol{r},\boldsymbol{F}) = \rho^{(0)}(\boldsymbol{r}) + \sum_i \rho^{(1)}(\boldsymbol{r})F^i + \frac{1}{2!}\sum_i \rho^{(2)}(\boldsymbol{r})F^iF^j + \frac{1}{3!}\sum_i \rho^{(3)}(\boldsymbol{r})F^iF^jF^k + \cdots . \tag{12}$$

Using Eq.(12), the dipole moment expansion can be represented as follows.

$$\begin{aligned}\mu^i(\boldsymbol{F}) &\equiv -\int q^i \rho(\boldsymbol{r},\boldsymbol{F})d\boldsymbol{r}^3 \\ &= -\int q^i \rho^{(0)}(\boldsymbol{r})d\boldsymbol{r}^3 - \sum_i \int q^i \rho^{(1)}(\boldsymbol{r})d\boldsymbol{r}^3 F^i - \frac{1}{2!}\sum_i \int q^i \rho^{(2)}(\boldsymbol{r})d\boldsymbol{r}^3 F^iF^i \\ &\quad - \frac{1}{3!}\sum_i \int q^i \rho^{(3)}(\boldsymbol{r})d\boldsymbol{r}^3 F^iF^iF^i - \cdots .\end{aligned} \tag{13}$$

Here, the q^i is the i component of the molecular coordinate.

From Eqs.(1) and (13),

$$\gamma_{iiii} = -\frac{1}{3!}\int q^i \rho^{(3)}(\boldsymbol{r})d\boldsymbol{r}^3 . \tag{14}$$

The charge density $(\boldsymbol{PS})_{ss}$ divided into each atomic orbital s is considered according to the Mulliken population analysis.

$$\rho(\boldsymbol{r}) = \sum_{st} (\boldsymbol{P})_{st} \phi_s(\boldsymbol{r}) \phi_t(\boldsymbol{r}), \tag{15}$$

where ϕ_s denotes the atomic orbital s. From Eq.(15),

$$\int \rho(\boldsymbol{r}) d\boldsymbol{r}^3 = \sum_{s} (\boldsymbol{PS})_{ss} = \sum_{s} \int \rho_s(\boldsymbol{r}) d\boldsymbol{r}^3. \tag{16}$$

Here, the $\boldsymbol{S}_{st}$ is the overlap matrix element and the $\boldsymbol{P}_{st}$ is the bond order matrix element. Equation (12) can be rewritten as follows by the use of the charge density function $\rho_s(\boldsymbol{r})$ divided into each atomic orbital s.

$$\rho(\boldsymbol{r},\boldsymbol{F}) = \sum_{s} \left\{ \rho^{(0)}(\boldsymbol{r}) + \sum_{i} \rho_s^{(1)}(\boldsymbol{r}) \boldsymbol{F}^i + \frac{1}{2!} \sum_{i} \rho_s^{(2)}(\boldsymbol{r}) \boldsymbol{F}^i \boldsymbol{F}^j + \frac{1}{3!} \sum_{i} \rho_s^{(3)}(\boldsymbol{r}) \boldsymbol{F}^i \boldsymbol{F}^j \boldsymbol{F}^k + \ldots \right\} . \tag{17}$$

Therefore,

$$\begin{aligned} \int \rho(\boldsymbol{r},\boldsymbol{F}) d\boldsymbol{r}^3 = & \\ & \sum_{s} \int \rho_s^{(0)}(\boldsymbol{r}) d\boldsymbol{r}^3 + \sum_{s} \sum_{i} \int \rho_s^{(1)}(\boldsymbol{r}) d\boldsymbol{r}^3 \boldsymbol{F}^i + \frac{1}{2!} \sum_{s} \sum_{i} \int \rho_s^{(2)}(\boldsymbol{r}) d\boldsymbol{r}^3 \boldsymbol{F}^i \boldsymbol{F}^i \\ & + \frac{1}{3!} \sum_{s} \sum_{i} \int \rho_S^{(3)}(\boldsymbol{r}) d\boldsymbol{r}^3 \boldsymbol{F}^i \boldsymbol{F}^i \boldsymbol{F}^i + \ldots . \end{aligned} \tag{18}$$

The following approximation is attempted to the charge density function $\rho_s(\boldsymbol{r})$.

$$\rho_s(r) = (PS)_{ss}\delta(r - r_s). \tag{19}$$

This approximation implies that the $\rho_s(r)$ is concentrated to the center r_s of the atomic orbital s. At this time, the following relation is hold.

$$\int \rho_s^{(i)}(r)dr^3 = (PS)_{ss}^{(i)} = \left(\int \rho_s(r)dr^3\right)^{(i)}. \tag{20}$$

By the use of this relation, Eq.(13) can be rewritten as follows.

$$\mu^i(F) \approx -\sum_s \{q_s^i(PS)_{ss}^{(0)} + \sum_i q_s^i(PS)_{ss}^{(1)}F^i + \frac{1}{2!}\sum_i q_s^i(PS)_{ss}^{(2)}F^iF^i + \frac{1}{3!}\sum_i q_s^i(PS)_{ss}^{(3)}F^iF^iF^i + \dots\}. \tag{21}$$

From this equation, we obtain

$$\gamma_{iiii} \approx -\frac{1}{3!}\sum_s (PS)_{ss}^{(3)} q_s^i. \tag{22}$$

where the q_s^i represent the i component of the coordinate of the atom located at the center of the atomic orbital s. We call the third derivative of $(PS)_{ss}$ the γ density. The spatial characteristics of the γ value can be obtained by the use of the plots of the magnitudes and signs of the γ densities on each atom. It is also possible to separate the density derivatives into the different contributions, for example, the σ and π contributions. The plus sign of the γ density implies that the second derivative of the charge density increases with the increase in

the field, while the minus sign implies the inverse effect. Plots of the γ density give the information about the magnitude and sign of the total γ shown in Fig.1. The third-derivative of the $(\boldsymbol{PS})_{ss}$, namely the γ_{iiii} density of atomic orbital s, is calculated by the four-point numerical derivative method as follows.

$$(\boldsymbol{PS})_{ss}^{(3)} = \frac{1}{2\boldsymbol{F}^3}\{(\boldsymbol{PS})_{ss}(2\boldsymbol{F}^i) - (\boldsymbol{PS})_{ss}(-2\boldsymbol{F}^i) + 2[(\boldsymbol{PS})_{ss}(-\boldsymbol{F}^i) - (\boldsymbol{PS})_{ss}(\boldsymbol{F}^i)]\} . \quad (23)$$

Here, the $(\boldsymbol{PS})_{ss}(\boldsymbol{F}^i)$ is the Mulliken charge density of the atomic orbital s in the presence of the field $\boldsymbol{F}^i$.

Appendix

1. Finite-field (FF) Method [13-15]

The fourth-order derivative of the total energy E with respect to the field is calculated by the following equations.

$$\gamma_{iiii} = -\frac{1}{6F^{i4}}\{56E(0)-39[E(F^i)+E(-F^i)]+12[E(2F^i)+E(-2F^i)] -[E(3F^i)+E(-3F^i)]\}, \quad (A.1)$$

$$\begin{aligned}\gamma_{iijj} = -\frac{1}{12F^{i2}F^{j2}}\{&-72E(0)-38[E(F^i)+E(-F^i)+E(F^j)+(-F^j)] \\ &+2[E(2F^i)+E(-2F^i)+E(2F^j)+E(-2F^j)] \\ &+20[E(F^i,F^j)+E(F^i,-F^j)+E(-F^i,F^j)+E(-F^i,-F^j)] \\ &-[E(2F^i,F^j)+E(2F^i,-F^j)+E(-2F^i,F^j)+E(-2F^i,-F^j) \\ &+E(F^i,2F^j)+E(F^i,-2F^j)+E(-F^i,2F^j)+E(-F^i,-2F^j)]\}. \quad (A.2)\end{aligned}$$

2. INDO CHF Method

2.1. INDO (intermediate neglect of differential overlap) Approximation [25]

Under the INDO approximation, the expressions for the unrestricted Fock matrix elements are

$$\begin{aligned}F^{\alpha}_{\mu\mu} = U_{\mu\mu} &+ \sum_{\lambda\in A}[P_{\lambda\lambda}(\mu\mu|\lambda\lambda) - P^{\alpha}_{\lambda\lambda}(\mu\lambda|\mu\lambda)] \\ &+ \sum_{B(\neq A)}(P_{BB} - Z_B)\gamma_{AB} \qquad \mu \text{ on atom } A, \quad (A.3)\end{aligned}$$

$$F^{\alpha}_{\mu\nu} = (2P_{\mu\nu} - P^{\alpha}_{\mu\nu})(\mu\nu|\mu\nu) - P^{\alpha}_{\mu\nu}(\mu\mu|\nu\nu). \tag{A.4}$$

Assuming $2s$ and $2p$ orbitals to have the same radial parts, the nonvanishing two-electron integrals are

$$(ss|ss) = (ss|xx) = F^0 = \gamma_{AA}, \tag{A.5}$$

$$(sx|sx) = \tfrac{1}{3}G^1, \tag{A.6}$$

$$(xy|xy) = \tfrac{3}{25}F^2, \tag{A.7}$$

$$(xx|xx) = F^0 + \tfrac{4}{25}F^2, \tag{A.8}$$

$$(xx|yy) = F^0 - \tfrac{2}{25}F^2, \tag{A.9}$$

and similar expressions for $(ss|zz)$, etc. The integral F^0 is calculated theoretically from Slater atomic orbitals. The values G^1 and F^2 are determined semiempirically. The values are listed in Table 1. The core integrals $U_{\mu\mu}$ are determined by the following relations :

Hydrogen :

$$-\tfrac{1}{2}(I+A)_s = U_{ss} + \tfrac{1}{2}\gamma_{HH}, \tag{A.10}$$

Boron to fluorine :

$$-\tfrac{1}{2}(I+A)_s = U_{ss} + (Z_A - \tfrac{1}{2})F^0 - \tfrac{1}{6}(Z_A - \tfrac{3}{2})G^1, \tag{A.11}$$

$$-\tfrac{1}{2}(I+A)_p = U_{pp} + (Z_A - \tfrac{1}{2})F^0 - \tfrac{1}{3}G^1 - \tfrac{2}{25}(Z_A - \tfrac{5}{2})F^2, \tag{A.12}$$

where Z_A is the core charge of atom A, and I and A denote the ionization potential and the electron affinity, respectively. Values for $(I+A)_s$ and $(I+A)_p$ are listed in Table 2.

2.2. CHF Method Based on the INDO Approximation [2]

The expression for the Fock matrix element of α spin in the presence of the electric field $\boldsymbol{F}$ is

$$F_{\mu\nu}^{\alpha} = H_{\mu\nu}^{core} + \boldsymbol{F}(\phi_\mu|\boldsymbol{r}_1|\phi_\nu) + \sum_{a}^{N^\alpha} [(\phi_\mu\phi_\nu|\Psi_a^\alpha\Psi_a^\alpha)-(\phi_\mu\Psi_a^\alpha|\Psi_a^\alpha\phi_\nu)] + \sum_{a}^{N^\beta} (\phi_\mu\phi_\nu|\Psi_a^\beta\Psi_a^\beta) . \quad \text{(A.13)}$$

Here, ϕ_μ denotes the μth atomic orbital and Ψ_a is the ath molecular orbital. The matrix elements $(\phi_\mu|\boldsymbol{r}_1|\phi_\nu)$ are expressed as

$$(\phi_{A\mu}|\boldsymbol{r}_1|\phi_{A\mu}) = \boldsymbol{R}_A + (\phi_{A\mu}|\boldsymbol{r}_A|\phi_{A\mu}) = \boldsymbol{R}_A , \quad \text{(A.14)}$$

$$(\phi_{A\mu}|\boldsymbol{r}_1|\phi_{A\nu}) = (\phi_{A\mu}|\boldsymbol{r}_A|\phi_{A\nu}) , \quad \text{(A.15)}$$

$$(\phi_{A\mu}|\boldsymbol{r}_1|\phi_{B\nu}) \approx \frac{1}{2}(\phi_{A\mu}|\phi_{B\nu})(\boldsymbol{R}_A+\boldsymbol{R}_B) \approx 0 , \quad \text{(A.16)}$$

where $\boldsymbol{r}_A$, $\boldsymbol{r}_1$ and $\boldsymbol{R}_A$ are shown in Fig.2. Here, $(\phi_{A\mu}|\boldsymbol{r}_A|\phi_{A\nu})$ are calculated by

$$(\phi_{2s}|z|\phi_{2p_z}) = (\phi_{2s}|x|\phi_{2p_x}) = (\phi_{2s}|y|\phi_{2p_y}) = \frac{5}{\sqrt{3}z^*} \times 0.529177 \text{ Å} , \quad \text{(A.17)}$$

$$(\phi_{2p_x}|\boldsymbol{r}_A|\phi_{2p_y}) = (\phi_{2p_y}|\boldsymbol{r}_A|\phi_{2p_z}) = (\phi_{2p_z}|\boldsymbol{r}_A|\phi_{2p_x}) = 0 , \quad \text{(A.18)}$$

in which z^* signifies the effective nuclear charge.

By solving the usual Hartree-Fock equation using the perturbed Fock matrix elements (A.13), the CHF orbitals and orbital energies can be obtained.

References

[1] M. Peng, Proc. R. Soc. Lond. **A178** (1941) 449.

[2] J. Zyss, J. Chem. Phys. **70** (1979) 3333.

[3] M. G. Papadopoulos, J. Waite and C. A. Nicolaides, J. Chem. Phys. **77** (1982) 2527.

[4] J. Waite and M. G. Papadopoulos, J. Chem. Phys. **82** (1985) 1427.

[5] C. P. deMelo and R. Silbey, Chem. Phys. Lett. **140** (1987) 537.

[6] P. Chopra, L. Carlacci, H. F. King and P. N. Prasad, J. Phys. Chem. **93** (1989) 7120.

[7] E. Perrin, P. N. Prasad, P. Mougenot and M. Dupuis, J. Chem. Phys. **91** (1989) 4728 .

[8] R. J. Bartlett and G. D. Purvis III, Phys. Rev. **A20** (1979) 1313.

[9] B. Kirtman and M. Hasan, Chem. Phys. Lett. **157** (1989) 123.

[10] R. Feynman, Phys. Rev. **56** (1939) 340. ; S. T. Epatein, Am. J. Phys. **22** (1954) 613. ; R. E. Stanton, J. Chem. Phys. **36** (1962) 1298.

[11] C. Møller and M. S. Plesset, Phys. Rev. **46** (1934) 618.

[12] P. O. Nerbrant, B. O. Roos and A. J. Sadleji, Int. J. Quantum Chem. **15** (1979) 135.

[13] H. D. Cohen and C. C. J. Roothaan, J. Chem. Phys. S34 (1965) 43.

[14] N. S. Hush and M. L. Williams, Chem. Phys. Lett. **5** (1970) 507.

[15] J. E. Gready and G. B. Bacskay and N. S. Hush, Chem. Phys. **22** (1977) 141.

[16] P. Jørgensen and J. Simons, Eds., *Geometrical Derivatives of Energy Surfaces and Molecular Properties* (Reidel, Dordrecht, 1986).

[17] J. Gerrat and I. M. Mills, J. Chem. Phys. **49** (1968) 1719, 1730.

[18] P. Pulay, Mol. Phys. **17** (1969) 197.

[19] J. A. Pople, R. Krishnan, H. B. Schlegel and J. S. Binkley, Int. J. Quantum Chem. Symp. **13** (1979) 225.

[20] G. Diercksen and R. J. McWeeny, J. Chem. Phys. **44** (1966) 3554.

[21] A. Komornicki, K. Ishida, K. Morokuma, R. Ditchfield and M. Conrad, Chem. Phys. Lett. **45** (1977) 595.

[22] J. L. Dodds, R. McWeeny, W. Raynes and J. P. Rieley, Mol. Phys. **33** (1977) 611.

[23] B. R. Brooks, W. D. Laidig, P. Saxw, N. C. Handy and H. F. Schaefer, Phys. Scr. **21** (1980) 312.

[24] G. J. B. Hurst, M. Dupuis and E. Clementi, J. Chem. Phys. **89** (1988) 385.

[25] J. A. Pople and D. L. Beveridge, *Approximate Molecular Orbital Theory* (McGraw-Hill, New York, 1970)

Table 1. Empirical values for G^1 and F^2.

Atom	G^1	F^2
C	0.267708	0.17372
N	0.346029	0.219055
O	0.43423	0.266415
F	0.532305	0.31580

Table 2. Values for $(I+A)_s/2$ and $(I+A)_p/2$ [eV].

	H	C	N	O	F
$(I+A)_s/2$	7.176	14.051	19.316	25.390	32.272
$(I+A)_p/2$		5.572	7.275	9.111	11.080

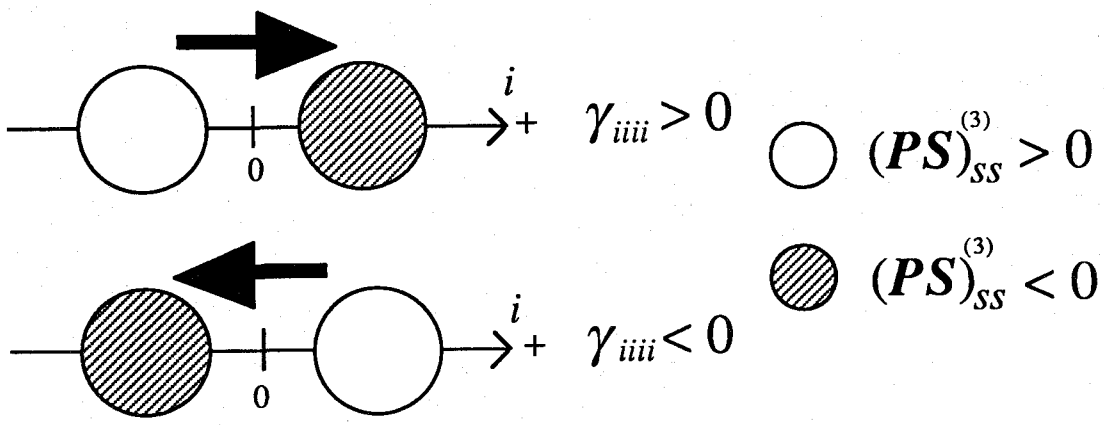

Fig.1. γdensity analysis. $(PS)^{(3)}_{ss}$ is the γ density.

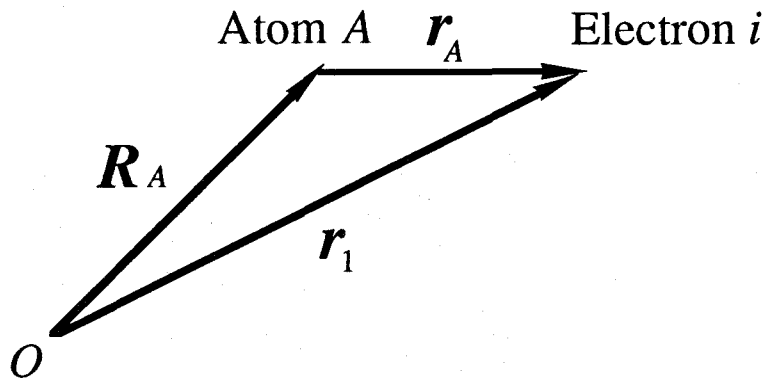

Fig.2. Coordinates of atom A and electron i

Chapter 2

General equations for the *n*th-order response to an external one-electron perturbation. Many-body perturbation and coupled-cluster treatments

General equations for the *n*th-order response properties with respect to an external time-independent one-electron perturbation are derived on the basis of the many-body perturbation theory (MBPT) and the coupled-cluster (CC) theory. The corresponding equations for the time-dependent case are also derived by the CC formalism, which is referred to as the time-dependent CC (TDCC) method. The theoretical expressions developed will be useful for analytical calculations of the response properties of any order , e.g., polarizability and hyperpolarizability.

1. Introduction

Wavefunctions which are adequate for calculations of the total electronic energies are known to be often inadequate for reasonable evaluations of physical properties [1]. Response properties to external perturbation are particularly cumbersome to calculate inasmuch as they involve quantities relating to the transition energies. Generally, the energy differences between states obtained by subtracting two expectation values calculated separately no longer have the upper bound property. Development of reliable methods for non-variational direct calculations of the response properties are thus a momentous matter of urgency. Methods of direct calculations of the response properties are placed in two categories, numerical and analytical. In the numerical methods, the response properties of a given order are determined by fitting the computed total electronic energies of the perturbed system to a power series of external field. The finite-field (FF) method [2-5] belongs to this category. However, the numerical procedures are liable to encounter some inherent difficulties. For example, choices of the basis sets describing polarization properly in the presence of the field and calculations of the total energies reliably for the varying field strength are difficult to achieve. In the analytical methods, on the other hand, responses to the external perturbation at various orders can be calculated on a unified ground. Derivations and comparisons of general equations which provide analytical expressions for the response properties most effectively are the purpose of the present work.

We first consider time-independent response properties with respect to an external one-electron perturbation in a general manner. Two non-variational approaches are examined. One is the Rayleigh-Schrödinger-type double perturbation theory (RSPT) (= many body perturbation theory (MBPT)) [1,2,6-8], which chooses the Hartree-Fock (HF) Hamiltonian as the unperturbed Hamiltonian, and regards both electron correlations and the external one-electron disorder as perturbation. The other is based on the coupled-cluster (CC) theory [9-14], which

can include higher electron correlations effectively. Finally, the dynamic responses to an external time-dependent one-electron perturbation will be dealt with in the formalism of the coupled-cluster(CC) theory [15,16].

2. Static Response Properties by the Time-independent Double Perturbation Theory

An external time-independent one-electron perturbation, e.g., electric field, is expressed as αH_1. The total electronic energy in the presence of the external perturbation can be expanded as the power series of α.

$$E_0(\alpha) = E_0(0) - \alpha E_1 - \frac{1}{2!}\alpha^2 E_2 - \frac{1}{3!}\alpha^3 E_3 - \frac{1}{4!}\alpha^4 E_4 \cdots . \tag{1}$$

If the unperturbed term is the HF Hamiltonian and if the perturbed terms are the potential V which represents the electron correlation effects and an external one-electron perturbation αH_1, the total Hamiltonian H is expressed as follows:

$$H = H_{HF} + \mu V + \lambda(\alpha H_1) . \tag{2}$$

where μ and λ signify the order parameters. The correlation potential V is expressed as

$$V = \sum_{i<j} r_{ij}^{-1} - \sum_i v^{HF}(i) . \tag{3}$$

Here, the first and second terms of the right-hand side of Eq.(3) represent the Coulomb repulsion and the HF potential, respectively.

Our objective here is to derive static response properties by the time-independent double perturbation theory [17,18]. The perturbed time-independent Schrödinger equation is written as

$$H\,|\Phi_0\rangle = E_0\,|\Phi_0\rangle\,, \tag{4}$$

where $|\Phi_0\rangle$ and E_0 represent the eigenvector and eigenvalue of the ground state, respectively. On the other hand, the unperturbed eigenvector $|\Psi_0(0,0)\rangle$ of the HF ground state and its eigenvalue $E_0(0,0)$ satisfy the following Schrödinger equation.

$$H_{\mathrm{HF}}\,|\Psi_0(0,0)\rangle = E_0(0,0)|\Psi_0(0,0)\rangle\,. \tag{5}$$

Here, two variables μ and λ in $|\Psi_0(\mu,\lambda)\rangle$ and $E_0(\mu,\lambda)$ indicate the order of the correlation effects and that of an external perturbation, respectively.

The total electronic energy E_0 can be expressed in the power series of $E_0(\mu,\lambda)$

$$\begin{aligned} E_0 &= E_0(0,0) + \sum_{n=0}^{1} \mu^{1-n}\lambda^n E_0(1-n,n) + \sum_{n=0}^{2} \mu^{2-n}\lambda^n E_0(2-n,n) + \cdots \\ &= \sum_{m=0}\sum_{n=0}^{m} \mu^{m-n}\lambda^n E_0(m-n,n) \end{aligned} \tag{6}$$

The perturbed ground state $|\Phi_0\rangle$ can be expanded similarly:

$$\begin{aligned} |\Phi_0\rangle &= |\Psi_0(0,0)\rangle + \sum_{n=0}^{1} \mu^{1-n}\lambda^n|\Psi_0(1-n,n)\rangle + \sum_{n=0}^{2} \mu^{2-n}\lambda^n|\Psi_0(2-n,n)\rangle + \cdots \\ &= \sum_{m=0}\sum_{n=0}^{m} \mu^{m-n}\lambda^n|\Psi_0(m-n,n)\rangle \end{aligned} \tag{7}$$

Substituting Eqs. (2), (6) and (7) into Eq. (4), we obtain

$$\sum_{m=0}\sum_{n=0}^{m}\mu^{m-n}\lambda^{n}H_{HF}\,|\Psi_0(m-n,n)\rangle + \sum_{m=0}\sum_{n=0}^{m}\mu^{m-n+1}\lambda^{n}V\,|\Psi_0(m-n,n)\rangle +$$
$$\sum_{m=0}\sum_{n=0}^{m}\mu^{m-n}\lambda^{n+1}(\alpha H_1)|\Psi_0(m-n,n)\rangle = \sum_{m''=0}\sum_{n''=0}^{m''}\mu^{m''-n''}\lambda^{n''}E_0(m-n,n)|\Psi_0(m'-n',n')\rangle \qquad (8)$$

where, $m''=m+m'$ and $n''=n+n'$.

We choose $|\Psi_0(\mu, \lambda)\rangle$ to satisfy the intermediate normalization condition as follows:

$$\langle\Psi_0(0,0)|\Phi_0\rangle = \langle\Psi_0(0,0)|\Psi_0(0,0)\rangle$$
$$+ \mu\langle\Psi_0(0,0)|\Psi_0(1,0)\rangle + \lambda\langle\Psi_0(0,0)|\Psi_0(0,1)\rangle + \cdots = 1,$$

where

$$\langle\Psi_0(0,0)|\Psi_0(m,n)\rangle = 0, \qquad (m \neq 0,\ n \neq 0). \qquad (9)$$

From each order term of Eq. (8), the following relations are obtained:

<u>$\mu=0,\ \lambda=0$</u>

$$H_{HF}\,|\Psi_0(0,0)\rangle = E_0(0,0)|\Psi_0(0,0)\rangle, \qquad (10)$$

<u>$\mu=1,\ \lambda=0$</u>

$$H_{HF}\,|\Psi_0(1,0)\rangle + V|\Psi_0(0,0)\rangle = E_0(1,0)|\Psi_0(0,0)\rangle + E_0(0,0)|\Psi_0(1,0)\rangle, \qquad (11)$$

<u>$\mu=0,\ \lambda=1$</u>

$$H_{HF}|\Psi_0(0,1)\rangle + (\alpha H_1)|\Psi_0(0,0)\rangle = E_0(0,1)|\Psi_0(0,0)\rangle + E_0(0,0)|\Psi_0(0,1)\rangle, \quad (12)$$

<u>μ=p, λ=q (p, q ≥ 1)</u>

$$H_{HF}|\Psi_0(p,q)\rangle + V|\Psi_0(p-1,q)\rangle + (\alpha H_1)|\Psi_0(p,q-1)\rangle = \sum_{r=0}^{p}\sum_{s=0}^{q} E_0(p-r,q-s)|\Psi_0(r,s)\rangle. \quad (13)$$

Operating $\langle\Phi_0(0,0)|$ on both sides of Eqs.(11)-(13) and using Eq.(9), we obtain

$$E_0(1,0) = \langle\Psi_0(0,0)|V|\Psi_0(0,0)\rangle, \quad (14)$$

$$E_0(0,1) = \langle\Psi_0(0,0)|\alpha H_1|\Psi_0(0,0)\rangle, \quad (15)$$

and

$$E_0(p,q) = \langle\Psi_0(0,0)|V|\Psi_0(p-1,q)\rangle + \langle\Psi_0(0,0)|\alpha H_1|\Psi_0(p,q-1)\rangle, \quad (p,q \geq 1). \quad (16)$$

From Eq.(11), it follows that

$$(E_0(0,0) - H_{HF})|\Psi_0(1,0)\rangle = (V - E_0(1,0))|\Psi_0(0,0)\rangle = (V - \langle\Psi_0(0,0)|V|\Psi_0(0,0)\rangle)|\Psi_0(0,0)\rangle . \quad (17)$$

We expand $|\Psi_0(1,0)\rangle$ as the function of $|\Psi_0(0,0)\rangle$:

$$|\Psi_0(1,0)\rangle = \sum_n C_n(1,0)|\Psi_n(0,0)\rangle. \quad (18)$$

Operating $\langle\Psi_0(0,0)|$ on both sides of Eq.(18), we can write

$$<\Psi_n(0,0)|\Psi_0(1,0)> = \sum_{n,n'} C_{n'}(1,0)<\Psi_n(0,0)|\Psi_{n'}(0,0)> = C_n(1,0). \quad (19)$$

From Eq.(9), $C_0(1,0)$ equals 0. Therefore,

$$|\Psi_0(1,0)> = \sum_{n}{}' |\Psi_n(0,0)><\Psi_n(0,0)|\Psi_n(1,0)>. \quad (20)$$

Here, the symbol Σ' indicates the summation over n except n=0. Operating $<\Psi_0(0,0)|$ on both sides of Eq. (17),

$$<\Psi_n(1,0)|(E_0(0,0)-H_{HF})|\Psi_0(1,0)> = <\Psi_n(0,0)|(V - <\Psi_0(0,0)|V\Psi_0(1,0)>)|\Psi_0(1,0)>.$$

Using Eq.(20), we obtain

$$<\Psi_n(0,0)|\Psi_0(1,0)> = \frac{<\Psi_n(0,0)|V\Psi_0(0,0)>}{E_0(0,0) - E_n(0,0)} . \quad (21)$$

In the same manner, from Eq.(12), we obtain

$$<\Psi_n(0,0)|\Psi_0(0,1)> = \frac{<\Psi_n(0,0)|\alpha H_1|\Psi_0(0,0)>}{E_0(0,0) - E_n(0,0)} . \quad (22)$$

From Eq.(13),

$$<\Psi_n(0,0)|\Psi_0(p,q)> = \frac{1}{E_0(0,0) - E_n(0,0)}[<\Psi_n(0,0)|V|\Psi_n(p-1,q)>$$

$$+ <\Psi_n(0,0)|\alpha H_1|\Psi_0(p,q-1)> - \sum_{r=0}^{p}{}' \sum_{s=0}^{q}{}' E_0(p-r,q-s)<\Psi_n(0,0)|\Psi_0(r,s)>], \quad (p,q \geq 1). \qquad (23)$$

Here, the symbol Σ' indicates the summation over r and s except the case: $r=s=0$ and $r=p$, $s=p$.

From the above Eqs.(14)-(16) and (21)-(23), any $E_0(\mu,\lambda)$ can be obtained. The analytical expressions of response properties (E_i, i = 1,2,...) can be calculated using the analytical expressions of $E_0(\mu,\lambda)$ and the following relations:

$$E_0 = E_0(0,0) + \sum_{\mu=0} E_0(\mu,1) + \sum_{\mu=0} E_0(\mu,2) + \sum_{\mu=0} E_0(\mu,3) + \sum_{\mu=0} E_0(\mu,4) + \cdots$$

$$= E_0(0) - \alpha E_1 - \frac{1}{2!}\alpha^2 E_2 - \frac{1}{3!}\alpha^3 E_3 - \frac{1}{4!}\alpha^4 E_4 - \cdots. \qquad (24)$$

When αH_1 represents a static electric field ($\alpha H_1 = \boldsymbol{F}\cdot\boldsymbol{r}$), E_1, E_2 and E_n (n≥3) give the permanent electric dipole moment, polarizability and hyperpolarizabilities, respectively. For example, the explicit expression of $E_0(0,4)$ is given by Eq. (14)-(16) and (21)-(23) as

$$E_0(0,4) = \sum_{n_1} \frac{<0|W|0>^2<0|W|n_1><n_1|W|0>}{(E_0(0,0) - E_{n_1}(0,0))^3}$$

$$- \sum_{n_1,n_2} \frac{<0|W|n_1><n_1|W|0><0|W|n_2><n_2|W|0>}{(E_0(0,0) - E_{n_1}(0,0))(E_0(0,0) - E_{n_2}(0,0))^2}$$

$$- \sum_{n_1,n_2} \frac{<0|W|0><0|W|n_1><n_1|W|n_2><n_2|W|0>}{(E_0(0,0) - E_{n_1}(0,0))(E_0(0,0) - E_{n_2}(0,0))^2}$$

$$- \sum_{n_1,n_2} \frac{<0|W|0><0|W|n_1><n_1|W|n_2><n_2|W|0>}{(E_0(0,0) - E_{n_1}(0,0))^2(E_0(0,0) - E_{n_2}(0,0))}$$

$$+ \sum_{n_1,n_2,n_3} \frac{<0|W|n_1><n_1|W|n_2><n_2|W|n_3><n_3|W|0>}{(E_0(0,0) - E_{n_1}(0,0))(E_0(0,0) - E_{n_2}(0,0))(E_0(0,0) - E_{n_3}(0,0))}, \qquad (25)$$

where

$$W = e \sum_i \boldsymbol{F} \cdot \boldsymbol{r}^i . \tag{26}$$

Here, the indices n_1, n_2, ... indicate the excited states. When |0> represents the HF ground state, the static third-order hyperpolarizability γ_{ijkl} which is obtained from the coefficient of $\boldsymbol{F}^i \boldsymbol{F}^j \boldsymbol{F}^k \boldsymbol{F}^l$ (i,j,k,l represent the x,y,z components) is expressed as

$$\begin{aligned}\gamma_{ijkl} = -\frac{1}{4!} S_{ijkl} \Bigg\{ & \sum_{a,r,s,t} \frac{\langle a|\mu^i|r\rangle\langle r|\mu^j|s\rangle\langle s|\mu^k|t\rangle\langle t|\mu^l|a\rangle}{(\varepsilon_a-\varepsilon_r)(\varepsilon_a-\varepsilon_s)(\varepsilon_a-\varepsilon_t)} \\ & + \sum_{a,b,c,r} \frac{\langle a|\mu^i|r\rangle\langle r|\mu^j|c\rangle\langle c|\mu^k|b\rangle\langle b|\mu^l|a\rangle}{(\varepsilon_a-\varepsilon_r)(\varepsilon_b-\varepsilon_r)(\varepsilon_c-\varepsilon_r)} \\ & - \sum_{a,b,r,s} \frac{\langle a|\mu^i|r\rangle\langle r|\mu^j|s\rangle\langle s|\mu^k|b\rangle\langle b|\mu^l|a\rangle}{(\varepsilon_a-\varepsilon_r)(\varepsilon_b-\varepsilon_r)(\varepsilon_b-\varepsilon_s)} \\ & - \sum_{a,b,r,s} \frac{\langle a|\mu^i|r\rangle\langle r|\mu^j|s\rangle\langle s|\mu^k|b\rangle\langle b|\mu^l|a\rangle}{(\varepsilon_a-\varepsilon_r)(\varepsilon_a-\varepsilon_s)(\varepsilon_b-\varepsilon_s)} \\ & - \sum_{a,b,r,s} \frac{\langle a|\mu^i|r\rangle\langle r|\mu^j|b\rangle\langle b|\mu^k|s\rangle\langle s|\mu^l|a\rangle}{(\varepsilon_a-\varepsilon_r)(\varepsilon_b-\varepsilon_s)(\varepsilon_a-\varepsilon_s)} \Bigg\} . \end{aligned} \tag{27}$$

and the unoccupied spin orbitals of the HF ground state, respectively. ε_i represents the i th orbital energy and μ^i represents the i component of the one-electron dipole operator. Details of calculations of the γ values by the use of Eq.(27) will be reported elsewhere [19].

3. Static Response Properties by the Coupled-Cluster Theory

The coupled-cluster (CC) method [1,9-14] can include the interactions among electrons within clusters and those between these clusters effectively. The CC method tends to give faster convergence of the wavefunction than does the configuration interaction (CI) method.

Prior to applications of the method to the response property problems, it will be beneficial to briefly outline the essence of the coupled-cluster theory. In order to introduce the cluster interactions, the wavefunction $|0\rangle$ is written as follows in terms of a cluster operator T :

$$|0\rangle = e^{T} |0^{(0)}\rangle . \tag{28}$$

The noninteracting reference function $|0^{(0)}\rangle$ is limited to a ket corresponding to a single Slater determinant here. The cluster operator T is expressed as the sum of one-, two-electron, etc., clusters

$$T = \sum_{i=1}^{N} T_i = T_1 + T_2 + \cdots + T_N \tag{29}$$

with

$$T_1 = \sum_{ar} t_a^r a_r^+ a_a \tag{30}$$

$$T_2 = \frac{1}{4} \sum_{abrs} t_{ab}^{rs} a_r^+ a_s^+ a_b a_a \tag{31}$$

$$\vdots$$

$$T_N = \frac{1}{(N!)^2} \sum_{\substack{a\,b\ldots \\ r\,s\ldots}} t_{ab\ldots}^{r\,s\ldots} a_r^+ a_s^+ \ldots a_b a_a \tag{32}$$

In these expressions, a, b, c, ... denote the occupied spin orbitals in $|0^{(0)}\rangle$, while r, s, t, ... denote the unoccupied ones. The symbols a^+ and a represent the creation and the annihilation

operators, respectively. One of the advantages of the CC method is that the size-consistency is satisfied on a truncation of T at any order.

By expanding Eq.(28) and collecting terms of common excitation level, we write

$$e^{T}|0^{(0)}\rangle = (1 + C_1 + C_2 + C_3 + \cdots)|0^{(0)}\rangle, \tag{33}$$

where the configuration excitation operators C_1, C_2, ... are

$$C_1 = T_1 \tag{34}$$

$$C_2 = T_2 + \frac{1}{2!}T_1^2 \tag{35}$$

$$C_3 = T_3 + \frac{1}{3!}T_1^3 + T_1T_2 \tag{36}$$

$$C_4 = T_4 + \frac{1}{4!}T_1^4 + \frac{1}{2!}T_2^2 + T_3T_1 + \frac{1}{2!}T_1^2T_2 \text{ , etc.} \tag{37}$$

These expressions are convenient to analyze the excitation level in the conventional CI and MBPT wavefunctions [20].

The cluster amplitudes $t_{ab\ldots}^{rs\ldots}$ are determined by the condition that the CC wavefunction $e^{T}|0^{(0)}\rangle$ satisfy the Schrödinger equation :

$$He^{T}|0^{(0)}\rangle = Ee^{T}|0^{(0)}\rangle . \tag{38}$$

When the above exponential series are collected together as commutators, Eq.(38) is rewritten as follows:

$$\left(H + [H,T] + \frac{1}{2!}[[H,T],T] + \frac{1}{3!}[[[H,T],T],T] + \frac{1}{4!}[[[[H,T],T],T],T]\right)|0^{(0)}> = E\,|0^{(0)}>. \tag{39}$$

The reason why the series truncates after four commutators is that H contains at most two-electron operators, which involve four general (particle and hole) operators. Equations for the amplitudes of any order are derived by noting that when the excited determinant $<0^{(0)}|$(excitation operators) operates on both sides of Eq. (39), the final equation yields zero. The excitations are chosen to include up through n-fold excitations from $|0^{(0)}>$ in the case where T has been truncated at T_n. Once these amplitudes are obtained, the total energy can be calculated by projecting Eq. (39) onto $|0^{(0)}>$. For this reason, the energy obtained is not variational. Although the variational approach, where $<0^{(0)}|e^{T\,+}$ operates on both sides of Eq. (36), can also be performed, the resultant commutator expression of the exponential operators cannot be truncated and comes to be complicated. Therefore, in general, the CC equations are treated nonvariationally.

We are now in a position to derive general equations for the nth-order response properties. In practice, we will follow the procedure by Monkhorst [15,16].

When an external one-electron perturbation (αH_1) is applied, the total electronic Hamiltonian is written as

$$H(\alpha) = H_0 + \alpha H_1. \tag{40}$$

The perturbed wavefunction $|0>$ is expressed as

$$|0> = e^{T(\alpha)} |0^{(0)}> . \tag{41}$$

The cluster operator $T(\alpha)$ can be expanded in powers of the field α :

$$T(\alpha) = T^{(0)} + \alpha T^{(1)} + \alpha^2 T^{(2)} + \alpha^3 T^{(3)} + \alpha^4 T^{(4)} + \cdots . \tag{42}$$

The total electronic energy $E(\alpha)$ can also be expanded in the same way :

$$E(\alpha) = E^{(0)} + \alpha E^{(1)} + \alpha^2 E^{(2)} + \alpha^3 E^{(3)} + \alpha^4 E^{(4)} + \cdots . \tag{43}$$

The equations for $E(\alpha)$ and the cluster amplitudes $t_{ab\ldots}^{rs\ldots}$ are

$$<0^{(0)}| e^{-T(\alpha)} H(\alpha) e^{T(\alpha)} |0^{(0)}> = E(\alpha) , \tag{44}$$

and

$$<_{ab\ldots}^{rs\ldots}| e^{-T(\alpha)} H(\alpha) e^{T(\alpha)} |0^{(0)}> = 0 . \tag{45}$$

Substituting Eqs.(40) and (42) into the left-hand side of Eqs.(44) and (45), we obtain

$$<0^{(0)}| e^{-T^{(0)}} e^{-\alpha T^{(1)} - \alpha^2 T^{(2)} - \cdots} (H_0 + \alpha H_1) e^{\alpha T^{(1)} + \alpha^2 T^{(2)} + \cdots} e^{T^{(0)}} |0^{(0)}>$$

and

$$<{}^{r\ s\ \cdots}_{a\ b\ \cdots}|\ e^{-T^{(0)}}\ e^{-\alpha T^{(1)}-\alpha^2 T^{(2)}-\cdots}\ (H_0+\alpha H_1)\ e^{\alpha T^{(1)}+\alpha^2 T^{(2)}+\cdots}\ e^{T^{(0)}}|0^{(0)}>\ .$$

Substitution of Eq.(43) into the right-hand side of Eq.(44) permits the equation of each order (n) to be rewritten as follows.

(i) $n = 0$

$$<0^{(0)}|\ e^{-T^{(0)}}\ H_0\ e^{T^{(0)}}\ |0^{(0)}> = E^{(0)}. \tag{46}$$

$$<{}^{r\ s\ \cdots}_{a\ b\ \cdots}|\ e^{-T^{(0)}}\ H_0\ e^{T^{(0)}}\ |0^{(0)}> = 0\ . \tag{47}$$

These equations are nothing but the original CC equations, Eqs.(44) and (45).

(ii) $n = 1$

$$<0^{(0)}|\ e^{-T^{(0)}}\ \left\{H_1 + H_0 T^{(1)} - T^{(1)} H_0\right\}\ e^{T^{(0)}}\ |0^{(0)}> = E^{(1)}.$$

Therefore,

$$<0^{(0)}|\ e^{-T^{(0)}}\ \left\{H_1 + [H_0, T^{(1)}]\right\}\ e^{T^{(0)}}\ |0^{(0)}> = E^{(1)}, \tag{48}$$

$$<{}^{r\ s\ \cdots}_{a\ b\ \cdots}|\ e^{-T^{(0)}}\ \left\{H_1 + [H_0, T^{(1)}]\right\}\ e^{T^{(0)}}\ |0^{(0)}> = 0\ . \tag{49}$$

(iii) $n = 2$

$$<0^{(0)}|\, e^{-T^{(0)}} \left\{ (H_1 T^{(1)} - T^{(1)} H_1) + \frac{1}{2}(H_0 T^{(1)2} - 2T^{(1)} H_0 T^{(1)} + T^{(1)2} H_0) \right.$$
$$\left. + (H_0 T^{(2)} - T^{(2)} H_0) \right\} e^{T^{(0)}} |0^{(0)}> = E^{(2)}.$$

Using the relation :

$$H_0 T^{(1)2} - 2T^{(1)} H_0 T^{(1)} + T^{(1)2} H_0 = [[H_0, T^{(1)}], T^{(1)}] \ ,$$

we obtain the following equations.

$$<0^{(0)}|\, e^{-T^{(0)}} \left\{ [H_1, T^{(1)}] + \frac{1}{2}[[H_0, T^{(1)}], T^{(1)}] + [H_0, T^{(2)}] \right\} e^{T^{(0)}} |0^{(0)}> = E^{(2)}. \qquad (50)$$

$$<^{r\,s\,\cdots}_{a\,b\,\cdots}|\, e^{-T^{(0)}} \left\{ [H_1, T^{(1)}] + \frac{1}{2}[[H_0, T^{(1)}], T^{(1)}] + [H_0, T^{(2)}] \right\} e^{T^{(0)}} |0^{(0)}> = 0 . \qquad (51)$$

These equations are identical to those derived by Monkhorst [15,16].

(iv) $n = 3$

$$<0^{(0)}|\, e^{-T^{(0)}} \left\{ (H_1 T^{(2)} - T^{(2)} H_1) + \frac{1}{2}(H_1 T^{(1)2} - 2T^{(1)} H_1 T^{(1)} + T^{(1)2} H_1) \right.$$
$$+ H_0 T^{(3)} - T^{(3)} H_0 + \frac{1}{6}(H_0 T^{(1)3} - 3T^{(1)} H_0 T^{(1)2} + 3T^{(1)2} H_0 T^{(1)} - T^{(3)} H_0)$$
$$\left. + (H_0 T^{(1)} T^{(2)} - T^{(1)} H_0 T^{(2)} - T^{(2)} H_0 T^{(1)} + T^{(2)} T^{(1)} H_0) \right\} e^{T^{(0)}} |0^{(0)}> = E^{(3)}.$$

Here, using the relations :

$$H_0T^{(1)}T^{(2)} - T^{(1)}H_0T^{(2)} - T^{(2)}H_0T^{(1)} + T^{(2)}T^{(1)}H_0 = [[H_0, T^{(1)}], T^{(2)}]$$
$$H_0T^{(1)3} - 3T^{(1)}H_0T^{(1)2} + 3T^{(1)2}H_0T^{(1)} - T^{(1)3}H_0 = [[[H_0, T^{(1)}], T^{(1)}], T^{(1)}],$$

we obtain

$$<0^{(0)}| e^{-T^{(0)}} \left\{ [H_1, T^{(2)}] + \frac{1}{2}[[H_1, T^{(1)}], T^{(1)}] + [H_0, T^{(3)}] \right.$$
$$\left. + \frac{1}{6}[[H_0, T^{(1)}], T^{(1)}], T^{(1)}] + [[H_0, T^{(1)}], T^{(2)}] \right\} e^{T^{(0)}} |0^{(0)}> = E^{(3)}, \qquad (52)$$

$$<^{r\,s\,\cdots}_{a\,b\,\cdots}| e^{-T^{(0)}} \left\{ [H_1, T^{(2)}] + \frac{1}{2}[[H_1, T^{(1)}], T^{(1)}] + [H_0, T^{(3)}] \right.$$
$$\left. + \frac{1}{6}[[H_0, T^{(1)}], T^{(1)}], T^{(1)}] + [[H_0, T^{(1)}], T^{(2)}] \right\} e^{T^{(0)}} |0^{(0)}> = 0. \qquad (53)$$

(v) $n = 4$

$$<0^{(0)}| e^{-T^{(0)}} \left\{ (H_1T^{(3)} - T^{(3)}H_1) + \frac{1}{6}(H_1T^{(1)3} - 3T^{(1)}H_1T^{(1)2} + 3T^{(1)2}H_1T^{(1)} - T^{(1)3}H_1) \right.$$
$$+ (H_1T^{(1)}T^{(2)} - T^{(2)}H_1T^{(1)} - T^{(1)}H_1T^{(2)} + T^{(2)}T^{(1)}H_1) + (H_0T^{(4)} - T^{(4)}H_0)$$
$$+ \frac{1}{24}(H_0T^{(1)4} - 4T^{(1)}H_0T^{(1)3} + 6T^{(1)2}H_0T^{(1)2} - 4T^{(1)3}H_0T^{(1)} + T^{(1)4}H_0)$$
$$+ \frac{1}{2}(H_0T^{(1)2}T^{(2)} - T^{(2)2}H_0T^{(1)2} - 2T^{(1)}H_0T^{(1)}T^{(2)} + 2T^{(2)}T^{(1)}H_0T^{(1)}$$
$$+ T^{(1)2}H_0T^{(2)} - T^{(2)}T^{(1)2}H_0) + \frac{1}{2}(H_0T^{(2)2} + T^{(2)2}H_0 - 2T^{(2)}H_0T^{(2)})$$
$$\left. + (H_0T^{(1)}T^{(3)} - T^{(3)}H_0T^{(1)} - T^{(1)}H_0T^{(3)} + T^{(3)}T^{(1)}H_0) \right\} e^{T^{(0)}} |0^{(0)}> = E^{(4)}.$$

Using the relations :

$$H_1T^{(1)}T^{(2)} - T^{(2)}H_1T^{(1)} - T^{(1)}H_1T^{(2)} + T^{(2)}T^{(1)}H_1 = [[H_1, T^{(1)}], T^{(2)}]$$

$$H_0T^{(1)4} - 4T^{(0)}H_0T^{(1)3} + 6T^{(1)2}H_0T^{(1)2} - 4T^{(1)3}H_0T^{(1)} + T^{(1)4}H_0$$
$$= [[[[H_0, T^{(1)}], T^{(1)}], T^{(1)}], T^{(1)}],$$

we reach

$$\begin{aligned}
&\langle 0^{(0)}| e^{-T^{(0)}} \Big\{ [H_1, T^{(3)}] + \frac{1}{6}[[[H_1, T^{(1)}], T^{(1)}], T^{(1)}] + [[H_1, T^{(1)}], T^{(2)}] \\
&+ [H_0, T^{(4)}] + \frac{1}{24}[[[[H_0, T^{(1)}], T^{(1)}], T^{(1)}], T^{(1)}] + \frac{1}{2}[[[H_0, T^{(1)}], T^{(1)}], T^{(2)}] \\
&+ \frac{1}{2}[[H_0, T^{(2)}], T^{(2)}] + [[H_0, T^{(1)}], T^{(3)}] \Big\} e^{T^{(0)}} |0^{(0)}\rangle = E^{(4)}, \qquad (54) \\
&\langle {}^{r\,s\,\cdots}_{a\,b\,\cdots}| e^{-T^{(0)}} \Big\{ [H_1, T^{(3)}] + \frac{1}{6}[[[H_1, T^{(1)}], T^{(1)}], T^{(1)}] + [[H_1, T^{(1)}], T^{(2)}] \\
&+ [H_0, T^{(4)}] + \frac{1}{24}[[[[H_0, T^{(1)}], T^{(1)}], T^{(1)}], T^{(1)}] + \frac{1}{2}[[[H_0, T^{(1)}], T^{(1)}], T^{(2)}] \\
&+ \frac{1}{2}[[H_0, T^{(2)}], T^{(2)}] + [[H_0, T^{(1)}], T^{(3)}] \Big\} e^{T^{(0)}} |0^{(0)}\rangle = 0. \qquad (55)
\end{aligned}$$

The above equations can be regularized by the use of the commutative relation among $T^{(i)}$. For example, Eq. (54) is rewritten as

$$\begin{aligned}
&\langle 0^{(0)}| e^{-T^{(0)}} \Big\{ [H_1, T^{(3)}] + \frac{1}{3!}[[[H_1, T^{(1)}], T^{(1)}], T^{(1)}] + \frac{1}{2!}([[H_1, T^{(1)}], T^{(2)}] \\
&+ [[H_1, T^{(2)}], T^{(1)}]) + [H_0, T^{(4)}] + \frac{1}{4!}[[[[H_0, T^{(1)}], T^{(1)}], T^{(1)}], T^{(1)}] \\
&+ \frac{1}{3!}([[[H_0, T^{(1)}], T^{(1)}], T^{(2)}] + [[[H_0, T^{(1)}], T^{(2)}], T^{(1)}] \\
&+ [[[H_0, T^{(2)}], T^{(1)}], T^{(1)}]) + \frac{1}{2!}[[H_0, T^{(2)}], T^{(2)}] \\
&+ \frac{1}{2!}([[H_0, T^{(1)}], T^{(3)}] + [[H_0, T^{(3)}], T^{(1)}]) \Big\} e^{T^{(0)}} |0^{(0)}\rangle = E^{(4)}. \qquad (56)
\end{aligned}$$

Equation (56) allows to express the CC equations for the nth-order ($n \geq 2$) response properties in a general form as follows:

$$<0^{(0)}| e^{-T^{(0)}} \left\{ \sum_{i=0}^{1} \sum_{N=1}^{n-i} \frac{1}{N!} P_{n_1, n_2, \ldots, n_N} ([\cdots [[H_i, T^{(n_1)}], T^{(n_2)}], \right.$$
$$\left. \cdots, T^{(n_N)}]) \right\} e^{T^{(0)}} |0^{(0)}> = E^{(n)}, \qquad (57)$$

$$<^{r\,s\,\cdots}_{a\,b\,\cdots}| e^{-T^{(0)}} \left\{ \sum_{i=0}^{1} \sum_{N=1}^{n-i} \frac{1}{N!} P_{n_1, n_2, \ldots, n_N} ([\cdots [[H_i, T^{(n_1)}], T^{(n_2)}], \right.$$
$$\left. \cdots, T^{(n_N)}]) \right\} e^{T^{(0)}} |0^{(0)}> = 0. \qquad (58)$$

with

$$\sum_{k=1}^{N} n_k = n - i, \qquad (n_k > 0, \text{ integer}). \qquad (59)$$

Here, $P_{n_1, n_2, \cdots, n_N}$ is the operator which represents the summation over all combinations of $(n_1, n_2, \ldots, n_N)$. It should be noted that the series in Eqs.(57) and (58) truncate after four commutators when H_i contains at most two-electron operators. The cluster operator $T^{(i)}$ is written as

$$T^{(i)} = \sum_{m=1}^{N} T_m^{(i)} = T_1^{(i)} + T_2^{(i)} + \cdots + T_N^{(i)}, \qquad (60)$$

where

$$T_1^{(i)} = \sum_{ar}{}^{(i)} t_a^r a_r^+ a_a \tag{61}$$

$$T_2^{(i)} = \frac{1}{4} \sum_{abrs}{}^{(i)} t_{ab}^{rs} a_r^+ a_s^+ a_b a_a \text{ , etc.} \tag{62}$$

Here, the index i represents the order of α. As can be seen from Eqs.(47), (49) and (58), calculations of the ith-order cluster amplitudes ${}^{(i)}t$ entail calculations of the cluster amplitudes of the (i-1)th-order. Therefore, Eqs.(47), (49) and (58) have to be solved successively up to the desired order of the cluster amplitudes. Once the cluster amplitudes are obtained, the response properties $E^{(n)}$ of any order can be calculated by the use of Eqs.(48) and (57).

4. Dynamic Response Property by the Coupled-Cluster Theory

Recently, Koch et al. have derived analytical expressions for the higher-order response properties by the CC response functional theory [21]. In the present paper, the corresponding equations to obtain analytical expressions for the time-dependent nth-order response properties will be derived according to the method proposed by Monkhorst [13]. We refer to this formalism as the time-dependent coupled-cluster (TDCC) method.

The time-dependent Schrödinger equation :

$$H(\alpha, t)\,|0\rangle = i \frac{\partial}{\partial t} |0\rangle \tag{63}$$

is used. Consider the total Hamiltonian

$$H(\alpha, t)\,|0\rangle = H_0 + \alpha H_1 (e^{i\omega t} + e^{-i\omega t}) e^{\varepsilon t}, \tag{64}$$

where the second term is an external time-dependent one-electron perturbation. A small positive number ε is used in order for this perturbation to be applied adiabatically.

The cluster operator $T(\alpha, t)$ can be expanded as follows:

$$T(\alpha, t) = T^{(0)} + \alpha T^{(1)}(t) + \alpha^2 T^{(2)}(t) + \alpha^3 T^{(3)}(t) + \alpha^4 T^{(4)}(t) + \cdots . \tag{65}$$

Here, the excitation operator $T^{(i)}$ of a given order i is written as

$$T^{(i)}(t) = \sum_{m=1}^{N} T_m^{(i)}(t) = T_1^{(i)}(t) + T_2^{(i)}(t) + \cdots + T_N^{(i)}(t) , \tag{66}$$

where

$$T_1^{(i)}(t) = \sum_{ar}^{(i)} t_a^r(t)\, a_r^+ a_a \tag{67}$$

$$T_2^{(i)}(t) = \frac{1}{4} \sum_{abrs}^{(i)} t_{ab}^{rs}(t)\, a_r^+ a_s^+ a_b a_a , \text{ etc.} \tag{68}$$

Here, It should be noted that the cluster amplitudes $t_{ab\ldots}^{rs\ldots}(t)$ depend on time.

The time-dependent wavefunction $|0>$ is expressed as

$$|0> = e^{T(\alpha,t) - i\delta(\alpha,t)} |0^{(0)}> . \tag{69}$$

The phase factor $\delta(\alpha, t)$ can be expanded as

$$\delta(\alpha, t) = E^{(0)} t + \alpha \delta^{(1)}(t) + \alpha^2 \delta^{(2)}(t) + \alpha^3 \delta^{(3)}(t) + \alpha^4 \delta^{(4)}(t) + \cdots . \tag{70}$$

Substitution of Eqs.(64) and (79) into Eq.(63) gives

$$[H_0 + \alpha H_1(e^{i\omega t} + e^{-i\omega t})e^{\varepsilon t}]\, e^{T(\alpha,t) - i\delta(\alpha,t)}|0^{(0)}> = i\frac{\partial}{\partial t} e^{T(\alpha,t) - i\delta(\alpha,t)}|0^{(0)}> . \quad (71)$$

Substituting Eqs.(65) and (70) into Eq.(71), we obtain

$$\begin{aligned}&[H_0 + \alpha H_1(e^{i\omega t} + e^{-i\omega t})e^{\varepsilon t}]\, e^{T(\alpha,t) - i\delta(\alpha,t)}|0^{(0)}> \\ &= \left\{ E^{(0)} + i\frac{\partial}{\partial t}[\alpha T^{(1)}(t) + \cdots] + \frac{\partial}{\partial t}[\alpha \delta^{(1)}(t) + \cdots] \right\} e^{T(\alpha,t) - i\delta(\alpha,t)}|0^{(0)}> . \end{aligned} \quad (72)$$

In the limit of time t approaching negative infinity, Eq. (72) should taken on the form

$$\begin{aligned}&H_0\, e^{T(\alpha,-\infty) - i\delta(\alpha,-\infty)}|0^{(0)}> = \\ &\left\{ E^{(0)} + \left[i\frac{\partial}{\partial t}(\alpha T^{(1)}(t) + \cdots) \right]_{t=-\infty} \right. \\ &\qquad \left. + \left[\frac{\partial}{\partial t}(\alpha \delta^{(1)}(t) + \cdots) \right]_{t=-\infty} \right\} e^{T(\alpha,-\infty) - i\delta(\alpha,-\infty)}|0^{(0)}> . \end{aligned} \quad (73)$$

The eigenvalue and the eigenvector of the unperturbed Hamiltonian H_0 in this limit are E_0 and $e^{T(\alpha,-\infty) - i\delta(\alpha,-\infty)}|0^{(0)}>$, respectively; that is,

$$H_0 e^{T(\alpha,-\infty) - i\delta(\alpha,-\infty)}|0^{(0)}> = E_0 e^{T(\alpha,-\infty) - i\delta(\alpha,-\infty)}|0^{(0)}> . \quad (74)$$

Therefore,

$$T^{(k)}(-\infty) = 0 \qquad (k = 1, 2, \ldots), \tag{75}$$

and

$$\delta^{(k)}(-\infty) = 0 \qquad (k = 1, 2, \ldots). \tag{76}$$

Operating $\langle 0^{(0)}| e^{-T(\alpha,t)+i\delta(\alpha,t)}$ on both sides of Eq. (72), and noting that $\delta(\alpha, t)$ can commute with H_0 and H_1, we obtain

$$\langle 0^{(0)}| e^{-T(\alpha,t)} [(H_0 + \alpha H_1(e^{i\omega t} + e^{-i\omega t})\, e^{\varepsilon t}]\, e^{T(\alpha,t)} |0^{(0)}\rangle = \frac{\partial}{\partial t}\delta(\alpha, t). \tag{77}$$

Using Eqs. (65) and (70), we may rewrite Eq.(77) as

$$\begin{aligned}&\langle 0^{(0)}| e^{-T^{(0)}} (e^{-\alpha T^{(1)}(t) - \alpha T^{(1)}(t) - \cdots}) [(H_0 + \alpha H_1(e^{i\omega t} + e^{-i\omega t})\, e^{\varepsilon t}] \\ &(e^{\alpha T^{(1)}(t) + \alpha T^{(1)}(t) + \cdots})\, e^{T^{(0)}} |0^{(0)}\rangle = E^{(0)} + \frac{\partial}{\partial t}(\alpha \delta^{(1)}(t) + \alpha^{(2)}\delta^{(2)}(t) + \cdots).\end{aligned} \tag{78}$$

Likewise by operating $\langle {}^{r\,s\,\cdots}_{a\,b\,\ldots}| e^{-T(\alpha,t)+i\delta(\alpha,t)}$ on both sides of Eq.(72), we obtain

$$\begin{aligned}&\langle {}^{r\,s\,\cdots}_{a\,b\,\ldots}| e^{-T^{(0)}} (e^{-\alpha T^{(1)}(t) - \alpha T^{(1)}(t) - \cdots}) [(H_0 + \alpha H_1(e^{i\omega t} + e^{-i\omega t})\, e^{\varepsilon t}] \\ &(e^{\alpha T^{(1)}(t) + \alpha T^{(1)}(t) + \cdots})\, e^{T^{(0)}} - i\frac{\partial}{\partial t}(T^{(0)} + \alpha T^{(1)}(t) + \cdots)|0^{(0)}\rangle = 0.\end{aligned} \tag{79}$$

From Eqs.(78) and (79), CC equations for the response properties of the order n are obtained as follows.

(i) $n = 0$

$$<0^{(0)}|\, e^{-T^{(0)}} H_0 e^{T^{(0)}} |0^{(0)}> = E^{(0)}. \tag{80}$$

$$<{}^{r\,s\,\cdots}_{a\,b\,\cdots}|\, e^{-T^{(0)}} H_0 e^{T^{(0)}} |0^{(0)}> = 0. \tag{81}$$

These equations are again nothing but the original CC expressions, Eqs.(46) and (47).

(ii) $n = 1$

$$<0^{(0)}|\, e^{-T^{(0)}} \left\{ H_1(e^{i\omega t+\varepsilon t} + e^{-i\omega t+\varepsilon t}) + [H_0, T^{(1)}(t)] \right\} e^{T^{(0)}} |0^{(0)}> = \frac{\partial \delta^{(1)}(t)}{\partial t}, \tag{82}$$

$$<{}^{r\,s\,\cdots}_{a\,b\,\cdots}|\, e^{-T^{(0)}} \left\{ H_1(e^{i\omega t+\varepsilon t} + e^{-i\omega t+\varepsilon t}) + [H_0, T^{(1)}(t)] \right\} e^{T^{(0)}} - i\frac{\partial T^{(1)}(t)}{\partial t} |0^{(0)}> = 0. \tag{83}$$

(iii) $n = 2$

$$<0^{(0)}|\, e^{-T^{(0)}} \left\{ [H_1, T^{(1)}(t)](e^{i\omega t+\varepsilon t} + e^{-i\omega t+\varepsilon t}) + \frac{1}{2}[[H_0, T^{(1)}(t)], T^{(1)}(t)] + [H_0, T^{(2)}(t)] \right\} e^{T^{(0)}} |0^{(0)}> = \frac{\partial \delta^{(2)}(t)}{\partial t}, \tag{84}$$

$$<{}^{r\,s\,\cdots}_{a\,b\,\cdots}|\, e^{-T^{(0)}} \left\{ [H_1, T^{(1)}(t)](e^{i\omega t+\varepsilon t} + e^{-i\omega t+\varepsilon t}) + \frac{1}{2}[[H_0, T^{(1)}(t)], T^{(1)}(t)] + [H_0, T^{(2)}(t)] \right\} e^{T^{(0)}} - i\frac{\partial T^{(2)}(t)}{\partial t} |0^{(0)}> = 0. \tag{85}$$

(iv) $n = 3$

$$<0^{(0)}|\, e^{-T^{(0)}} \left\{ [H_1, T^{(2)}(t)](e^{i\omega t+\varepsilon t} + e^{-i\omega t+\varepsilon t}) + \frac{1}{2}[[H_1, T^{(1)}(t)], T^{(1)}(t)] \right.$$
$$(e^{i\omega t+\varepsilon t} + e^{-i\omega t+\varepsilon t}) + [H_0, T^{(3)}(t)] + \frac{1}{6}[[H_0, T^{(1)}(t)], T^{(1)}(t)], T^{(1)}(t)]$$
$$\left. + [[H_0, T^{(1)}(t)], T^{(2)}(t)] \right\} e^{T^{(0)}}\, |0^{(0)}> = \frac{\partial \delta^{(3)}(t)}{\partial t}, \qquad (86)$$

$$<^{r\ s\ \cdots}_{a\ b\ \cdots}|\, e^{-T^{(0)}} \left\{ [H_1, T^{(2)}(t)](e^{i\omega t+\varepsilon t} + e^{-i\omega t+\varepsilon t}) + \frac{1}{2}[[H_1, T^{(1)}(t)], T^{(1)}(t)] \right.$$
$$(e^{i\omega t+\varepsilon t} + e^{-i\omega t+\varepsilon t}) + [H_0, T^{(3)}(t)] + \frac{1}{6}[[H_0, T^{(1)}(t)], T^{(1)}(t)], T^{(1)}(t)]$$
$$\left. + [[H_0, T^{(1)}(t)], T^{(2)}(t)] \right\} e^{T^{(0)}} - i\frac{\partial T^{(3)}(t)}{\partial t}|0^{(0)}> = 0. \qquad (87)$$

(v) $n = 4$

$$<0^{(0)}|\, e^{-T^{(0)}} \left\{ [H_1, T^{(3)}(t)](e^{i\omega t+\varepsilon t} + e^{-i\omega t+\varepsilon t}) + \frac{1}{6}[[[H_1, T^{(1)}(t)], T^{(1)}(t)], \right.$$
$$T^{(1)}(t)](e^{i\omega t+\varepsilon t} + e^{-i\omega t+\varepsilon t}) + [[H_1, T^{(1)}(t)], T^{(2)}(t)](e^{i\omega t+\varepsilon t} + e^{-i\omega t+\varepsilon t})$$
$$+ [H_0, T^{(4)}(t)] + \frac{1}{24}[[[[H_0, T^{(1)}(t)], T^{(1)}(t)], T^{(1)}(t)], T^{(1)}(t)]$$
$$+ \frac{1}{2}[[[H_0, T^{(1)}(t)], T^{(1)}(t)], T^{(2)}(t)] + \frac{1}{2}[[H_0, T^{(2)}(t)], T^{(2)}(t)]$$
$$\left. + [[H_0, T^{(1)}(t)], T^{(3)}(t)] \right\} e^{T^{(0)}}\, |0^{(0)}> = \frac{\partial \delta^{(4)}(t)}{\partial t}. \qquad (88)$$

$$<0^{(0)}|\, e^{-T^{(0)}} \Big\{ [H_1, T^{(3)}(t)](e^{i\omega t+\varepsilon t} + e^{-i\omega t+\varepsilon t}) + \frac{1}{6}[[[H_1, T^{(1)}(t)], T^{(1)}(t)],$$
$$T^{(1)}(t)](e^{i\omega t+\varepsilon t} + e^{-i\omega t+\varepsilon t}) + [[H_1, T^{(1)}(t)], T^{(2)}(t)](e^{i\omega t+\varepsilon t} + e^{-i\omega t+\varepsilon t})$$
$$+ [H_0, T^{(4)}(t)] + \frac{1}{24}[[[[H_0, T^{(1)}(t)], T^{(1)}(t)], T^{(1)}(t)], T^{(1)}(t)]$$
$$+ \frac{1}{2}[[[H_0, T^{(1)}(t)], T^{(1)}(t)], T^{(2)}(t)] + \frac{1}{2}[[H_0, T^{(2)}(t)], T^{(2)}(t)]$$
$$+ [[H_0, T^{(1)}(t)], T^{(3)}(t)] \Big\}\, e^{T^{(0)}}\, |0^{(0)}> = \frac{\partial \delta^{(4)}(t)}{\partial t}, \tag{89}$$

The general CC equations for the nth-order ($n \geq 2$) response properties are also expressible in the form as follows:

$$<0^{(0)}|\, e^{-T^{(0)}} \Big\{ \sum_{i=0}^{1} \sum_{N=1}^{n-i} \frac{1}{N!} P_{n_1, n_2, \ldots, n_N}([\cdots [[H_i(t), T^{(n_1)}(t)], T^{(n_2)}(t)],$$
$$\cdots, T^{(n_N)}(t)]) \Big\}\, e^{T^{(0)}}\, |0^{(0)}> = \frac{\partial \delta^{(n)}(t)}{\partial t}. \tag{90}$$

$$<^{r\,s\,\cdots}_{a\,b\,\cdots}|\, e^{-T^{(0)}} \Big\{ \sum_{i=0}^{1} \sum_{N=1}^{n-i} \frac{1}{N!} P_{n_1, n_2, \ldots, n_N}([\cdots [[H_i(t), T^{(n_1)}(t)], T^{(n_2)}(t)],$$
$$\cdots, T^{(n_N)}(t)]) \Big\}\, e^{T^{(0)}} - i \frac{\partial T^{(n)}(t)}{\partial t} |0^{(0)}> = 0. \tag{91}$$

with

$$H_i(t) = \begin{cases} H_0, & (i = 0) \\ H_1(e^{i\omega t+\varepsilon t} + e^{-i\omega t+\varepsilon t}), & (i = 1) \end{cases} \tag{92}$$

$$\sum_{k=1}^{N} n_k = n - i, \qquad (n_k > 0, \text{ integer}) \tag{93}$$

Here, $P_{n_1, n_2, \cdots, n_N}$ is the operator which represents the summation over all combinations of $(n_1, n_2, \ldots, n_N)$. The series in Eqs.(90) and (91) are truncated after four commutators when H_i contains at most two-electron operators. Solving Eq.(90), the time-averaged nth-order response properties, i. e., he first- order polarizability and the second-order hyperpolarizability (α and γ, respectively) may be evaluated with the aid of the following relations:

$$\overline{E^{(2)}(\omega)} = \frac{\omega}{2\pi} \int_0^{2\pi/\omega} \frac{\partial \delta^{(2)}(t)}{\partial t} dt = -\frac{1}{4}\alpha(\omega). \tag{94}$$

$$\overline{E^{(4)}(\omega)} = \frac{\omega}{2\pi} \int_0^{2\pi/\omega} \frac{\partial \delta^{(4)}(t)}{\partial t} dt = -\frac{1}{64}\gamma(\omega). \tag{95}$$

5. Concluding Remarks

In calculating physical properties numerically, we often encounter difficulties related to the choice of proper basis sets describing the accurate total energies under the electric field of given strengths. As an alternative approach, some analytical expressions for the response properties are badly needed. In the present work, general equations for analytical expressions of the nth-order response properties have been derived on the basis of the MBPT and the CC methods. These methods can include higher-order correlation effects systematically. In the MBPT double perturbation method, however, correlation effects included are usually rather limited for a practical reason related to the expense for calculating many higher-order perturbational terms. Moreover, most higher-order response properties tend to need higher-order correlation effects in order to result in correct results [2-8,22-23]. The time-dependent coupled-cluster (TDCC) analytical method presented here will be most appropriate for quantitative calculations of the higher-order response properties. Recently it has also been

pointed out that qualitative calculations of the higher-order polarizabilities for open-shell systems are difficult [3,30]. For these systems, the augmentations of the basis set seem to be mandatory. Further, for reasonable treatments of the properties of the systems which cannot be described adequately by a single-reference zeroth-order wavefunction, we would have to develop the present approach on the basis of the multi-reference CC (MRCC) method [34-37].

References

[1] P. Jørgensen and J. Simons, *Second Quantization Based Methods in Quantum Chemistry* (Academic Press, New York, 1981).

[2] R. J. Bartlett and G. D. Purvis III, Phys. Rev. **A20** (1979) 1313.

[3] C. A. Nicolaides, Th. Mercouris, G. Aspromallis, J. Opt. Soc. Am. **B7** (1990) 494.

[4] P. Chopra, L. Carlacci, H. F. King and P. N. Prasad, J. Phys. Chem. **93** (1989) 7120.

[5] E. Perrin, P. N. Prasad, P. Mougenot and M. Dupuis, J. Chem. Phys. **91** (1989) 4728.

[6] R. J. Bartlett and G. D. Purvis III, Phys. Rev. **A23** (1981) 1594.

[7] H. Sekino and R. J. Bartlett, J. Chem. Phys. **84** (1986) 2726 .

[8] H. Sekino and R. J. Bartlett, J. Chem. Phys. **85** (1986) 976.

[9] F. Coester, Nucl. Phys. **7** (1958) 421.

[10] F. Coester and H. Kümmel, Nucl. Phys. **17** (1960) 477.

[11] J. Cizek and J. Paldus, Int. J. Quantum Chem. **5** (1971) 359.

[12] J. Paldus, J. Cizek and I. Shavitt, Phys. Rev. **A5** (1972) 50.

[13] R. J. Bartlett and G. D. Purvis, Int. J. Quantum Chem. **16** (1978) 561.

[14] R. J. Bartlett, J. Phys. Chem. **93** (1989) 169.

[15] H. J. Monkhorst, Int. J. Quantum Chem. **S11** (1977) 421.

[16] E. Dalgaard and H. J. Monkhorst, Phys. Rev. **A28** (1983) 1217.

[17] H. P. Kelly, Adv. Chem. Phys. **14** (1969) 129.

[18] R. J. Bartlett and D. M. Silver, Int. J. Quantum Chem. **S9** (1978) 83.

[19] M. Nakano, K. Yamaguchi and T. Fueno, submitted for publication.

[20] H. J. Monkhorst and T. Zivkonic, J. Math. Phys. **19** (1978) 1007.

[21] H. Koch and P. Jørgensen, J. Chem. Phys. **93** (1990) 3333.

[22] C. W. Bauschlicher and P. R. Taylor, Theoret. Chim. Acta. **71** (1987) 263.

[23] G. Maroulis and A. J. Thakkar, Chem. Phys. Lett. **156** (1989) 87.

[24] M. Urban, I. Cernusak, V. Kello and J. Noga, Methods Comput. Chem. **1** (1987) 117.

[25] C. E. Dykstra, *Ab initio calculation of the structures and properties of molecules* (Elsevier, Amsterdam, 1988).

[26] C. Pouchan and D. M. Bishop, Phys. Rev. **A29** (1984) 1.

[27] S. Canuto, W. Duch, J. Geertsen, F. Müller-Plathe, J. Oddershede and G. E. Scuseria, Chem. Phys. Lett. **147** (1988) 435.

[28] V. Carravetta, H. Ågren, H. J. A. Jensen, P. Jørgensen and J. Olsen, J. Phys. **B22** (1989) 2133.

[29] D. P. Chong and S. P. Langhoff, J. Chem. Phys. **93** (1990) 570.

[30] E. F. Archibong and A. J. Thakkar, Chem. Phys. Lett. **173** (1990) 579.

[31] G. J. Hurst, M. Dupuis and E. Clementi, J. Chem. Phys. **89** (1988) 385.

[32] S. P. Karna and M. Dupuis, Chem. Phys. Lett. **171** (1990) 201.

[33] C. Daniel and M. Dupuis, Chem. Phys. Lett. **171** (1990) 209.

[34] D. Mukherjee, Chem. Phys. Lett. **125** (1986) 207. ;
Int. J. Quantum Chem. **S20** (1986) 409.

[35] U. Kaldor, Int. J. Quantum Chem. **S20** (1986) 445.

[36] S. Pal, M. Rittby, R. J. Bartlett, D. Sinha and D. Mukherjee, J. Chem. Phys. **88** (1988) 4357.

[37] M. Rittby, S. Pal and R. J. Bartlett, J. Chem. Phys. **90** (1989) 3214.

PART III

CALCULATIONS OF THE THIRD-ORDER HYPERPOLARIZABILITIES FOR ORGANIC NONLINEAR OPTICAL SYSTEMS

Introduction

Calculation methods as mentioned in parts I and II are used for the evaluation of the hyperpolarizabilities for several representative existing organic nonlinear systems. Nonlinear systems studied here are classified to the monomolecular, charge-transfer (CT) and polymeric systems. For these classified systems, each specific mechanism inducing the nonlinear optical effects are investigated and then some new models of nonlinear optical systems are proposed.

In chapter 1, the monomolecular systems are examined. Comparisons of the results obtained by the ab initio coupled-Hartree-Fock (CHF) and the semi-empirical uncoupled-Hartree-Fock (UCHF) and CHF calculations are carried out. It is well known that the augmented basis set is mandatory for the calculation of the semiquantitative hyperpolarizability of the small-size system. Therefore, the augmented basis set which is appropriate for the calculation of the third-order hyperpolarizability is presented.

In chapters 2-4, the static third-order hyperpolarizabilities (γ) of π-conjugated polyacetylene and polydiacetylene systems are calculated by the use of the TDPT(time-dependent perturbation theory), UCHF and CHF methods combined with the semi-empirical INDO approximation. Characteristics of γ calculated for these systems are investigated in relation to the chain-length effect. In the TDPT approach, three types of the virtual excitation processes for the systems are investigated. In CHF approach, the plotting of the third derivatives of the Mulliken charge densities (γ density analysis) against the electric field is proposed for the analysis of the spatial contributions of γ.

In chapter 5, the static third-order hyperpolarizabilities (γ_{yyyy}) of alternate donor (D)-acceptor (A) stacks and of segregated molecular stacks in the column direction are calculated by the CHF method based on the INDO approximation. It is found that both the mixed and the neutral/ionic segregated stacks exhibit large γ_{yyyy} values.

In chapter 6, the third-order organic nonlinear optical systems are classified based on the mechanism of the occurrence of third-order nonlinear effects and several appropriate calculation methods of their third-order hyperpolarizabilities (γ) are discussed. The criteria of the classification are the symmetry of charge distributions (centro- and noncentro-symmetric charge distributions) and the types of the interactions which induce the charge-transfer (CT) effects (through-bond and through-space interactions). Moreover, based on the classification, new types of polymeric systems with polar side chains which involve both the through-bond and through-space interactions are proposed.

Chapter 1

Ab initio and Semiempirical Calculations of the Third-order Hyperpolarizabilities for Centro- and Noncentro- Symmetric π-Conjugated Molecules

The static third-order hyperpolarizabilities are calculated for centro- and noncentro-symmetric π-conjugated systems via ab initio and semiempirical methods. The basis set augmentations to a standard 6-31G basis set are carried out at the ab initio coupled-Hartree-Fock (CHF) level. At the semiempirical level, the INDO Rayleigh-Schrödinger perturbation theory (RSPT), the CHF and CHF combined with Møller-Plesset second-order (MP2) perturbation theory are employed. Results for the INDO and ab initio CHF methods are in agreement qualitatively well each other. The γ density analysis is also employed to understand the spatial contributions of the γ values. This analysis reveals the differences of π and σ contributions, and of the contributions of α and β electrons in the case of the open-shell molecules.

1. Introduction

It has been recognized that the delocalized π-electrons contribute to the remarkable enhancement of the nonlinear polarizabilities [1,2]. The nonlinear systems with large nonlinear effects tend to possess noncentrosymmetric charge distributions [3,4]. These systems involve the intramolecular charge-transfer (CT) effects. In this work, the centro- and noncentro-symmetric systems are mainly examined.

In this report, several variational and perturbational approaches at the ab initio and semiempirical levels are employed. For the ab initio coupled-Hartree-Fock (CHF) and coupled-perturbed-Hartree-Fock (CPHF) methods [5-18], it is well known that the choice of basis set is very important for small molecules [5-9]. In the present work, the augmentations to the standard 6-31G basis sets for C, N and O atoms are performed according to the method by Hurst et al. [5]. It is expected that the nonlinear optical properties for small molecules are reproduced semiquantitatively well by ab initio CHF method with the augmented basis sets. For the aniline, nitrobenzene and *p*-nitroaniline, it is found that the qualitative agreements between the ab initio and semiempirical CHF values are achieved well.

There are indications that the electron correlation effects are somewhat larger for third-order hyperpolarizabilities [10,11,13,19,20]. Therefore, the Møller-Plesset second-order (MP2) perturbation theory [21] is employed combined with the INDO CHF calculations [22,23]. Further, the Rayleigh-Schrödinger perturbation theory (RSPT) [22,24,25] without electron-correlation effects is attempted. This method is referred to as the RSPT0 method [22] hereafter.

In the previous paper [22], we proposed the γ density analysis as a convenient procedure which can exhibit the spatial contributions of γ values. In this work, the γ density analysis at the semiempirical CHF level for π and σ electrons, and/or α and β electrons.

Details of the RSPT0 and CHF(+MP2) are the same as those described previously [22].

2. Calculated methods and systems

The ab initio and semiempirical methods are employed to obtain the third-order hyperpolarizabilities for the butadiene (a), diacetylene (b) and benzene (c) shown in Fig.1. Bond lengths and angles for butadiene (a), diacetylene (b), benzene (c) and dicyanoetylene (g) are taken from experimental data. The ab initio quantum chemistry program HONDO7 [26] is used. The selection of basis set is known to be very crucial for the calculation of the qualitatively correct γ value [5]. Hurst et al. proposed the basis set augmentation appropriate for the calculation of γ value in the chain direction for regular polyene [5]. In the present work, we extend the standard 6-31G basis for the C, N and O atoms nearly according to the method by Hurst et al. [5]. The diffuse *p* functions are generated from the most diffuse 6-31G exponents in the way that their ratio make a geometric series. The polarization *d* functions have the same exponents. These diffuse *p* and polarization *d* functions are added to the standard 6-31G basis sets for C, N and O atoms. The augmentation to the basis of H atom is not carried out since it little affects the γ values for the systems studied here. Details of the augmentations are given in Table 1. This augmented 6-31G basis set is referred to as the 6-31G+PD hereafter. At the semiempirical level, the INDO RSPT0, CHF and CHF+MP2 methods are employed. In the CHF method, the numerical differentiations are used. The minimum field strength is 0.005 a.u., which seems to be most appropriate to assess the calculated results.

mono- and di- Substituted benzenes with donor (D) and acceptor (A) groups; aniline (d), nitrobenzene (e) and *p*-nitroaniline (f), are examined. These molecular geometries are optimized at 6-31G+PD and 6-31+G [27]. These systems possess the noncentrosymmetric charge distributions. The CHF and CHF+MP2 methods are used for the calculations of the hyperpolarizabilities for these systems. Results by the ab initio CHF and CHF+MP2 methods with 6-31+PD and 6-31+G [28] are compared with the INDO calculated values.

The system (g) is trans-dicyanoethylene with centrosymmetric charge distributions. The INDO RSPT0, CHF and CHF+MP2 methods are applied to this system. The ionic trans-dicyanoethylene $(g)^-$ is also examined.

3. γ density analysis

The approximated γ_{zzzz} in the γ density analysis is expressed as follows [22] :

$$\gamma_{zzzz} \approx -\frac{1}{3!}\sum_{s} (\boldsymbol{PS})^{(3)}_{ss} q^z_s \,. \tag{1}$$

The q^z_s represents the z component of the coordinate of the atom located at the center of the atomic orbital s. The $(\boldsymbol{PS})_{ss}$ is the Mulliken charge density divided to the atomic orbitals s. $\boldsymbol{S}_{st}$ is the overlap matrix element and $\boldsymbol{P}_{st}$ is the bond order matrix element. This approximation implies that the charge densities are concentrated on the center of the atomic orbital s. The spatial characteristics of γ can be obtained by the use of the plots of the magnitude and sign of the γ density on each atom. The plus sign of the γ density implies that the second derivative of the charge density increases with the increase in the field, while the minus sign implies the inverse effect. In the γ density plot, the size of a circle on each atomic site indicates the magnitude of the γ_{zzzz} densities, while the black and white circles correspond to the increased and decreased γ_{zzzz} densities, respectively.

4. Results and discussion

4.1. Comparisons of several calculation methods for the small-size systems

The γ_{zzzz} values for butadiene (a), diacetylene (b) and benzene (c) calculated by the ab initio and INDO methods are listed in Table 2. The results from the ab initio CHF method are in

good agreement with the results of Chopra et al. [9]. The INDO method tends to give the smaller $|\gamma|$ values than the ab initio results. However, the qualitative tendencies of γ_{zzzz} values at the INDO level except the RSPT0 method for (a), (b) and (c) are in good agreement with those of the ab initio CHF values. The degree of the electron correlation effects at the INDO level is found to vary with the systems remarkably. For example, the γ_{zzzz} value for butadiene (a) at the INDO CHF+MP2 level is 2.0 times as large as the values at the ab initio CHF level, while the value for benzene (c) at the INDO CHF+MP2 level is 1.4 times as large as the values at the INDO CHF level.

4.2. Analysis of the contributions of π and σ electrons by the use of the γ density

For butadiene (a) and diacetylene (b), the plots of the γ_{zzzz} densities are employed to interpret their spatial characteristics. The results by the INDO CHF method are used. Figure 2 shows both the π - and σ - γ_{zzzz} densities. For butadiene (a), although the contributions of π - γ_{zzzz} densities for the central two C atoms and those for the C atoms at both ends are opposite in sign, the contributions of the central two C atoms are much larger than those of the C atoms at both ends. As a result, for both butadiene (a) and diacetylene (b), the π - γ_{zzzz} densities give large positive contributions, while the σ - γ_{zzzz} densities give small negative contributions. Therefore, in these systems, the characteristics of whole the γ_{zzzz} are determined mainly by the contributions of π electrons. The variations in γ_{zzzz} densities for diacetylene (b) indicate the non-local effects ranging from the right half of the molecule to the left half. These non-local separation of the γ_{zzzz} densities suggests the nonlinear dependence of γ value in the chain direction on the chain length.

4.3. Comparisons of the semiempirical and ab initio CHF methods for the medium-size noncentrosymmetric systems

By the large-scale ab initio calculations for the long regular polyenes, Hurst et al. pointed out that the basis augmentations are much less important with increasing chain length [5]. Considering from this fact, the CHF at the semiempirical level are expected to give the reasonable γ values for the medium and large-size systems. As the example of the noncentrosymmetric medium-size systems, aniline (d), nitrobenzene (e) and *p*-nitroaniline (f) are examined. The INDO calculated γ_{zzzz} values are listed in Table 3. From these results, the MP2 effects slightly increase the CHF results. In the INDO CHF and CHF+MP2 methods, the γ_{zzzz} values increase in the order : (d)<(e)<(f). In the ab initio CHF methods with 6-31G+PD basis and CHF+MP2 with 6-31+G basis, the γ_{zzzz} values increase in the same order : (d)<(e)<(f). In the CHF method, the ratios of the INDO/ab initio values are aniline (d) 0.16, nitrobenzene (e) 0.16, and *p*-nitroaniline (f) 0.27. In the CHF+MP2 method, the ratios of the INDO/ab initio values are aniline (d) 0.25, nitrobenzene (e) 0.15, and *p*-nitroaniline (f) 0.21. From these results, the semiempirical INDO method can simulate the ab initio hyperpolarizability with a scaling method. Both INDO and ab initio CHF+MP2 results indicated that the γ_{zzzz} values for nitrobenzene (e) are slightly larger than aniline (d), whereas the γ_{zzzz} values for *p*-nitroaniline (f) are about 5 times as large as the values for nitrobenzene (e). This implies that the intramolecular CT effects from D to A groups mainly contribute to enhance the total γ_{zzzz} values of *p*-nitroaniline (f). Ab initio CHF+MP2 calculations with 6-31G+PD basis are expected to investigate the γ_{zzzz} values for these systems more precisely.

From the spatial characteristics of the γ_{zzzz} densities for *p*-nitroaniline (f) by the INDO CHF method shown in Fig.2, the contributions of π and σ electrons are found to be opposite in sign. Large variations in the γ_{zzzz} densities on the amino and nitro groups are mainly related to these contributions. The contributions of π electrons, which are positive in sign, are much

larger than those of σ electrons, which are negative in sign, so that the net γ_{zzzz} comes to be positive in sign.

4.3. INDO CHF hyperpolarizability and the γ density analysis for the open-shell system

System (g) is the acceptor molecule with centrosymmetric charge distributions. The γ_{zzzz} values calculated by the INDO method are listed in Table 4. For the neutral and anion systems $(g)^0$ and $(g)^-$, the tendencies of the RSPT0 values agree well with those of the CHF values although the values by the CHF method are much smaller than those by the RSPT0 method. At the RSPT0 and CHF levels, the γ_{zzzz} value of ionic dicyanoethylene $(g)^-$ is found to be about twice as large as that of neutral dicyanoethylene $(g)^0$. At the CHF+MP2 level, in contrast to the results by the RSPT0 and CHF methods, the γ_{zzzz} value for the ionic dicyanoethylene $(g)^-$ is smaller than that of the neutral dicyanoethylene $(g)^0$. Ab initio CHF method has to be needed to confirm the above tendencies more precisely.

The γ_{zzzz} densities for $(g)^0$ and $(g)^-$ are illustrated in Figs.3. From the γ_{zzzz} densities for the neutral dicyanoethlene $(g)^0$, the central CC double bonds exhibit the negative contributions to the γ_{zzzz} value, whereas the cyano groups at both ends exhibit the positive contributions. From the definition of γ density, the contributions for more remote cyano groups from the center of the molecule are larger than those of the central CC double bonds, so that the total γ_{zzzz} value comes to be positive in sign. The γ_{zzzz} densities for the ionic dicyanoethlene $(g)^-$ are divided into the contributions of α and β electrons. It is found that the contributions of α electrons are distributed on the cyano groups, while those of β electrons are on the central CC double bonds and the N atoms in the cyano groups. The contributions of α electrons are positive in sign, while those of β electrons are negative in sign. The contributions of α electrons are larger than those of β electrons, so that the total γ_{zzzz} values come to be positive in sign. This implies that one excess α electron increase the γ_{zzzz} densities of α electron on

the cyano groups and those of β electrons on the central CC double bonds and the N atoms in the cyano groups.

From the large-scale ab initio calculations for the small-size molecules, it is noted that the augmentations of basis sets and the inclusions of the higher-order electron correlation effects are very important for the calculation of the hyperpolarizability for the anion system [16-18]. Ab initio CHF calculations based on the coupled-cluster (CC) theory [18] are now in progress to confirm the tendency of hyperpolarizabilities for the anion systems.

References

[1] *Nonlinear Optical Properties of Polymers*, edited by A. J. Heeger, J. Orenstein and D. R. Ulrich, Vol. **109** (Material Research Society Publication, Pittsburgh, 1988).

[2] *Nonlinear Optical Properties of Organic and Polymeric Materials*, edited by D. J. Williams (Am. Chem. Soc., Washington, D. C. , 1983).

[3] M. Nakano, M. Okumura, K. Yamaguchi and T. Fueno, Mol. Cryst. Liq. Cryst. **182A** (1990) 1.

[4] M. Nakano, K. Yamaguchi and T. Fueno, in *Nonlinear Optics of Organics and Semiconductors*, edited by T. Kobayashi, Springer Proceedings in Physics **36** (1989) 98 ; 103.

[5] G. J. B. Hurst, M. Dupuis and E. Clementi, J. Chem. Phys. **89** (1988) 385.

[6] C. J. Jameson and P. W. Fowler, J. Chem. Phys. **85** (1986) 3432 .

[7] P. A. Christiansen and E. A. McCullough, Chem. Phys. Lett. **51** (1977) 468.

[8] P. A. Christiansen and E. A. McCullough, Chem. Phys. Lett. **63** (1979) 570.

[9] P. Chopra, L. Carlacci, H. F. King and P. N. Prasad, J. Phys. Chem. **93** (1989) 7120.

[10] E. Perrin, P. N. Prasad, P. Mougenot and M. Dupuis, J. Chem. Phys. **91** (1989) 4728 .

[11] B. M. Pierce, J. Chem. Phys. **91** (1989) 791.

[12] C. P. de Melo and R. Silbey, Chem. Phys. Lett. **140** (1987) 537 ; J. Chem. Phys. **88** (1987) 2558, 2567.

[13] R. J. Bartlett and G. D. Purvis III, Phys. Rev. **A20** (1979) 1313.

[14] S. P. Karna and M. Dupuis, Chem. Phys. Lett. **171** (1990) 201.

[15] C. Daniel and M. Dupuis, Chem. Phys. Lett. **171** (1990) 209.

[16] C. A. Nicolaides, Th. Mercouris, G. Aspromallis, J. Opt. Soc. Am. **B7** (1990) 494.

[17] D. P. Chong and S. P. Langhoff, J. Chem. Phys. **93** (1990) 570.

[18] E. F. Archibong and A. J. Thakkar, Chem. Phys. Lett. **173** (1990) 579.

[19] J. R. Heflin, K. Y. Wong, O. Zamani-Khamiri and A. F. Garito, Phys. Rev. **B38** (1988) 1573.

[20] A. F. Garito and J. R. Heflin, K. Y. Wong and O. Zamani-Khamiri, in Organic Materials for Nonlinear Optics, edited by D. J. Andre and D. Bloor (1988).

[21] C. Møller and M. S. Plesset, Phys. Rev. **46** (1934) 618.

[22] M. Nakano, K. Yamaguchi and T. Fueno submitted.

[23] J. A. Pople and D. L. Beveridge, *Approximate Molecular Orbital Theory* (McGraw-Hill, New York, 1970).

[24] E. F. McIntyre and H. F. Hameka, J. Chem. Phys. **68** (1978) 3481 ; 5534 ; **69** (1978) 4814 ; **70** (1979) 2215.

[25] O. Zamani-Khamiri, E. F. McIntyre and H. F. Hameka, J. Chem. Phys. **71** (1979) 1607 ; **72** (1980) 1280 ; **72** (1980) 5906.

[26] M. Dupuis, J. D. Watts, H. O. Villar and G. J. B. Hurst, HONDO(7.0), available from QCPE, Indiana University.

[27] T. Clark, J. Chandrasekhar, G. W. Spitznagel and P. R. Schleyer, J. Comput. Chem. 4 (1983) 294.

[28] K. Ohta, T. Fukumi, T. Sakaguchi, M. Nakano, K. Yamaguchi and T. Fueno, unpublished.

Table 1. Exponents for diffuse and polarization Gaussian orbitals for 6-31G+PD.

Atom	*p*	*d*
C	0.05230	0.05230
N	0.05822	0.05822
O	0.07191	0.07191

Table 2. γ_{zzzz} values [a.u.] calculated by the ab initio and INDO methods for butadiene (a), diacetylene (b) and benzene (c).

System	Ab initio CHF	INDO		
		RSPT0	CHF	CHF+MP2
(a)	4316.3	426.3	372.0	743.3
(b)	3929.4	498.2	303.0	488.1
(c)	2336.7	255.5	140.2	191.6

Table 3. γ_{zzzz} values [a.u.] calculated by the ab initio and INDO methods for aniline (d), nitrobenzene (e) and *p*-nitroaniline (f) shown in Fig.1.

System	Ab initio		INDO		INDO/Ab initio	
	CHF [a)]	CHF+MP2 [b)]	CHF	CHF+MP2	CHF	CHF+MP2
(d)	5033.1	4452.6	817.9	1113.4	0.163	0.250
(e)	5804.2	7945.1	921.4	1195.1	0.159	0.150
(f)	16906.8	31993.7	4504.7	6830.9	0.266	0.214

a) 6-31G+PD basis set. Orbital exponents of augmented *p* and *d* functions are 0.0438 for C, 0.0639 for N and 0.0845 for O.

b) 6-31+G basis set [28].

Table 4. γ_{zzzz} values [a.u.] calculated by the INDO method for the neutral and ionic dicyanoethylenes $(g)^0$ and $(g)^-$.

System	INDO		
	RSPT0	CHF	CHF+MP2
$(g)^0$	202.4	34.7	362.8
$(g)^-$	451.5	77.7	276.9

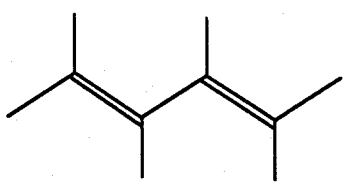

(a) Butadiene

(b) Diacetylene

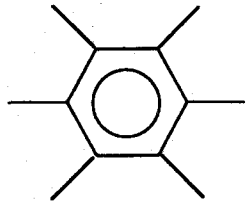

(c) Benzene

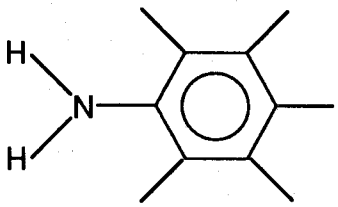

(d) Aniline

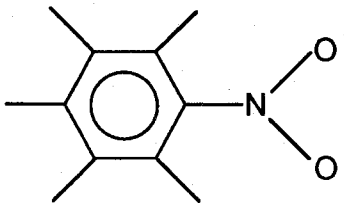

(e) Nitrobenzene

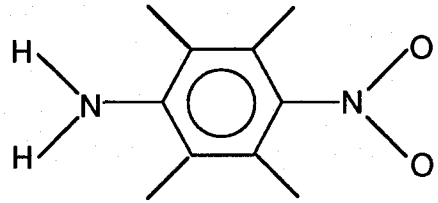

(f) *p*-Nitroaniline

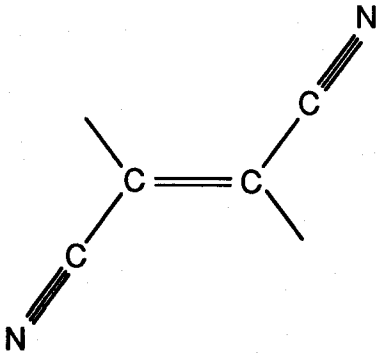

(g) Dicyanoethylene

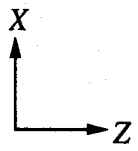

Fig.1. π-Conjugated molecules studied.

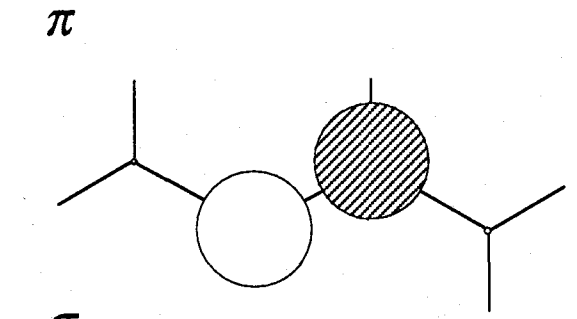

(a) Butadiene

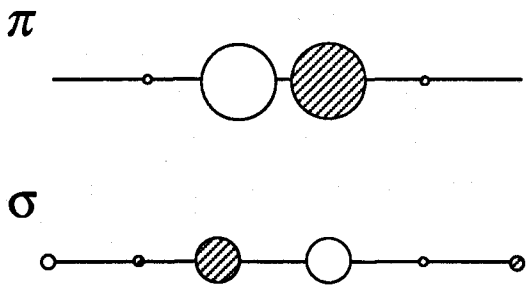

(b) Diacetylene

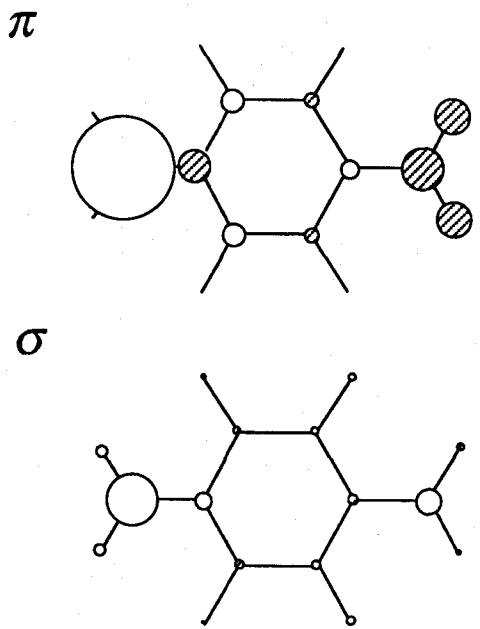

(f) *p*-Nitroaniline

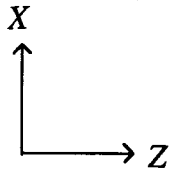

Fig.2. γ_{zzzz} densities contributed from π and σ electrons for butadiene (a), diacetylene (b) and *p*-nitroaniline (f).

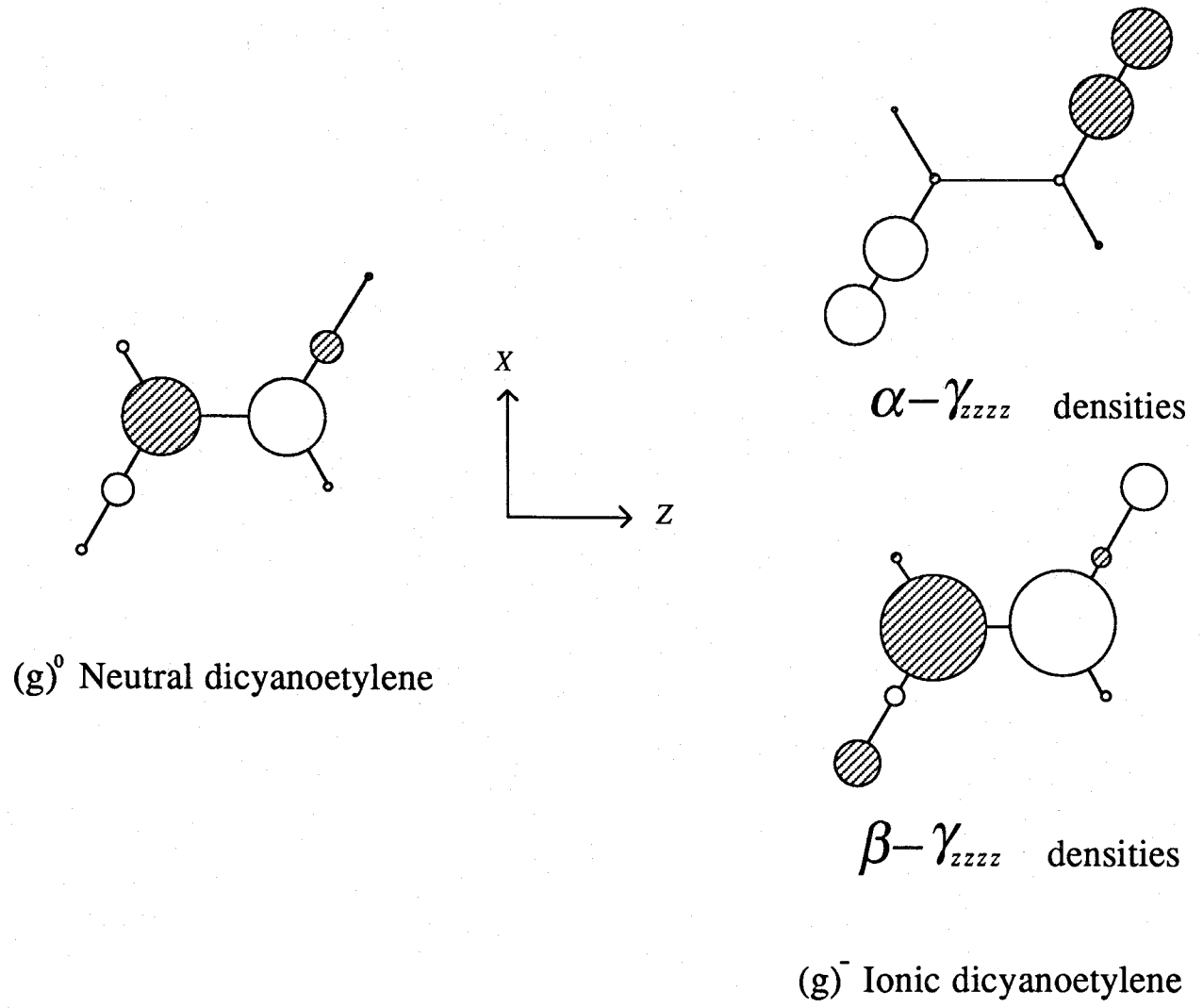

Fig.3. γ_{zzzz} densities for the neutral and ionic dicyanoethylenes $(g)^0$ and $(g)^-$.

Chapter 2

CNDO/S-CI Calculations of Hyperpolarizabilities : Regular Polyenes, Charged Polyenes, Disubstituted Polyenes, Polydiacetylene and Related Species

The analytic formula for the third-order hyperpolarizability $\gamma_{ijkl}(-3\omega;\omega,\omega,\omega)$ can be derived from the time-dependent perturbation theory. An approximate formula of γ_{ijkl} in a static electric field is presented here. The γ_{zzzz} values (the chain axis components) for regular polyenes, charged polyenes, donor(D)-acceptor(A) disubstituted polyenes, polydiacetylene and related species are evaluated by the use of several quantities calculated for low-lying excited states by the CNDO/S-CI method. The signs and magnitudes of γ_{zzzz} and the effects of variations in chain length are investigated on the basis of the calculated results. For regular polyenes, the calculated γ_{zzzz} values are positive and a power law dependence on the chain length N is found with an exponent of 4.14. In contrast, the calculated values of γ_{zzzz} for charged polyenes(+) are negative, but possess a similar N-dependence with an exponent of 4.44. The signs, magnitudes and N-dependences of γ_{zzzz} for disubstituted polyenes with donor(D) and acceptor(A) groups and polydiacetylene are discussed in relation to the experimental data available.

1. Introduction

The third-order hyperpolarizability $\gamma_{ijkl}(-3\omega;\omega,\omega,\omega)$ has been receiving intense interest recently. The analytic expression for $\gamma_{ijkl}(-3\omega;\omega,\omega,\omega)$ is derived here from time-dependent perturbation theory [1] in a similar fashion to the derivation of the second-order hyperpolarizability $\beta_{ijk}(-2\omega;\omega,\omega)$ treated in previous papers [2,3]. However, the expression for $\gamma_{ijkl}(-3\omega;\omega,\omega,\omega)$ is considerably more complex and the higher excited states contribute to γ_{ijkl} significantly. Therefore, approximations of terms in the full formula of $\gamma_{ijkl}(-3\omega;\omega,\omega,\omega)$ are presented. The approximations clarify the virtual excitation processes [4,5] for the third-order nonlinear coefficients, and reduce the labors of calculation on the basis of the full formula. The approximate formula is applied to the evaluation of the γ_{zzzz} values (the chain axis components) for relatively short π-conjugated compounds. As previously [2,3], the excitation energies, transition moments and the differences of dipole moments between excited and ground states are calculated by the CNDO/S single-excitation CI (SCI) procedure.

There are three objectives of this study : first, to examine the magnitudes and signs of the γ_{zzzz} values for regular polyenes and charged polyenes (+) and (-) and to clarify their dependences on the number N of carbon-atom sites [7-9]; second, to investigate the γ_{zzzz} values for disubstituted polyenes with donor(D)-acceptor(A), D-D, A-A groups and related species; and third, to calculate the γ_{zzzz} values for polydiacetylene and to examine the calculated results in relation to the experiments [10,11].

2. Theoretical Methods

A theoretical formulation for the third-order hyperpolarizability $\gamma_{ijkl}(-3\omega;\omega,\omega,\omega)$ is given by time-dependent perturbation theory [1]. However, the full expression for $\gamma_{ijkl}(-3\omega;\omega,\omega,\omega)$ is too complicated to provide a clear picture of the virtual excitation processes [4,5]. Thus, the processes have been separated into three different contributions [5] as shown in

Fig.1. In order further to clarify the characteristics of the processes, the following approximations are introduced : (1) in compounds with π-conjugated linear chains, the chain axis component of $\gamma_{ijkl}(-3\omega;\omega,\omega,\omega)$ is assumed to be predominant, so that $\gamma_{iiii}(-3\omega;\omega,\omega,\omega)$, which corresponds to $\gamma_{zzzz}(-3\omega;\omega,\omega,\omega)$, is adopted as the characteristic quantity of the third-order hyperpolarizability; (2) for contributions of type (I) in Fig.1, all terms are considered; (3) for contributions of type (II) in Fig.1, the predominant term is considered to be the process ($0n$-$n0$-$0n$-$n0$). When n is set to n', the term obtained is denoted type (II)'; (4) for contributions of type (III) in Fig.1, a reduction to the process ($0n$-nm-mn-$n0$) is made by eliminating the terms with $n\neq n'$ from the process ($0n'$-$n'm$-mn-$n0$). The reduced term is then denoted type (III)'.

Approximations (3) and (4) are illustrated in Fig.2. These are considered to be reliable unless many higher excited states contribute to the third-order nonlinear excitation processes. Approximations (3) and (4) are expected to be applicable to small molecules and/or relatively short conjugated chains. The approximate analytic formula for $\gamma_{iiii}(-3\omega;\omega,\omega,\omega)$ is given, using the above approximations, as

$$\gamma_{iiii}(-3\omega;\omega,\omega,\omega) =$$

$$\left.\sum_{n=1}(\mu^i_{n0})^2(\Delta\mu^i_{n0})^2\frac{E_{n0}(E_{n0}^2+(\hbar\omega)^2)}{(E_{n0}^2-(3\hbar\omega)^2)(E_{n0}^2-(2\hbar\omega)^2)(E_{n0}^2-(\hbar\omega)^2)}\right\}\text{(I)}$$

$$\left.-\sum_{n=1}(\mu^i_{n0})^4\frac{E_{n0}}{(E_{n0}^2-(3\hbar\omega)^2)(E_{n0}^2-(\hbar\omega)^2)}\right\}\text{(II)'}$$

$$\left.+\sum_{\substack{m,n=1\\ m\neq n}}(\mu^i_{n0})^2(\mu^i_{mn})^2\frac{E_{n0}^2E_{m0}+4E_{n0}(\hbar\omega)^2-3E_{n0}(\hbar\omega)^2}{(E_{n0}^2-(3\hbar\omega)^2)(E_{n0}^2-(\hbar\omega)^2)(E_{m0}^2-(2\hbar\omega)^2)}\right\}\text{(III)'} \quad (1)$$

In the case of a static electric field, Eq.(1) is reduced to Eq.(2).

$$\gamma_{iiii}(-0;0,0,0) = \sum_{n=1} \frac{(\mu_{n0}^{i})^2(\Delta\mu_{n0}^{i})^2}{E_{n0}^{3}} - \sum_{n=1} \frac{(\mu_{n0}^{i})^4}{E_{n0}^{3}} + \sum_{\substack{m,n=1 \\ m\neq n}} \frac{(\mu_{n0}^{i})^2(\mu_{mn}^{i})^2}{E_{n0}^{2}E_{m0}}, \qquad (2)$$

where the first, second and third terms correspond to the type (I), type (II)' and type (III)' contributions of Fig.1, respectively. From Eq.(2), the terms expressed by type (I) and type (III)' contributions are positive in sign, while the type (II)' contribution is a negative. Therefore, the overall sign of γ_{iiii} is determined by the detailed balance between the (I+III')- and (II')-terms.

In order to calculate γ_{iiii} by the use of Eq.(2), the excitation energies (E_{n0}), transition moments (μ_{0n}, μ_{nm}) and the differences of dipole moments (μ_{nm}) between excited and ground states are needed to be known. Here, the CNDO/S approximation [6] including the single-excitation configuration interaction (SCI) is employed to calculate these quantities. In these SCI calculations [2,3], only the π electron orbitals are included because π-π^* excitations contribute predominantly to low-lying excited states and because the π-electron contribution to γ_{ijkl} is known to be more dominant than the σ-electron contribution [4,5].

3. Results

Organic systems studied here are schematically shown in structural formula (A)-(I) of Fig.3. The compounds are placed on the z-x plain, and the coordinate z axis is chosen along the chain axis. Under this assumption, a dominant component of γ_{ijkl} is given by γ_{zzzz}. Bond lengths and bond angles for these systems are assumed on the basis of experimental data and the bond alternation has been taken into account. For regular polyenes, lengths of 1.35 and 1.45 Å are assumed for the double and single bonds, respectively. For the charged polyenes, it

is assumed that the alternation between single and double bonds is inverted at the center of the chain.

Table 1 summarizes the γ_{zzzz} values in a static electric field and the values of the three types of contribution for the varying number N of carbon-atom sites in systems (A)-(I). Figures 4-12 show the log-log plots of the absolute value of γ_{zzzz}, i.e., $|\gamma_{zzzz}|$, and each part of $|\gamma_{zzzz}|$ versus the number N of carbon-atom sites. Table 2 shows virtual excitation process which makes the most dominant contribution to each part, together with the γ_{zzzz} values at N=9 for (B), (C), (G) and at N=8 for the remaining systems.

From the calculated results, it is seen : (a) that the first excited state is predominant in type (I) and type (II)' contributions; (b) that both the first and second excited states are contribute to type (III)' contributions in centrosymmetric systems such as a regular polyene; and (c) that plurality of excited states, including a few higher states, contribute to type (III)' contributions in noncentrosymmetric systems such as a D-A disubstituted polyene.

The contributions of type (I) for the regular polyene (A) are found to be zero since the $\Delta\mu$ disappears because of the centrosymmetric structure. In type (II)' and (III)' contributions for the regular polyene (A), the absolute values of the type (III)' contribution are larger than those of the part (II)' contribution, so that the net γ_{zzzz} values are positive in sign. In this system, the process (01-10-01-10) is dominant in the type (II)' contribution while the process (01-12-21-10) is dominant in the type (III)' contribution throughout all the numbers N of carbon-atom sites. Figure 4 shows that the calculated values of type (II)', type (III)' and γ_{zzzz} all fit well expressions of the form:

$$\gamma_{zzzz} = a N^{k} . \qquad (3)$$

From Fig.4, these terms have power law dependences on the number N of carbon-atom sites with exponents (k) of 4.09, 4.10 and 4.14, respectively. The results are in good agreement with the previously reported results [4,7-9].

Ab initio calculations of γ_{ijkl} in a static electric field for regular polyenes have been carried out by Hurst et.al. [12]. Their calculations using the CPHF method give γ_{ijkl} in a static electric field by differentiating the ground state energy at the Hartree-Fock level obtained variationally in the presence of an electric field. They investigate the dependences of some basis sets on γ_{ijkl} and propose the basis set named 6-31G+PD by which reasonable results of the chain axis component can be obtained. In order to compare their results with those obtained by the present authors, the chain axis components were calculated from their equation of extrapolation and their values are plotted together with our results in Fig.13. Our γ_{zzzz} are about 60% of their values at the 6-31G+PD. As for the dependence of γ_{zzzz} on N, our k value (4.14) agrees well with theirs (k=3.91) at 6-31G+PD. This suggests that the three-type approximation with CNDO/S-CI method is appropriate to reproduce the dependences of γ_{zzzz} on chain length of medium-size polyenes, which are obtained by the large scale ab initio CPHF method with the augmented basis sets.

The calculated results for the charged polyenes (+) (B) show that the |type (I)| values are zero because of the centrosymmetric structure as in the case of regular polyenes, while the |type (II)'| values are larger than |type (III)'| values unlike the regular polyene, resulting in a γ_{zzzz} that is negative in sign. The result is in good accord with the calculated result for the charged soliton (+) reported by Silbey et.al. [7-9]. From Fig.5, it is seen that |type (II)'|, |type (III)'| and $|\gamma_{zzzz}|$ of charged polyene (+) have the power law dependences on N with the exponents 4.57, 4.61 and 4.44, respectively. Similarly, Fig.6 shows that |type (II)'|, |type (III)'| and $|\gamma_{zzzz}|$ of charged polyene (-) exhibit similar power law dependences with the exponents 4.25, 4.26 and 4.25, respectively.

The system (F) represents the largest $|\gamma_{zzzz}|$ value among the disubstituted systems: (D) with amino groups as electron donors, (E) with nitro groups as acceptors and (F) with both amino and nitro groups. The γ values decrease in the order: (F) > (E) > (D), as shown in Table 1. However, the N dependences of $|\gamma_{zzzz}|$ in Figs.7-9 show that k values for (D), (E) and (F) are 3.64, 2.37 and 2.70, respectively. From comparison with the N dependence of each part for the regular polyenes (A), it is found that system (D) exhibits smaller N dependences of E_{10} and E_{20} than system (A), and that the N dependences of E_{10}, E_{20} and $|\mu_{12}|$ for system (E) are smaller than those of system (A). Since D-A disubstituted system (F) is not centrosymmetric in structure, the contribution of type (I) to (F) is not zero, whereas types (II)' and (III)' contributions are nearly cancelled as shown in Fig.9. Therefore, the N dependence of |type (I)| contribution seems to be reflected mainly in the N dependence of the total $|\gamma_{zzzz}|$ value of (F).

It seems that the dipole moment difference ($\Delta\mu$) most contributing to type (I) contributions, is not simply proportional to the number N of carbon-atom sites. This behavior of $\Delta\mu$ is responsible for the smaller N dependence of $|\gamma_{zzzz}|$ for system (E). In fact, in the D-A disubstituted polyene, the charge displacement by the 0-1 transition increases linearly with N in the case of short chains, whereas the charge for long chains is more or less localized in the vicinity of the carbon-atom sites connected with D and A substituted groups, rather than showing a direct charge transfer from a D to an A group. Consequently, $\Delta\mu$ causes the saturation for long chains.

For the system (G) with a carbonyl group at the middle of the chain, $|\gamma_{zzzz}|$ values are positive in sign. In this system, the $|\mu_{01}|$ and $|\mu_{12}|$ are smaller than those for the charged polyenes. In Fig.10, |type (II)'| exhibits a larger N dependence than does |type (III)'|. Hence, the N dependence of $|\gamma_{zzzz}|$ is calculated to be small (k=3.29).

γ_{zzzz} values for system (H), which has a C=N backbone, become larger than those of the regular polyene. From Fig.11, the N dependence of $|\gamma_{zzzz}|$ is the largest with k=4.53 among all the calculated systems except for the polydiacetylene. This large third-order hyperpolarizability is probably due to the large polarization in the main chain. Ab initio calculations such as CPHF are necessary to confirm this tendency.

The k values for the polydiacetylene (I) are found to be 6.67, 6.36 and 6.85, respectively, from the N dependences of |type (II)'|, |type (III)'| and $|\gamma_{zzzz}|$ shown in Fig.12. The magnitudes of k are the largest among all the calculated systems. The γ_{zzzz} values for system (I) are, however, enormously negative. This is attributable to the N dependences of the transition moments ($|\mu_{01}|$, $|\mu_{12}|$) and the excitation energies (E_{10}, E_{20}); i.e., the $|\mu_{01}|$ values are much larger than $|\mu_{12}|$ and the N dependences of $|\mu_{01}|$ and E_{20} are larger than those of $|\mu_{12}|$ and E_{10}, respectively. Probably these differences are the origins of the characteristic behavior of γ_{zzzz} values for polydiacetylene system (I).

4. Discussion and Conclusions

These CNDO/S-CI calculations show that the approximate formula Eq.(2) is sufficiently reliable in reproducing the tendencies for γ_{zzzz} observed for relatively short π conjugated linear chains [5]. Table 3 summarizes the dependences of |type (II)'|, |type(III)'| and total $|\gamma_{zzzz}|$ on the number N of the carbon-atom sites, and the signs of γ_{zzzz} for all the systems treated here.

From Table 3, it is seen that the signs of γ_{zzzz} for the charged polyenes (B) and (C) are opposite to those for the regular polyenes and that their dependences(k) are larger than those for the regular polyenes. These tendencies seem to be attributable mainly to the fact that $|\mu_{01}|$ is smaller than $|\mu_{12}|$ in the case of the regular polyenes, while $|\mu_{01}|$ for charged polyenes become large owing to the charge transfer from the neutral carbon sites to the charged site, so that |type (II)'| dominates over |type (III)'|.

For the systems disubstituted by donor (D) and acceptor (A) groups, it is proved that $|\gamma_{zzzz}|$ values are larger than those for the regular polyenes, although the N dependences become smaller for the former systems. The present calculations demonstrate that the $|\gamma_{zzzz}|$ values for D-A disubstituted polyenes are determined mainly by the type (I) contribution because of the cancellation of type (II)' and (III)' contributions. The calculations also indicate that the type (I) contribution is affected primarily by the $|\Delta\mu|$ value. It suffers saturation in long chain systems because the charge localization in the vicinity of the carbon-atom sites connected with the D- and A- groups occurs with the increase of the number N of carbon-atom sites. This tendency probably leads to the characteristic behaviors of γ_{zzzz} concluded for D-A disubstituted polyenes.

However, in the system (H), which might be expected to show the same characteristics as do the D-A disubstituted system, it is found that a large charge displacement in the main chain provides a large $|\gamma_{zzzz}|$ value, and furthermore, that the N dependence of $|\gamma_{zzzz}|$ does not exhibit so much saturation in contrast to the case of D-A disubstituted polyenes. It is suggested that synthesis of type (H) compounds is worth attempting.

For the polydiacetylene system (I), the calculated γ_{zzzz} values are found to be negative in sign, and their magnitudes and the N dependences exhibit the largest values in all the calculated systems. According to the recent experiments [10,11], the signs of γ observed for this system are variable from plus to minus, depending on the experimental conditions. This suggests that the γ value of the system is very sensitive to subtle changes in the molecular structure and environmental effects. As can be seen from Eq.(2), small changes for relationships of the magnitudes between type (II)' contributions and the other types can induce an inversion of the sign of γ_{zzzz}. In fact, the present calculations do indicate that the introduction or elimination of charge at the center of polyene, which corresponds to the case of charged polyenes here, can change the sign, magnitude and the dependence of γ_{zzzz} on N.

Therefore, it is not surprising that the inversion of the sign of γ_{zzzz} occurs with small changes of the molecular structure for the polydiacetylene systems.

In conclusion, the approximate formula Eq.(2) derived here is suitable for effective computation and analysis of the third-order hyperpolarizability $\gamma_{ijkl}(-3\omega;\omega,\omega,\omega)$ for organic molecules, such as long chain polyenes with donor and acceptor groups. The CNDO/S-SCI method employed in the present calculations provides reasonable results at least in qualitative sense. However, more careful examination of the contributions of double excitations [4,5] will be necessary in the case of long polyenes. Ab initio calculations are also desirable for confirmation of the qualitative tendencies revealed by the present CNDO/S-SCI calculations. They are in progress in this laboratory.

References

[1] J. A. Armstrong, N. Bloembergen, J. Ducuing and P. S. Pershan, Phys. Rev. **127** (1962) 1918.

[2] M. Nakano, K. Yamaguchi and T. Fueno, ' *CNDO/S-CI Calculations of Hyperpolarizabilities. I.*' : in *Nonlinear Optics of Organics and Semiconductors*, edited by T. Kobayashi, Springer Proceedings in Physics. 36 (1989) 98.

[3] M. Nakano, K. Yamaguchi and T. Fueno, ' *CNDO/S-CI Calculations of Hyperpolarizabilities. I.* ' in : *Nonlinear Optics of Organics and Semiconductors*, edited by T. Kobayashi, Springer Proceedings in Physics. 36 (1989) 103.

[4] J. R. Heflin, K. Y. Wong, O. Zamani-Khamiri and A. F. Garito, Phys. Rev. **B38** (1988) 1573 .

[5] A. F. Garito and J. R. Heflin, K. Y. Wong and O. Zamani-Khamiri, in : *Organic Materials for Nonlinear Optics*, edited by R. A. Hann and D. Bloor, Special Publication No. **69** (Royal Society of Chemistry, London, 1988).

[6] J. Del Bene and H. H. Jaffe, J. Chem. Phys. **48** (1968) 1807.

[7] C. P. de Melo and R. Silbey, Chem. Phys. Lett. **140** (1987) 537.

[8] C. P. de Melo and R. Silbey, J. Chem. Phys. **88** (1988) 2558.

[9] C. P. de Melo and R. Silbey, J. Chem. Phys. **88** (1988) 2567.

[10] F. Kajar and J. Messier, in : *Polydiacetylenes*, NATO ASI ser. **E102**, 325, eds. D. Bloor and R.R. Chance (Nijhoff, The Hague, 1985).

[11] G. M. Carter, Y. J. Chen and S. K. Tripathy, Appl. Phys. Lett. **43** (1983) 841.

[12] GJ. B. Hurst, M. Dupuis and E. Clementi, J. Chem. Phys. **89** (1988) 385.

Table 1. Calculated values of the three types of contribution and the total γ_{zzzz} x 10^{36} [esu] for system (A)-(I).

(A)

N	0,*n*-*n*,*n*-*n*,*n*-*n*,0	0,*n*-*n*,0-0,*n*-*n*,0	0,*n*-*n*,*m*-*m*,*n*-*n*,0	Total
4	0.0	-2.09	2.98	0.887
6	0.0	-12.0	17.5	5.60
8	0.0	-39.3	58.1	18.8
10	0.0	-94.0	138	43.9
12	0.0	-184	266	81.9

(B)

N	0,*n*-*n*,*n*-*n*,*n*-*n*,0	0,*n*-*n*,0-0,*n*-*n*,0	0,*n*-*n*,*m*-*m*,*n*-*n*,0	Total
5	0.0	-9.18	6.86	-2.33
9	0.0	-145	111	-33.8
13	0.0	-712	551	-160

(C)

N	0,*n*-*n*,*n*-*n*,*n*-*n*,0	0,*n*-*n*,0-0,*n*-*n*,0	0,*n*-*n*,*m*-*m*,*n*-*n*,0	Total
5	0.0	-14.2	11.6	-2.59
9	0.0	-184	150	-33.8
13	0.0	-822	673	-149

(D)

N	0,*n*-*n*,*n*-*n*,*n*-*n*,0	0,*n*-*n*,0-0,*n*-*n*,0	0,*n*-*n*,*m*-*m*,*n*-*n*,0	Total
4	0.0	-6.27	8.22	1.86
6	0.0	-25.6	35.1	9.47
8	0.0	-68.9	96.3	27.4
10	0.0	-145	203	57.9
12	0.0	-261	361	99.3

(E)

N	0,*n*-*n*,*n*-*n*,*n*-*n*,0	0,*n*-*n*,0-0,*n*-*n*,0	0,*n*-*n*,*m*-*m*,*n*-*n*,0	Total
4	0.0	-7.61	19.8	12.2
6	0.0	-33.2	67.1	33.9
8	0.0	-91.7	157	65.0
10	0.0	-194	305	111
12	0.0	-347	514	166

(F)

N	0,*n*-*n*,*n*-*n*,*n*-*n*,0	0,*n*-*n*,0-0,*n*-*n*,0	0,*n*-*n*,*m*-*m*,*n*-*n*,0	Total
4	14.8	-7.46	9.58	17.0
6	42.7	-30.6	38.0	50.1
8	90.4	-82.4	102	110
10	157	-172	216	202
12	237	-304	394	327

(G)

N	0,*n*-*n*,*n*-*n*,*n*-*n*,0	0,*n*-*n*,0-0,*n*-*n*,0	0,*n*-*n*,*m*-*m*,*n*-*n*,0	Total
5	0.0	-1.01	4.29	3.28
9	0.0	-18.8	45.8	27.1
13	0.0	-96.1	170	73.4

(H)

N	0,*n*-*n*,*n*-*n*,*n*-*n*,0	0,*n*-*n*,0-0,*n*-*n*,0	0,*n*-*n*,*m*-*m*,*n*-*n*,0	Total
4	1.05	-1.04	1.55	1.57
6	6.83	-5.29	9.59	11.1
8	23.2	-15.1	32.0	40.1
10	52.5	-32.0	77.2	97.7

(I)

N	0,*n*-*n*,*n*-*n*,*n*-*n*,0	0,*n*-*n*,0-0,*n*-*n*,0	0,*n*-*n*,*m*-*m*,*n*-*n*,0	Total
4	0.0	-26.9	11.8	-15.1
8	0.0	-1210	557	-659
12	0.0	-16000	5040	-11000

Table 2. More or most contributing process (according to type contribution) to γ_{zzzz} for (A)-(I)[a].

System	(I)	(II)'	(III)'
(A)		01-10-01-10	01-12-21-10
		(-39.3)	(50.0)
(B)		01-10-01-10	01-12-21-10
		(-145)	(76.8)
(C)		01-10-01-10	01-12-21-10
		(-184)	(107)
(D)		01-10-01-10	01-12-21-10
		(-68.9)	(81.4)
(E)		01-10-01-10	01-12-21-10
		(-91.6)	(102)
(F)	01-11-11-10	01-10-01-10	01-12-21-10
	(87.2)	(-81.9)	(20.2)
			01-13-31-10
			(44.6)
(G)		01-10-01-10	01-12-21-10
		(-18.3)	(19.4)
(H)	01-11-11-10	01-10-01-10	01-12-21-10
	(22.2)	(-14.9)	(21.7)
(I)		01-10-01-10	01-12-21-10
		(-16000)	(4870)

a) $\gamma_{zzzz} \times 10^{36}$ [esu] values of the contributions in three parts are shown in parentheses.

Table 3. k Values and the signs of γ_{zzzz} for (A)-(I).

System	k(I)	k(II)'	k(III)'	k(Total)	Sign of γ_{zzzz}
(A)		4.09	4.10	4.14	+
(B)		4.57	4.61	4.44	−
(C)		4.25	4.26	4.25	−
(D)		3.40	3.46	3.64	+
(E)		3.49	2.97	2.37	+
(F)	2.54	3.39	3.39	2.70	+
(G)		4.78	3.87	3.29	+
(H)	4.29	3.76	4.27	4.53	+
(I)		6.67	6.36	6.85	−

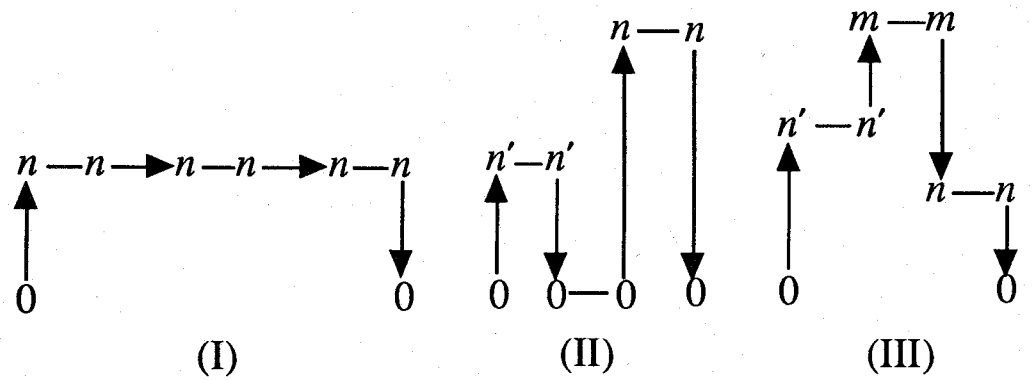

Fig.1. Three types of contributing terms to γ

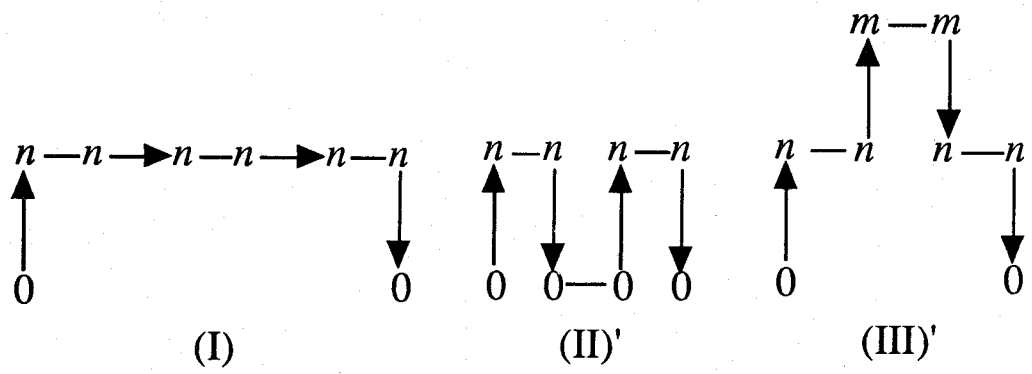

Fig.2. Approximation of terms illustrated by types (II) and (III) contributions in Fig.1.

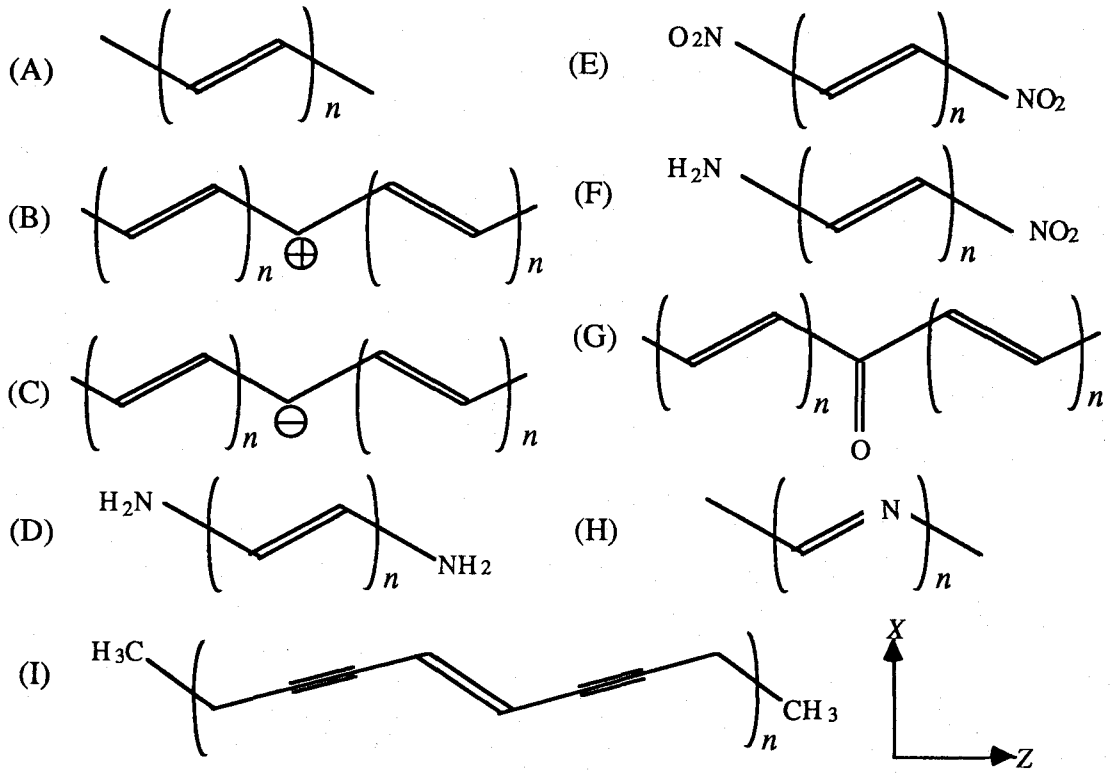

Fig.3. Schematic diagrams of the systems studied .

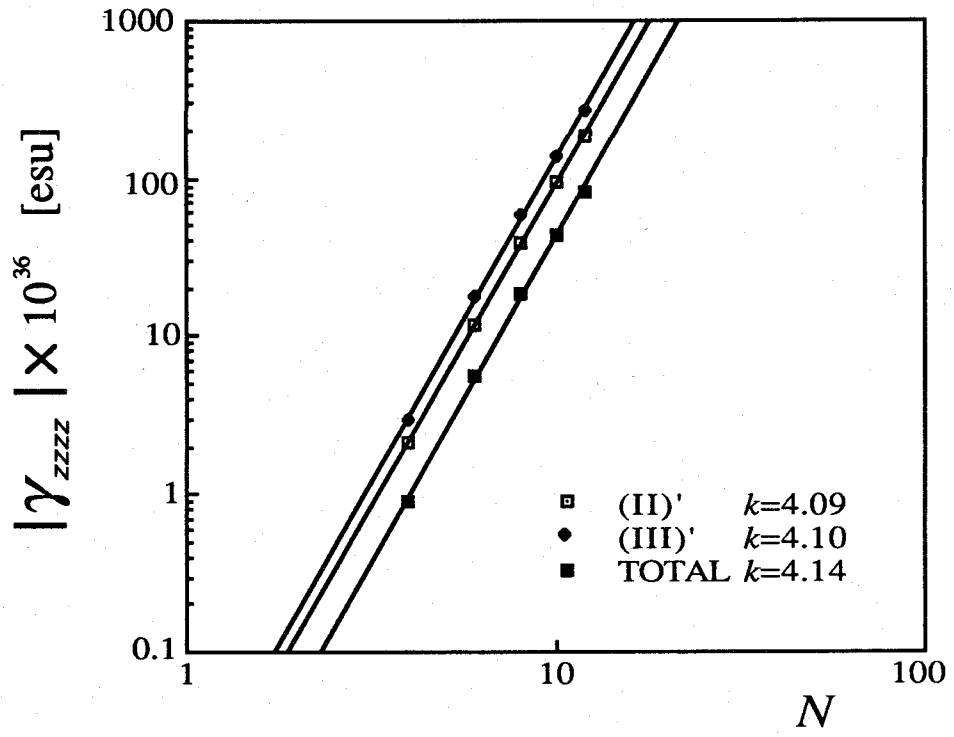

Fig.4. log -log plot of $|\gamma_{zzzz}|$ versus the number of carbon atoms N for (A). k ; slope

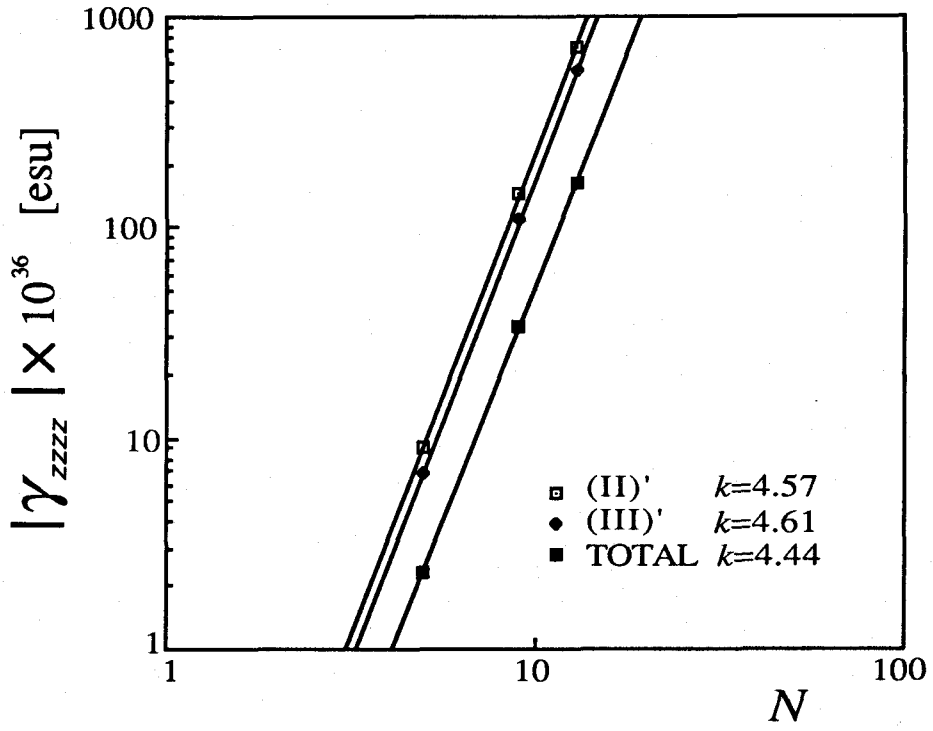

Fig.5. log -log plot of $|\gamma_{zzzz}|$ versus the number of carbon atoms N for (B). k ; slope

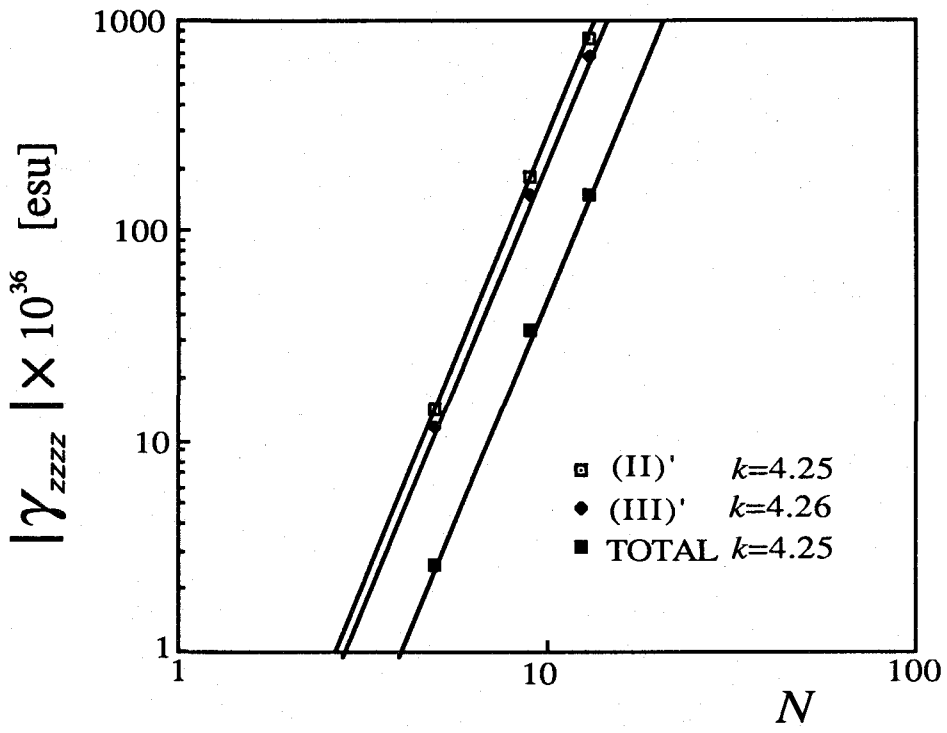

Fig.6. log -log plot of $|\gamma_{zzzz}|$ versus the number of carbon atoms N for (C). k ; slope

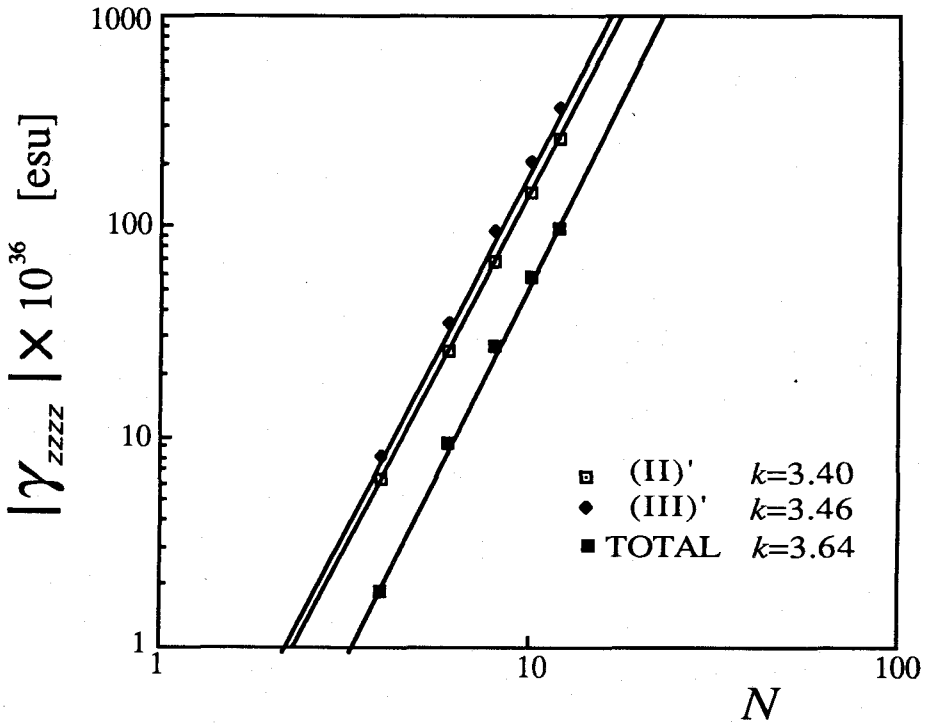

Fig.7. log -log plot of $|\gamma_{zzzz}|$ versus the number of carbon atoms N for (D). k; slope

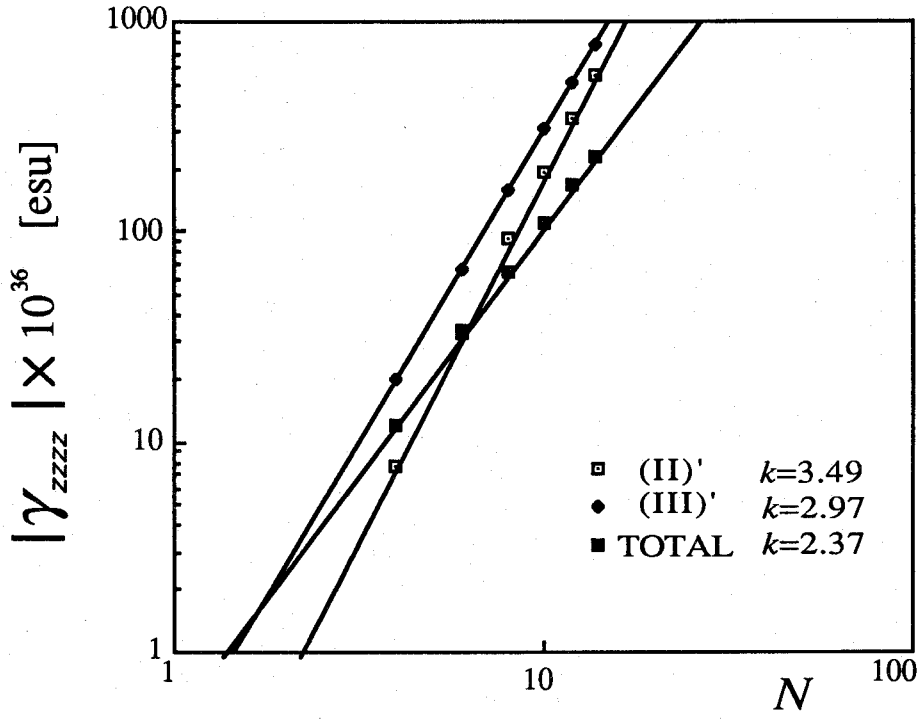

Fig.8. log -log plot of $|\gamma_{zzzz}|$ versus the number of carbon atoms N for (E). k ; slope

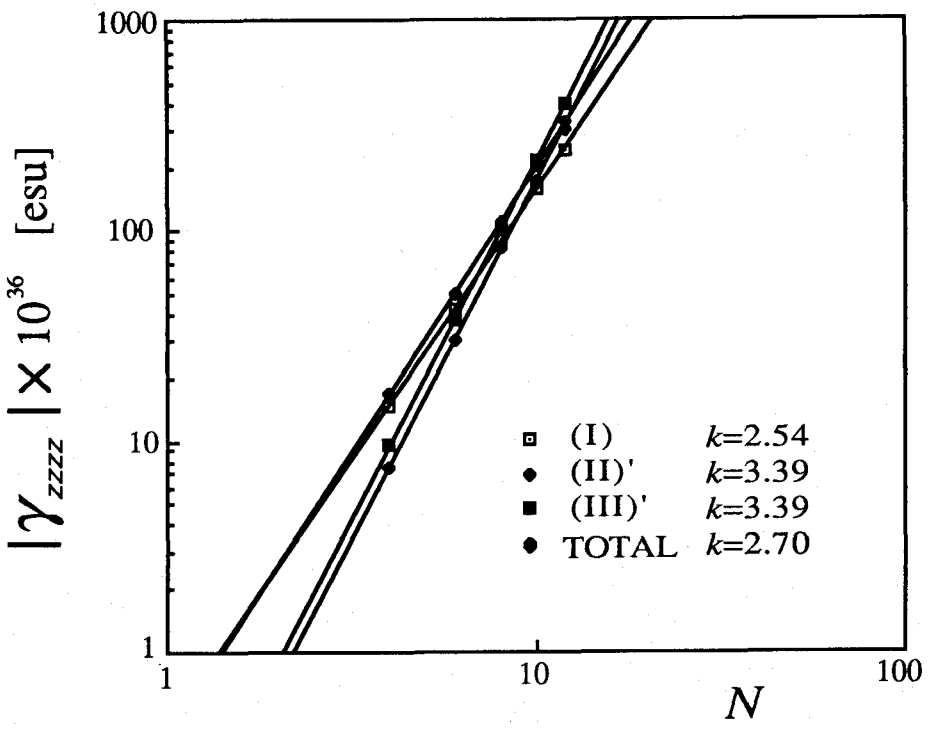

Fig.9. log -log plot of $|\gamma_{zzzz}|$ versus the number of carbon atoms N for (F). k ; slope

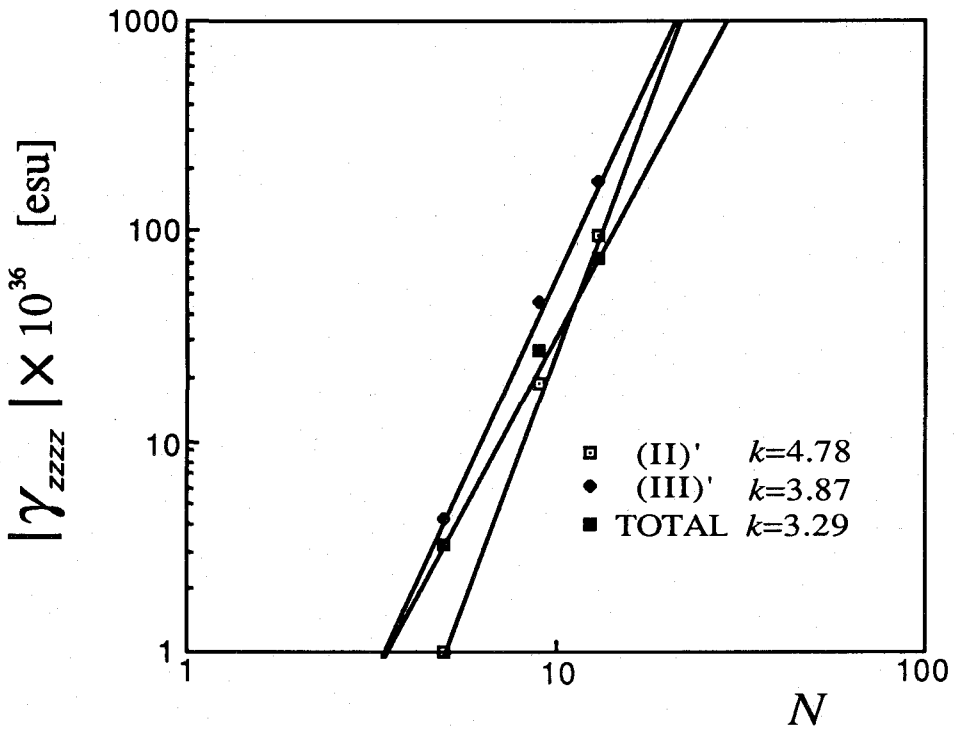

Fig.10. log -log plot of $|\gamma_{zzzz}|$ versus the number of carbon atoms N for (G). k; slope

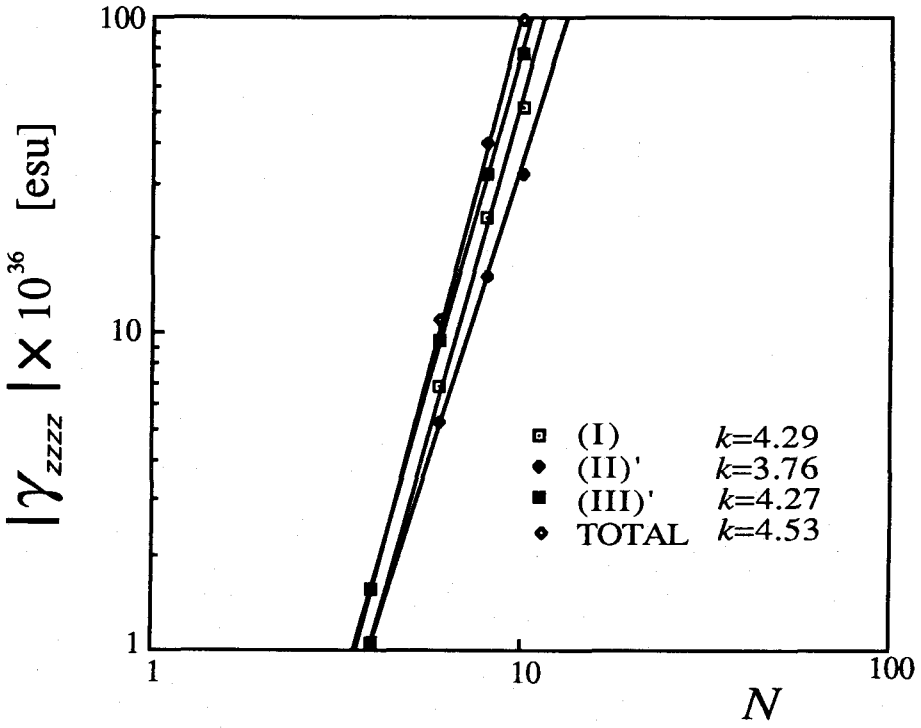

Fig.11. log -log plot of $|\gamma_{zzzz}|$ versus the number of carbon atoms N for (H). k; slope

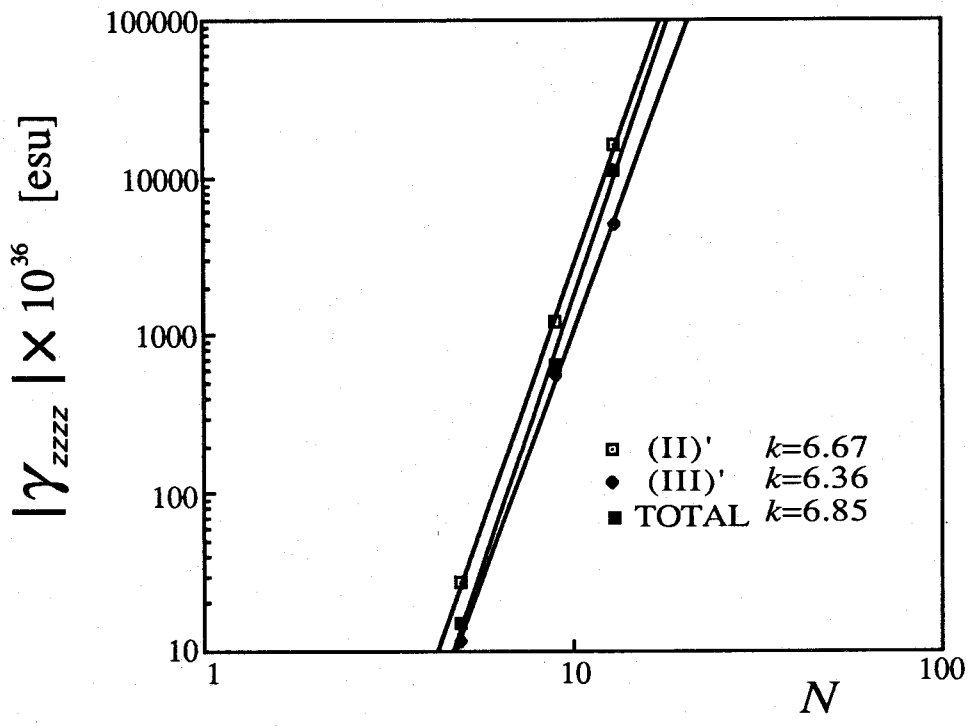

Fig.12. log -log plot of $|\gamma_{zzzz}|$ versus the number of carbon atoms N for (I). k ; slope

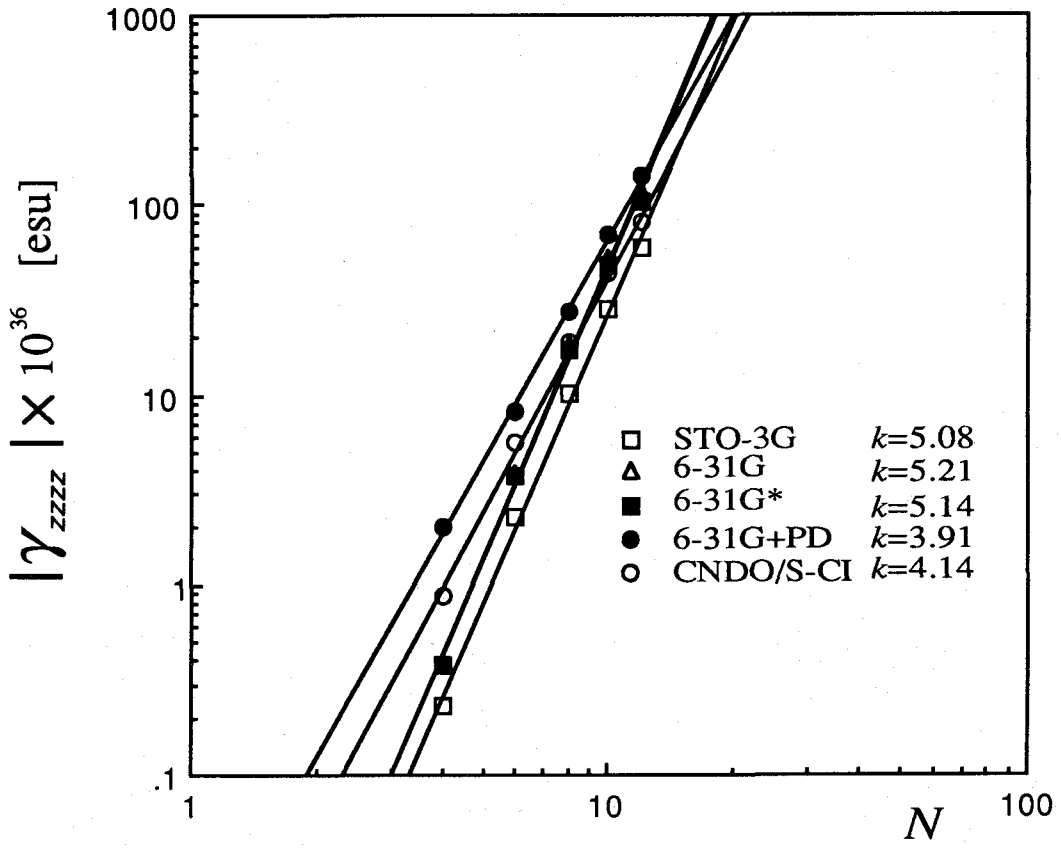

Fig.13. log -log Plot of $|\gamma_{zzzz}|$ versus the number of carbon atoms *N*.

Chapter 3

Uncoupled- and Coupled-Haretree-Fock Calculations of the Third-order Hyperpolarizabilities of π-Conjugated Polyenes with and without Defects

The static third-order hyperpolarizabilities (γ) of π-conjugated polyenes are calculated by the use of the uncoupled- and coupled-Hartree-Fock methods combined with the semi-empirical INDO approximation. Characteristics of γ calculated for regular polyenes, soliton-like polyenes and donor(D)-acceptor(A) disubstituted polyenes are investigated, particularly in relation to the chain-length effect. Plotting of the third derivatives of the Mulliken charge densities (γ density analysis) against the electric field is proposed for the analysis of the local contributions of the constituent atoms to γ. Results for the finite polyenes are extrapolated to an infinity of the chain length to predict the intrinsic γ values per unit carbon-carbon (CC) bond of polymeric chains.

1. Introduction

Considerable attention has been given to the investigations of the nonlinear optical properties of π-conjugated polyenes [1,2], in which delocalized π-electrons effect extremely large longitudinal hyperpolarizabilities. Recently, a number of ab initio and semi-empirical theoretical studies have been carried out [1-15]. The methods used in these studies can be divided into two categories; one is the variational [3-8] method while the other, perturbational [9-15]. Both methods involve the time-dependent and time-independent treatments.

Melo et al. [6] have performed theoretical calculations of the third-order hyperpolarizabilities for regular polyene, soliton-like polyene, and polaron-like polyene at the Pariser-Parr-Pople (PPP) level [16]. Their method is based on the perturbative expansion of the Hartree-Fock (HF) density matrix [17]. They have concluded that the conformational defects can make a non-negligible additive contribution to the total polarization response of the system. For example, the γ values along the chain lengths for charged soliton-like polyenes are negative in sign. In our previous work [9] based on the time-dependent perturbation theory (TDPT) with the CNDO/S [18] single-excitation CI (SCI) procedure, the γ values for charged soliton-like polyenes are likewise found to be negative. Recently, however, it is pointed out that the SCI procedure is often insufficient for reasonable predictions of the sign and the magnitude of γ [11-13].

Results of ab initio calculations to date unanimously indicate the necessity of the use of large augmented basis sets for obtaining reasonable γ values for small molecules such as hydrogen fluoride. However, such rigorous calculations can hardly be carried out for large molecules. Fortunately, Hurst et al. [3] have shown that the basis set dependence of γ becomes small when the lengths of polyenes are sufficiently large. Moreover, according to Kirtman and Hasan [7], the scaling procedure by the use of the finite-field (FF) INDO SCF

calculations is able to reproduce the tendency of the results obtained by ab initio large-scale calculations for the longitudinal hyperpolarizabilities of long polydiacetylenes [7].

In this article, the coupled-Hartree-Fock (CHF) method [3-5,8] based on the INDO [16] time-independent variational approach is employed to investigate the signs and magnitudes of the static γ values for regular polyenes, soliton-like polyenes and donor (D)-acceptor (A) disubstituted polyenes. The γ values are evaluated by the numerical differentiation of the self-consistent-field (SCF) energy of molecules in the presence of an electric field of finite strengths. A method termed the γ density analysis is proposed for an elucidation of local contributions of the constituent atoms to γ.

2. Methods of calculations

In our FF CHF treatments, the γ value is calculated by differentiating the ground state energy or dipole moment with respect to the external electric field. In general, the γ values by the FF CHF method are liable to involve some numerical errors. However, when precise calculation of the total energy and appropriate numerical differentiation are carried out under careful selection of the field strength, the numerical errors can be minimized [4]. One advantage of the FF CHF method is that it can be applied to almost any quantum chemical formalism, for example, Møller-Plesset perturbation theory (MPPT), in which the analytical computation of γ is not feasible at the present time [5].

The following equation is used for numerical computation of the longitudinal γ value in the chain direction (z) as the fourth-order derivative of the total energy with respect to the electric field :

$$\gamma_{zzzz} = \frac{1}{6F^4}\Big\{ -E(3F^z)+12E(2F^z)-39E(F^z)+56E(0) \\ -39E(-F^z)+12E(-2F^z)-E(-3F^z) \Big\}. \qquad (1)$$

Here, $E(F^z)$ is the total energy in the presence of the field F^z applied in the z direction. The minimum field strength employed here is 0.002 a.u., which seems to be most appropriate to assess the calculated results.

The relationships between the coupled-Hartree-Fock (CHF) and other approaches can easily be understood on the basis of the double-perturbation theory [8,14,15], in which both electron correlation and external field are regarded as perturbation. The theory is also referred to as the Rayleigh-Schrödinger perturbation theory (RSPT). Thus, the total energy in the presence of the field F is expanded as the power series of the field. The coefficient of the fourth-order field is $\gamma_{ijkl}(0;0,0,0)$. This expression seems to be convenient for calculation since only the quantities related to the ground state are required. Yet, the orders of electron correlations are usually limited to rather small ranks on account of practical reasons related to cumbersomeness and expense in evaluating their contributions. It is well known that the RSPT method including the first order of electron correlation is equivalent to the CHF method. In this work, the RSPT method including no correlation effects (RSPT0 method) is employed. This method is equivalent to the uncoupled-Hartree-Fock method [8].

The derivatives of the charge densities with respect to the applied field provide useful information for an interpretation of the spatial characteristics of the γ value. The charge density function can be expanded in powers of the field F [4]. The γ_{zzzz} value is expressed as

$$\gamma_{zzzz} = -\frac{1}{3!}\int q^z \rho^{(3)}(r) dr^3 \ . \qquad (2)$$

Here, q^z is the z component of the molecular coordinate and $\rho^{(3)}(r)$ is the third derivative of the electronic density function $\rho(r)$.

The γ value is approximately given by the Mulliken charge density $(PS)_{ss}$ divided to the atomic orbitals s involved :

$$\gamma_{zzzz} \approx -\frac{1}{3!}\sum_{s} (PS)^{(3)}_{ss} q^z_s \,, \tag{3}$$

in which

$$(PS)_{ss} = \sum_{t} (P)_{st}(S)_{ts} \,, \tag{4}$$

where S_{ts} is the overlap matrix element and where P_{st} is the bond order matrix element. The q^z_s represents the z component of the coordinate of the atom located at the center of the atomic orbital s. The approximation implies that the charge densities are concentrated at the atomic orbital centers. We refer to the third derivative of $(PS)_{ss}$ as the γ density. It is calculated by the four-point numerical derivative method as follows :

$$(PS)^{(3)}_{ss} = \frac{1}{2F^3}\left\{ (PS)_{ss}(2F^z) - (PS)_{ss}(-2F^z) + 2\left[(PS)_{ss}(-F^z) - (PS)_{ss}(F^z) \right] \right\}, \tag{5}$$

where the $(PS)_{ss}(F^z)$ is the Mulliken charge density of the atomic orbital s in the presence of the external field F^z .

The spatial characteristics of γ can be elucidated by the use of the plots of the magnitude and sign of the γ density on each atom. It is also possible to separate the density derivatives into different contributions, for example, the σ and π contributions [4]. The plus sign of the γ

density indicates that the second derivative of the charge density increases with the increase in the field, while the minus sign indicates the inverse effect.

3. Results and discussion

The molecular structures of polymeric compounds studied here are shown in Fig.1. The direction of chain length is taken as the z direction. Bond lengths and angles for these systems are all taken from the standard geometry data. For the regular polyenes, the lengths of 1.35 and 1.45 Å are assumed for the double and single bonds, respectively. For the soliton-like polyenes, it is assumed that the alternation between single and double bonds is inverted at the center of the chain. The γ_{zzzz} values per unit carbon-carbon (CC) bond, namely, γ_{zzzz} / N, calculated by the RSPT0 and CHF methods are listed in Table 1.

The logarithms of (γ_{zzzz} / N) versus N are plotted in Fig.2. Variations in $\log(\gamma_{zzzz} / N)$ with the increasing chain length exhibit similar trends for both methods. However, the magnitudes of the $\log(\gamma_{zzzz} / N)$ for several polymers obtained by the RSPT0 method are smaller than those by the CHF method. Moreover, the relative magnitudes of the $\log(\gamma_{zzzz} / N)$ by the RSPT0 method considerably differ from those by the CHF method combined with the INDO UHF approximation. For example, the magnitudes for neutral solitons (d), which are open-shell molecules, are much smaller than those for other systems. Nevertheless, the uncoupled-Hartree-Fock (=RSPT0) approach might be useful for qualitative understanding of the relative tendencies for these systems. However, since RSPT0 is admittedly less reliable than RSPT1(= CHF), only the CHF results will be discussed below.

The variation pattern of the chain-length dependence of γ for charged soliton-like polyenes (c) is found to be noticeably different from the patterns for other polyenes (a), (b) and (d); its γ increases most dramatically with the increasing chain length. The γ_{zzzz} / N values

for D-A disubstituted polyenes (b) at small N are greater than those for other polyenes but, at larger N, they are smaller than those for (a) and (c).

In order to compare the characteristics of the spatial contributions of γ_{zzzz}, the γ_{zzzz} density analysis is carried out for these systems with both larger and smaller N. The γ_{zzzz} density plots are shown in Fig.3. The size of the circles on each atom site exhibits the magnitude of the γ_{zzzz} densities and the black and white circles correspond to the increased and decreased γ_{zzzz} densities, respectively. At smaller N, the distribution patterns of the γ_{zzzz} densities for the D-A disubstituted polyene (b) are similar to those for regular polyene (a). However, the magnitude of the γ_{zzzz} densities for the D-A disubstituted polyene (b) are much larger than those for the regular polyene (a). For the soliton-like polyenes at small N, the charged soliton (c) exhibits two contributions of γ_{zzzz} densities whose signs are opposite to each other in contrast to the neutral soliton (d), so that the total γ_{zzzz} values for the charged soliton (c) are smaller than those for the neutral soliton (d). At large N, the magnitudes of γ_{zzzz} densities for the regular polyene (a) and the D-A disubstituted polyene (b) are much smaller than those for soliton-like polyenes. This implies that for greater chain lengths, the variation is localized in the vicinity of the carbon atom sites connected with D and A substituted groups, without delocalization due to direct charge transfer from D to A group, so that the γ_{zzzz} / N values tend to be saturated for long chains. For the charged soliton (c), the mutually opposite contributions of γ_{zzzz} densities are exhibited around the middle of the chain, while the end of the chain contributes the plus γ_{zzzz} values. On the other hand, for the neutral soliton (d), the magnitudes of γ_{zzzz} densities are relatively small as compared to those for the charged soliton (c), and the mutually opposite contributions of γ_{zzzz} densities are exhibited from one end to the other of the chain. Therefore, the behavior of the γ_{zzzz} / N values on the chain lengths for charged and neutral solitons (c) and (d) comes to be remarkably different. The

rapid saturation effect of γ_{zzzz}/N values for the neutral soliton (d) seems to have been caused by the localization of an extra electron at the middle of the chain.

Melo et al. reported that, according to the PPP variational perturbation approach [6], the γ values for the charged soliton-like polyenes are negative in sign in contrast to the present INDO CHF results. However, judging from the reliability of the INDO CHF calculations for large-size molecules, the results that the charged soliton-like polyenes exhibit positive γ values seem to be reasonable in the long chain region. Detailed investigations by the ab initio CHF method are desirable to confirm the validity of our results.

The γ_{zzzz}/N values for infinitely long polymeric chains are estimated by extrapolation. In this study, the extrapolation procedure presented by Hurst et al. [3] is applied. Thus, the γ_{zzzz}/N values are fitted by least squares to

$$\log A(N) = a + \frac{b}{N} + \frac{c}{N^2} , \qquad (6)$$

where N is the number of the unit CC bonds and where $A(N)$ is the γ_{zzzz}/N. The extrapolated values for infinite polyenes are $A(\infty) = 10^a$. The fitting parameters and extrapolated values are listed in Table 2. The limiting γ_{zzzz}/N value for the charged soliton-like polyene is found to be larger by about two orders of magnitude than that for the D-A disubstituted polyene. It is reported that the extrapolated γ_{zzzz}/N values have considerably large uncertainties [7]. Therefore, the γ_{zzzz}/N values for larger polyenes would have to be evaluated by the semiempirical scaling procedure in order to obtain reliable γ_{zzzz}/N values [7].

Finally, it should be noted that, at the ab initio level, augmentations of the basis sets are required in order to reproduce the characteristics of the third-order hyperpolarizability correctly [3,8]. For small-size systems, in particular, use of modest basis functions often

leads to incorrect representations of the third-order hyperpolarizability. In this connection, Hurst et al. pointed out that the basis augmentations become less important as the chain length increases[3]. The present CHF calculations at the semiempirical level appear to provide correct tendencies of the γ values for medium- and large-size systems as examined here. Although, in this work, the electron-electron correlation effects are neglected, the characteristics of the third-order hyperpolarizability demonstrated will probably be reliable. The Møller-Plesset perturbation theory (MPPT) [19] will be applied to estimate the correlation effects at the next stage.

References

[1] *Nonlinear Optical Properties of Polymers*, edited by A. J. Heeger, J. Orenstein and D. R. Ulrich, Vol. **109** (Material Research Society Publication, Pittsburgh, 1988).

[2] *Nonlinear Optical Properties of Organic and Polymeric Materials*, edited by D. J. Williams (Am. Chem. Soc., Washington, D. C. , 1983).

[3] G. J. B. Hurst, M. Dupuis and E. Clementi, J. Chem. Phys. **89** (1988) 385.

[4] P. Chopra, L. Carlacci, H. F. King and P. N. Prasad, J. Phys. Chem. **93** (1989) 7120.

[5] E. Perrin, P. N. Prasad, P. Mougenot and M. Dupuis, J. Chem. Phys. **91** (1989) 4728 .

[6] C. P. de Melo and R. Silbey, Chem. Phys. Lett. **140** (1987) 537 ; J. Chem. Phys. **88** (1987) 2558, 2567.

[7] B. Kirtman and M. Hasan, Chem. Phys. Lett. **157** (1989) 123.

[8] R. J. Bartlett and G. D. Purvis III, Phys. Rev. **A20** (1979) 1313.

[9] M. Nakano, M. Okumura, K. Yamaguchi and T. Fueno, Mol. Cryst. Liq. Cryst. **182A** (1990) 1.

[10] M. Nakano, K. Yamaguchi and T. Fueno, in *Nonlinear Optics of Organics and Semiconductors*, edited by T. Kobayashi, Springer Proceedings in Physics **36** (1989) 98 ; 103.

[11] J. R. Heflin, K. Y. Wong, O. Zamani-Khamiri and A. F. Garito, Phys. Rev. **B38** (1988) 1573.

[12] A. F. Garito and J. R. Heflin, K. Y. Wong and O. Zamani-Khamiri, in Organic Materials for Nonlinear Optics, edited by D. J. Andre and D. Bloor (1988).

[13] B. M. Pierce, J. Chem. Phys. **91** (1989) 791.

[14] E. F. McIntyre and H. F. Hameka, J. Chem. Phys. **68** (1978) 3481 ; 5534 ; **69** (1978) 4814 ; **70** (1979) 2215.

[15] O. Zamani-Khamiri, E. F. McIntyre and H. F. Hameka, J. Chem. Phys. **71** (1979) 1607 ; **72** (1980) 1280 ; **72** (1980) 5906.

[16] J. A. Pople and D. L. Beveridge, *Approximate Molecular Orbital Theory* (McGraw-Hill, New York, 1970).

[17] G. Diercksen and R. McWeeny, J. Chem. Phys. **44** (1966) 3554;
R. McWeeny and G. Diercksen, J. Chem. Phys. **49** (1968) 4852;
J. L. Dodds, R. McWeeny, W. T. Raynes and J. P. Riley, Mol. Phys. **33** (1977) 611.

[18] J. Del Bene and H. H. Jaffe, J. Chem. Phys. **48** (1968) 1807.

[19] C. Møller and M. S. Plesset, Phys. Rev. **46** (1934) 618.

Table 1. Values of γ_{zzzz}/N [a.u.] for polyene molecules (a) - (d).
N is the number of CC bonds.

N	INDO RSPT0				INDO CHF			
	(a)	(b)	(c)	(d)	(a)	(b)	(c)	(d)
7	2029	3813			3196	7835		
8			2431	1268			544	5207
11	6123	7307			13504	19485		
12			9215	2953			5565	15435
15	11224	10327			32018	33600		
16			22288	4771			25945	29750
19	16000	12468			55558	47305		
20			41690	6390			77900	45102
23	19933	13922			80202	59220		
24			65960	7738			172342	59420
27	23007	14944			103247	68600		
28			92586	8846			304100	71866

Table 2. Fitting parameters a, b and c for Eq.(5) and extrapolated values of $A(N) = \gamma_{zzzz}/N$ [a.u.] for $N \longrightarrow \infty$.

System	a	b	c	$A(\infty)$
(a)	5.7641	-21.596	40.412	0.581×10^6
(b)	5.2966	-13.123	23.085	0.198×10^6
(c)	7.2139	-53.487	141.37	16.4×10^6
(d)	5.4478	-17.404	28.354	0.280×10^6

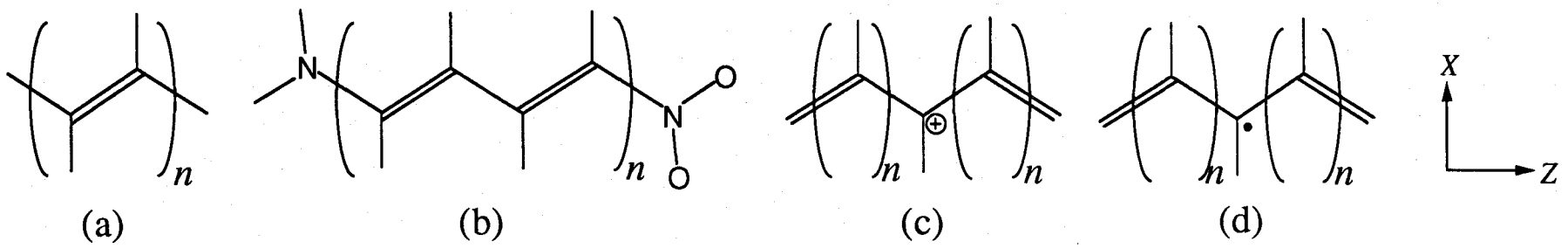

(a) (b) (c) (d)

Fig.1. Structures of the π-conjugated polymeric systems.

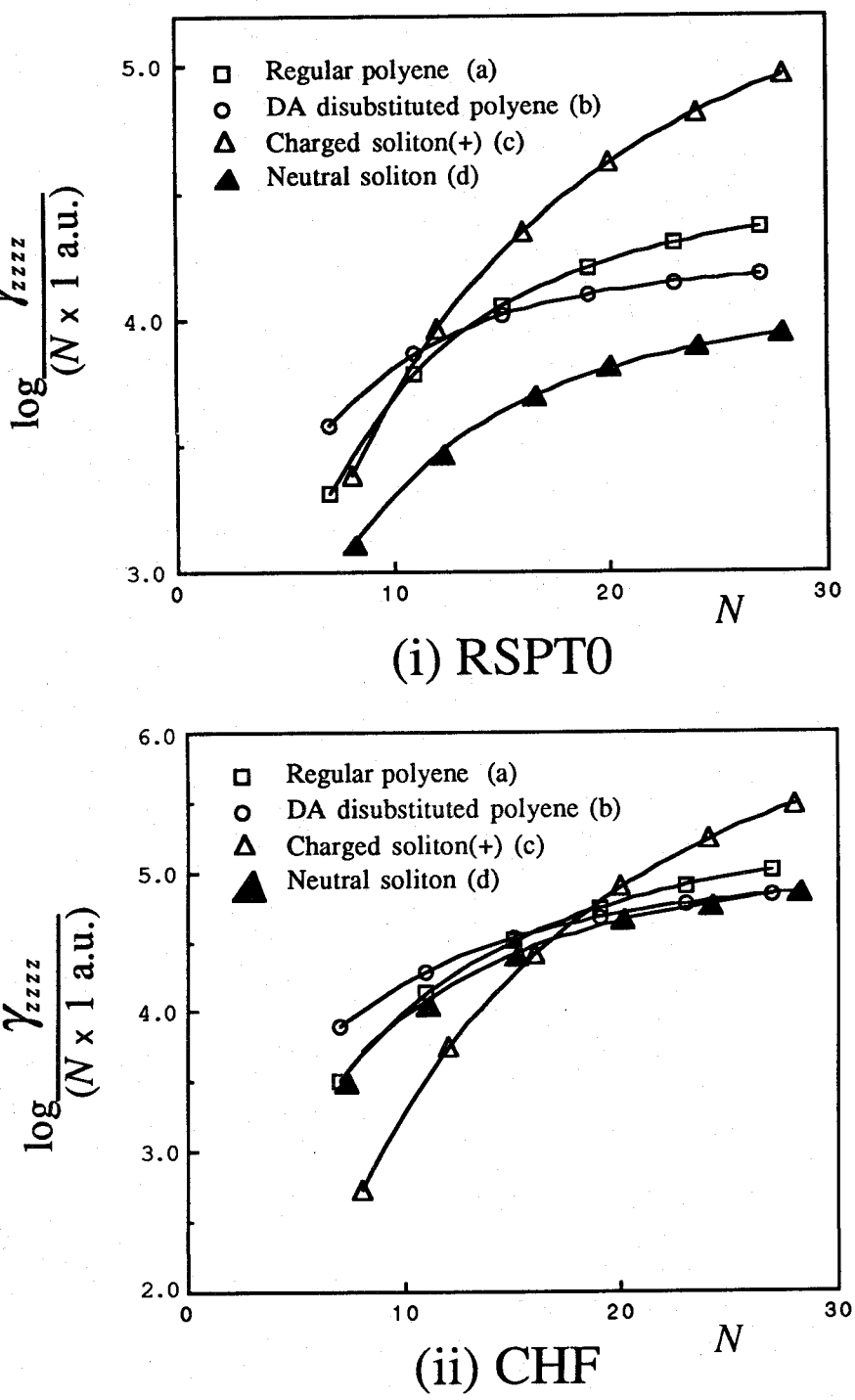

Fig.2. Plots of log(γ_{zzzz}/N) vs. N by the INDO CHF method. N is the number of CC bonds.

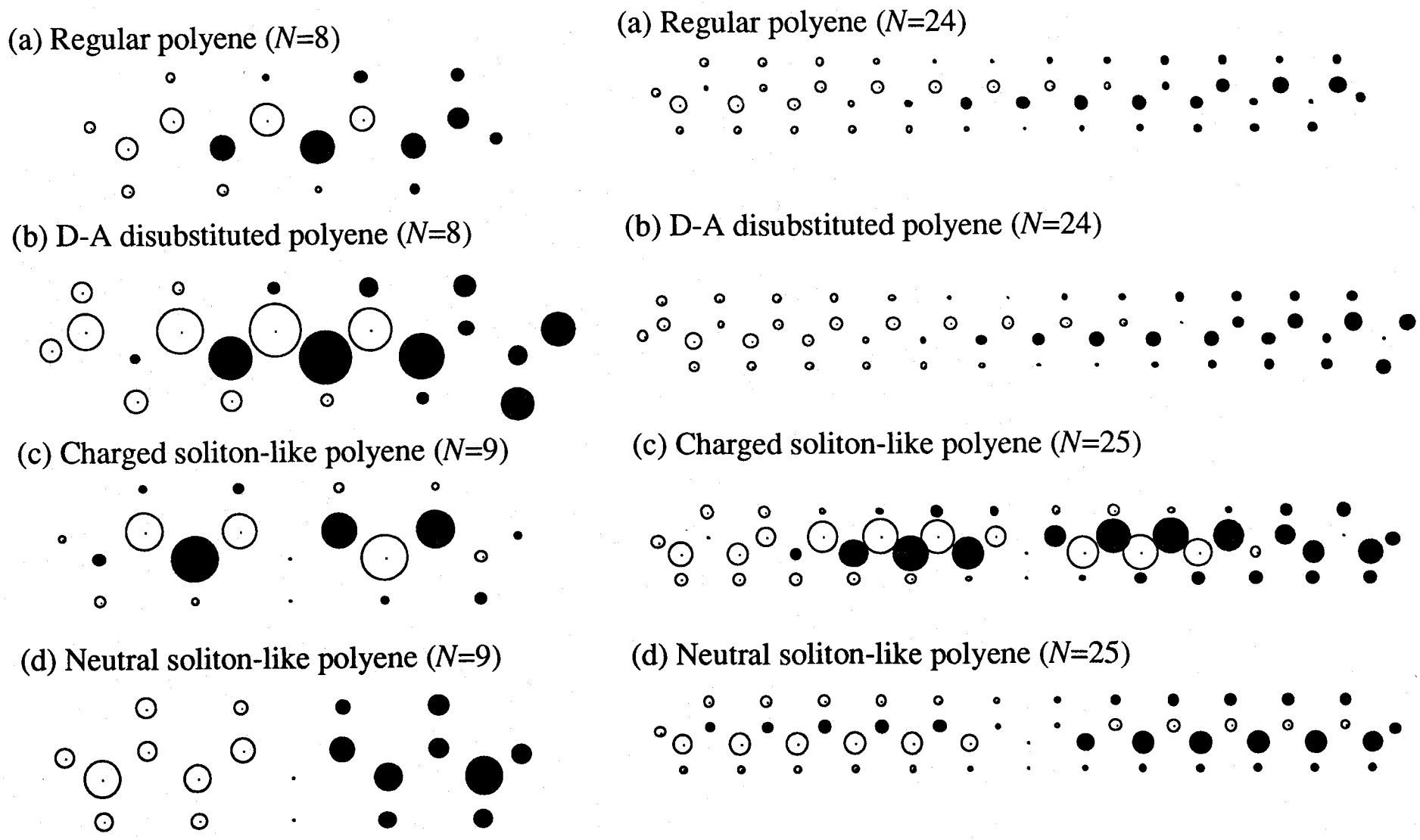

Fig.3. Plots of γ_{zzzz} densities for polymeric systems (a)-(d) by the INDO CHF method.

Chapter 4

Coupled-Haretree-Fock Calculations of the Third-order Hyperpolarizabilities of Substituted Polydiacetylenes

Coupled-Hartree-Fock calculations of the static third-order hyperpolarizabilities (γ) in the chain direction for regular polydiacetylene and several donor(D)-acceptor(A) substituted polydiacetylene oligomers through $C_{42}H_{24}$ are carried out at the level of the INDO approximation. The modes of the variations in γ with the increasing chain length are investigated for the different types of polydiacetylene systems. The γ density analysis is carried out to elucidate the spatial characteristics of γ. Results for sufficiently long oligomers are extrapolated to an infinity of the chain length to predict the intrinsic γ values per repeating unit of the polydiacetylenic chains.

1. Introduction

Recently, a large number of π-conjugated polymers have been investigated in relation to nonlinear optics. The longitudinal components of their hyperpolarizabilities are generally large and increase nonlinearly with the size of the chain length [1-8]. The polydiacetylene systems have attracted particular attention and are expected as the materials having large third-order nonlinear characteristics.

The chain length dependence of the third-order hyperpolarizabilities for conjugated polymers are thought to be an issue of practical significance. Kirtman and Hasan [5] calculated the static longitudinal hyperpolarizabilities γ for the polydiacetylene and polybutatriene oligomers through $C_{26}H_{16}$ by the coupled-Hartree-Fock (CHF) [5-12] method in both the INDO [13] and the ab initio formalisms [7-11]. The results of the INDO calculations have proved to reproduce the chain length dependence of the ab initio results, provided a certain scaling parameter is invoked.

In this work, the longitudinal γ values for regular polydiacetylene and six types of donor(D)-acceptor(A) substituted polydiacetylene oligomers through $C_{42}H_{24}$ are investigated by the INDO CHF method. Differences in mode of the variations in γ with the increasing chain lengths are examined for the different types of polydiacetylenes. The longitudinal γ values per unit cell of infinitely long polydiacetylenic chains are predicted by the extrapolation of the results of calculations for the polydiacetylene oligomers of finite lengths.

2. Calculation methods

Details of the CHF method used have been described previously [6]. Briefly, the third-order hyperpolarizability (γ) is expressed as the fourth-order derivative of the total energy with respect to the external electric field applied. The following equation is used for numerical computation of the longitudinal γ value in the chain direction (z) :

$$\gamma_{zzzz} = \frac{1}{6F^4}\left\{ 4(E(F^z)+E(-F^z)) - (E(2F^z)-E(-2F^z)) - 6E(0) \right\}, \qquad (1)$$

where $E(F^z)$ is the total energy in the presence of the field F^z applied in the z direction. The minimum field strength that is large enough to affect the numerical results without sacrifice of precision is chosen to be 0.002 a.u., a strength which seems to be most appropriate for our present purpose.

The γ density analysis is found to be useful to understand the spatial characteristics of γ [6]. The approximate γ_{zzzz} value in this analysis is expressed as follows [6] :

$$\gamma_{zzzz} \approx -\frac{1}{3!}\sum_s (PS)^{(3)}_{ss} q^z_s, \qquad (2)$$

where q^z_s represents the z component of the coordinate of the atom located at the center of the atomic orbital s and where $(PS)^{(3)}_{ss}$ is the third derivative of

$$(PS)_{ss} = \sum_t (P)_{st}(S)_{ts} \qquad (3)$$

with S_{ts} and P_{st} as the overlap and the bond-order matrix elements, respectively. The approximation presumes that the charge densities are concentrated on the centers of the atomic orbitals. The third derivative $(PS)^{(3)}_{ss}$ is referred to as the γ density. The spatial characteristics of γ can be elucidated most conveniently by visualizing the magnitudes and the signs of the γ densities on the atoms.

3. Calculated systems

Figure 1 shows structures of the polydiacetylene systems studied here. The structure of the polydiacetylenic main chain is the one that was obtained by Karpfen [14] according to the infinite polymer band structure calculations. The direction of chain length is taken as the z direction.

System (a), which is designated as R, is regular polydiacetylene. System (b) denoted by DA is the polydiacetylene which is substituted with the D and A groups at either end, and systems (c)-(g) are the polydiacetylenes whose side chains are all substituted by the D and/or A groups. The systems (e)DDDD, (f)AAAA and (g)DAAD as well as (a)R possess centrosymmetric charge distributions, while the systems (b)DA, (c)DADA and (d)DDAA are noncentrosymmetric. The amino ($-NH_2$) and nitro ($-NO_2$) groups are chosen as the D and A substituents, respectively.

4. Results and discussion

The longitudinal third-order hyperpolarizabilities (γ_{zzzz}) for the various model systems of the varying chain length N were calculated by the CHF method. The calculated γ values per unit cell, i.e., γ_{zzzz}/N, are summarized in Table 1. Figure 2 shows the logarithms of (γ_{zzzz}/N) versus N.

From Table 1 and Fig. 2, it appears possible to classify the systems into three categories. The first category includes systems (a)R, (b)DA, (c)DADA and (d)DDAA, which show relatively small γ_{zzzz}. Systems (e)DDDD and (f)AAAA form the second category exhibiting the γ_{zzzz} values of medium magnitude. Thirdly, system (g) DAAD is unique in that it exhibits anomalously large γ_{zzzz} values.

Systems (b), (c) and (d) of the first category are the noncentrosymmetric systems in the sense described above. According to the analysis based on the TDPT (= time-dependent

perturbation theory) [3,4,15-17] three-type approximation [3], the noncentrosymmetric systems should generally tend to exhibit larger γ values than do the centrosymmetric systems because of a large contribution of the intramolecular charge-transfer(CT) excitation involved. For systems (c) and (d), however, the CT effects from D to A groups are operative primarily across the main chain. Therefore, although the components of γ across the main chain may well be enhanced, those along the chain under consideration will be little affected. Correpondingly, in system (b), the CT effects along the main chain must be small because of the weak interactions between D and A substituents placed at a large separation.

The second category, i.e., systems (e) and (f), is centrosymmetric. The substituents attached to each double bond unit either donate or attract electrons all together. As a result, all the double bonds are rendered either electron-rich or -deficient as compared to the non-substituted chain. It appears that these situations somehow assist polarization of the main chain, thus leading to a slight enhancement of γ in the chain direction.

The third category, i.e., system (g), can exhibit a large local CT in the chain direction; the neighboring double bonds bear either A or D substituents. The situation accounts for its markedly large γ_{zzzz}.

The γ density analysis permits visualization of the origin of the γ values calculated. Plots of the γ_{zzzz} densities for systems (a)-(g) at N=6 are shown in Fig. 3. The size of a circle on each atomic site indicates the magnitude of the γ_{zzzz} densities, while the black and white circles correspond to the increased and decreased γ_{zzzz} densities, respectively. In all instances, the signs of γ densities are seen to be inversed in the middle of the chains.

Minute inspection of the density distributions shows that the γ_{zzzz} densities for the first category (a)-(d) are somewhat smaller than those for other systems. The γ_{zzzz} densities for systems (e) and (f) as the members of the second category are slightly larger than those for the first category. For system (g), the magnitudes of the γ_{zzzz} densities at each double bond unit

and the C-C≡C-C unit are found to be much larger than for other systems. These characteristics are all in line with the tendencies noted for the relative magnitudes of the γ values listed in Table 1.

The γ_{zzzz} / N values for infinitely long polydiacetylenic chains are estimated by extrapolation. Hurst et al. [7] proposed an extrapolation procedure of a physical quantity $A(N)$ by the least-squares fitting to an equation of the form:

$$\log A(N) = a + \frac{b}{N} + \frac{c}{N^2} , \qquad (4)$$

where N is the number of the unit cells and where $A(N)$ stands here for γ_{zzzz} / N. The limiting value at $N \rightarrow \infty$ is thus $A(\infty) = 10^a$. The fitting parameters a, b and c determined for our polydiacetylene oligomers are listed in Table 2, together with the extrapolated values $A(\infty)$. The limiting γ_{zzzz} / N value for system (g) is found to be considerably larger than the values for the remaining polydiacetylene systems.

According to Kirtman and Hasan [5], the ratio (γ_{zzzz} values by INDO)/(γ_{zzzz} values by ab initio (4-31G)) for the regular polydiacetylene (R) is estimated to be 0.20 ± 0.04 for sufficiently long chains. Using this scaling factor, the limiting value for (a)R in the ab initio framework is predicted to be (6.8 ± 1.4) x 10^5 a.u., which agrees reasonably well with the value ((5.33 ± 1.17) x 10^5 a.u.) obtained by Kirtman and Hasan. The corresponding limiting value for the case of (g)DAAD is as large as 2.7 x 10^6 a.u.

In conclusion, the centrosymmetric systems (e)DDDD, (f)AAAA and (g)DAAD, are predicted to exhibit fairly large γ_{zzzz} values in the chain direction. The system (g)DAAD, in particular, will have anomalously large γ_{zzzz}. The γ density analysis seems to be useful for a

pictorial understanding of the origin of large longitudinal hyperpolarizabilities possible with conjugated polymeric chains.

References

[1] *Nonlinear Optical Properties of Polymers*, edited by A. J. Heeger, J. Orenstein and D. R. Ulrich, Vol. **109** (Material Research Society Publication, Pittsburgh, 1988).

[2] *Nonlinear Optical Properties of Organic and Polymeric Materials*, edited by D. J. Williams (Am. Chem. Soc., Washington, D. C. , 1983).

[3] M. Nakano, M. Okumura, K. Yamaguchi and T. Fueno, Mol. Cryst. Liq. Cryst. **182A** (1990) 1.

[4] M. Nakano, K. Yamaguchi and T. Fueno, in *Nonlinear Optics of Organics and Semiconductors*, edited by T. Kobayashi, Springer Proceedings in Physics **36** (1989) 98 ; 103.

[5] B. Kirtman and M. Hasan, Chem. Phys. Lett. **157** (1989) 123.

[6] M. Nakano, K. Yamaguchi and T. Fueno, submitted.

[7] G. J. B. Hurst, M. Dupuis and E. Clementi, J. Chem. Phys. **89** (1988) 385.

[8] C. P. de Melo and R. Silbey, Chem. Phys. Lett. **140** (1987) 537 ; J. Chem. Phys. **88** (1987) 2558, 2567.

[9] P. Chopra, L. Carlacci, H. F. King and P. N. Prasad, J. Phys. Chem. **93** (1989) 7120.

[10] E. Perrin, P. N. Prasad, P. Mougenot and M. Dupuis, J. Chem. Phys. **91** (1989) 4728 .

[11] R. J. Bartlett and G. D. Purvis III, Phys. Rev. **A20** (1979) 1313.

[12] S.P. Karna and M. Dupuis, Chem. Phys. Lett. **171** (1990) 201;
C. Daniel and M. Dupuis, Chem. Phys. Lett. **171** (1990) 209.

[13] J. A. Pople and D. L. Beveridge, *Approximate Molecular Orbital Theory* (McGraw-Hill, New York, 1970).

[14] A. Karpfen, J. Phys. **C13** (1980) 5673.

[15] J. R. Heflin, K. Y. Wong, O. Zamani-Khamiri and A. F. Garito, Phys. Rev. **B38** (1988)

1573.

[16] A. F. Garito and J. R. Heflin, K. Y. Wong and O. Zamani-Khamiri, in *Organic Materials for Nonlinear Optics*, edited by D. J. Andre and D. Bloor (1988).

[17] B. M. Pierce, J. Chem. Phys. **91** (1989) 791.

Table 1. γ_{zzzz} / N [a.u.] values calculated for systems (a)-(g) by the CHF methods. N is the number of the repeating units of polydiacetylenic chain.

N	(a)R	(b)DA	(c)DADA	(d)DDAA	(e)DDDD	(f)AAAA	(g)DAAD
2	9343	10490	9874	9411	10530	9892	12730
4	31740	33310	28270	30980	41220	39760	74960
6	51250	52680	43290	48190	68930	68520	144500
8	64550	65750	53790	59550	88020	88910	197900
10	73560	74560	61000	67170	100800	103000	236200

Table 2. Fitting parameters a, b and c for Eq.(5) and extraporated values of $A(N) = \gamma_{zzzz} / N$ [a.u.] values for $N \rightarrow \infty$.

	(a)R	(b)DA	(c)DADA	(d)DDAA	(e)DDDD	(f)AAAA	(g)DAAD
a	5.1331	5.1298	5.0356	5.0648	5.2806	5.3141	5.7256
b	-2.6966	-2.6108	-2.5756	-2.3835	-2.7735	-3.0430	-3.5277
c	0.74105	0.78438	0.98600	0.40093	0.51222	0.80905	0.57023
$A(\infty)$	1.36×10^5	1.35×10^5	1.09×10^5	1.16×10^5	1.90×10^5	2.06×10^5	5.32×10^5

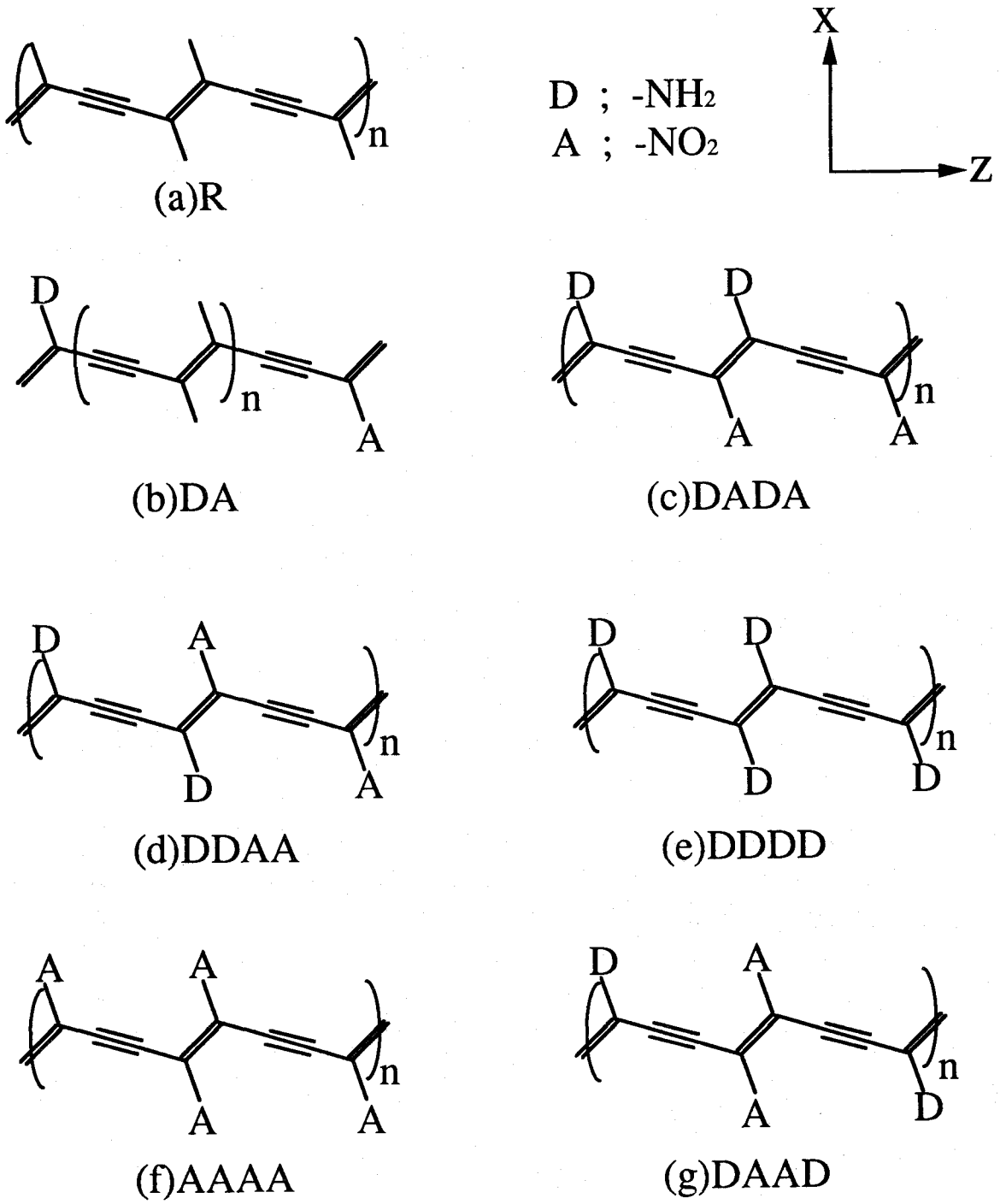

Fig.1. Structures of the polydiacetylene systems studied.

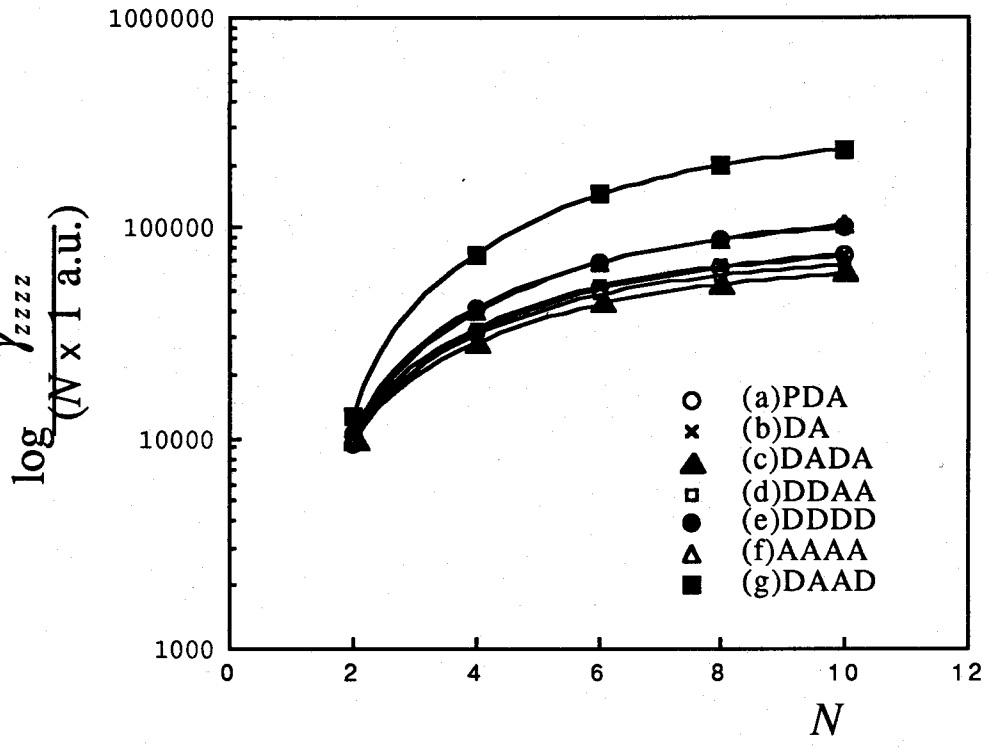

Fig.2. Plots of $\log(\gamma_{zzzz}/N)$ vs. N by the INDO CHF method. N is the number of the repeating units of the polydiacetylene chains.

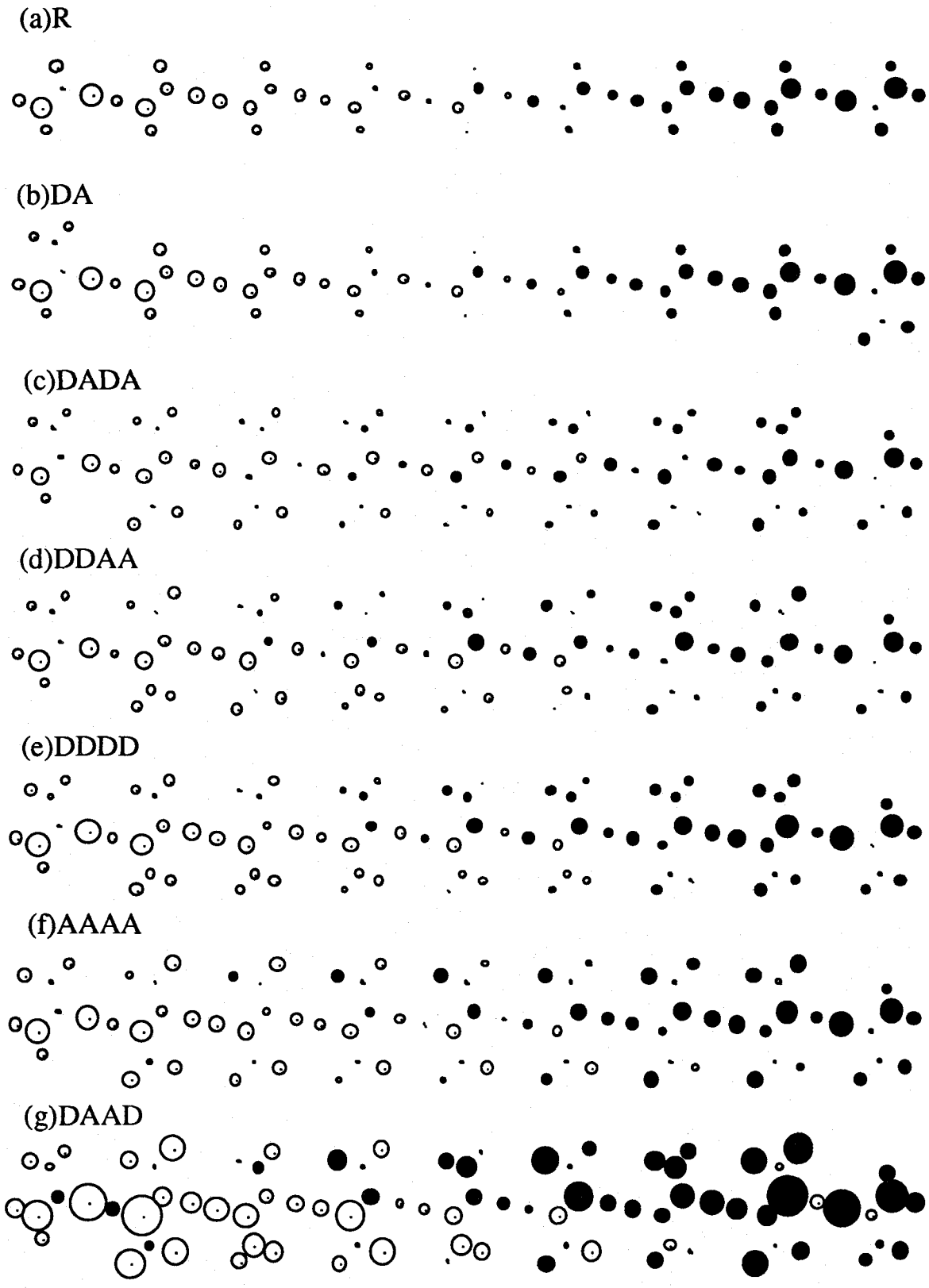

Fig.3. Plots of the γ_{zzzz} densities for systems (a)-(g) at N =8 according to the INDO CHF method.

Chapter 5

Coupled-Hartree-Fock Calculations of the Third-order Hyperpolarizabilities for Mixed and Segregated Charge-transfer Clusters

Static third-order hyperpolarizabilities (γ_{yyyy}) of alternate donor (D)-acceptor (A) stacks and of segregated molecular stacks in the column direction are calculated by the coupled-Hartree-Fock (CHF) method based on the INDO approximation. It is found that both the mixed and the neutral/ionic segregated stacks exhibit large γ_{yyyy} values.

1. Introduction

Organic materials which exhibit strong nonlinear optical properties have attracted considerable attention, and materials with large nonlinear effects have been investigated actively in recent years [1-13]. Most third-order nonlinear materials involve the intramolecular charge delocalization to effect large hyperpolarizability γ. Interestingly, nonlinear optical systems with the intermolecular charge-transfer (CT) interactions have also been studied [14]. Recently, it has been reported that the mixed stack of tetracyanoquinodimethane (TCNQ) with perylene exhibits enormously large γvalues [15].

In this paper, molecular aggregates in which donor (D) and acceptor (A) molecules stack alternatively or segregatively, namely the mixed and segregated stacks [16], are investigated, in order to analyze the effects of the intermolecular interactions and to propose new models of the third nonlinear systems involving the intermolecular charge-transfer (CT) effects. The coupled-Hartree-Fock (CHF) method in the INDO approximation is used to evaluate the static third-order hyperpolarizabilities (γ_{yyyy}) in the column direction. Dependence of γ_{yyyy} on the size of cluster is also investigated. The γ density analysis proposed in a previous paper [17] is applied to the examination of the spatial contributions of γ_{yyyy} for the CT clusters. Details of the CHF method and of the γ density analysis are the same as those described previously [17].

2. Method

2.1. Model systems

Figure 1 shows spatial arrangements of the alternate D-A stacks (a) and the segregated A stacks (b) treated here. trans-Diaminoethylene and trans-dicyanoethylene are adopted as the D and A molecules, respectively. The intermolecular distance was fixed at 3.0 Å. In the alternate stacks (a), the D and A molecules are assumed to be placed in such a

manner that the intermolecular overlap be maximal. For the segregated stack (b) as a model of the A column in the segregated D and A molecular stacks, three models are considered: (i) the ionic stack ($(b)^{N-}$), (ii) the mixed-valence stack($(b)^{0.5N-}$) and (iii) the neutral stack($(b)^{0}$), where N is the number of the monomers involved. The models (i), (ii) and (iii) correspond respectively to the representative states involving complete CT, incomplete CT and no CT from the D to A column in many existing CT complexes [16].

Geometries of the D and A component molecules were assumed on the basis of relevant experimental structural data. Those for the charged A molecules are assumed to remain the same as for the neutral trans-dicyanoethylene.

2.2. γ density analysis

The γ density variation in the column direction is examined in order to elucidate the effect of intermolecular CT interaction on γ. The approximated γ_{yyyy} in the γ density analysis is expressed as follows [17] :

$$\gamma_{yyyy} \approx -\frac{1}{3!}\sum_{s} (\boldsymbol{PS})_{ss}^{(3)} q_s^y \,. \tag{1}$$

Here, q_s^y represents the y component of the coordinate of the atom located at the center of the atomic orbital s. $(\boldsymbol{PS})_{ss}$ is the Mulliken charge density divided to the atomic orbitals s. S_{st} is the overlap matrix element and $\boldsymbol{P}_{st}$ is the bond order matrix element. The approximation is based on the assumption that the charge densities be concentrated on the centers of the atomic orbitals involved. The spatial characteristics of γ can be obtained by the use of the plots of the magnitude and sign of the γ density on each atom. The plus sign of the γ density implies that the second derivative of the charge density increases with the increase in the field, while the

minus sign implies the inverse effect. In the γ density plot, the size of a circle on each atomic site indicates the magnitude of the γ_{yyyy} densities, while the black and white circles correspond to the increased and decreased γ_{yyyy} densities, respectively.

3. Results

3.1. Mixed stacks

The γ_{yyyy} values calculated for the mixed stacks (a) with N = 2, 4, 6 and 8 are listed in Table 1. The mixed dimer (N=2) exhibits a positive γ_{yyyy} value as large as 1229. The γ_{yyyy} densities shown in Fig.2 are negative and positive in sign for D and A molecules, respectively. The CT effects from D to A thus lead to a large positive γ_{yyyy} value.

As Table 1 shows, the γ_{yyyy} values for the mixed stacks (a) increase almost linearly with the increasing stack size N. The distributions of γ_{yyyy} densities shown in Fig.2 suggest that the γ_{yyyy} densities at the both ends of the dimer (N=2) are carried over without loss to the top and bottom molecules for the hexamer (N=6). The distance between the top and bottom molecules are 5 times as large as that for the dimer (N=2), so that the total γ_{yyyy} value for the hexamer is 5 times as large as that for the dimer. As a general trend, the γ_{yyyy} / (N-1) values appear to be constant over different size of clusters as can be seen in Fig.3. The results can be interpreted as an indication that the effect of the intermolecular CT interaction between the nearest neighboring molecules as noted in the dimer is propagated without decay along the column of the alternate stacks of the increasing stack size.

3.2. Segregated stacks

As Table 1 shows, the neutral segregated dimer $(b)^0$ (N=2) exhibits a relatively small positive γ_{yyyy} value. From the γ_{yyyy} densities shown in Fig.4, it is evident that the γ_{yyyy} value is yet caused by the CT effects. Needless to say, these effects are much smaller than

those for the mixed dimer. The dominant spatial contributions of the γ_{yyyy} densities are found to be located on the cyano groups.

Again, the γ_{yyyy} values are (N-1) times as large as the value for the dimer $(b)^0$ (N=2), as can be seen in Fig.2. The γ_{yyyy} densities shown in Fig.4 indicate that the distributions of γ_{yyyy} densities for the top and bottom molecules are similar to those of the dimer. Apparently, the γ_{yyyy} value is determined only by the interaction between the nearest neighboring molecules as in the case of the mixed stack (a).

For the ionic dimer $(b)^{2-}$ (N=2) in the triplet state, the relatively large positive γ_{yyyy} value is obtained as compared to that of the neutral dimer $(b)^0$ (N=2) (Table 1). As is shown in Fig.5, the γ_{yyyy} densities on each atomic site are opposite in sign for α and β electrons. The contributions of α electrons are dominant in the central CC double bonds and CH bonds. By contrast, the contributions of β electrons are dominant in the N atoms in the cyano groups. Both contributions are positive in sign, so that the total γ_{yyyy} values come to be positive in sign. Compared with the neutral dimer $(b)^0$ (N=2), the γ_{yyyy} values for $(b)^{2-}$ (N=2) are calculated to become larger on account of two excessive α electrons existing in $(b)^{2-}$ (N=2).

As can be seen in Fig.3, the ionic segregated stack $(b)^{N-}$ exhibits a nonlinear increase when the size of the cluster is small. However, the $\gamma_{yyyy} / (N\text{-}1)$ values approach a constant level for large-size clusters. The γ_{yyyy} densities for the hexamer (Fig.5) show that the densities for the top and bottom molecules are much larger than those for the dimer $(b)^{2-}$ (N=2). However, the contributions from the molecules lying inside the stack are contrary in sign to those of the top and bottom molecules. The net results are that the nonlinear increase of the $\gamma_{yyyy} / (N\text{-}1)$ values tends to become saturated rapidly.

For the mixed-valence dimer $(b)^-$ (N=2) in the doublet state, the electric charge on each monomer comes to be -0.5 in the molecular orbital (MO) picture. The CT energy of this mixed-valence stack is clearly much lower than the values for other CT stacks, since the former does

not have a strong Coulomb repulsion energy. Therefore, extraordinarily large γ_{yyyy} values are to be obtained. The mixed-valence stack has been regarded as a high conducting system [16]. Thus, the electrons tend to transfer between the neighboring molecules along the column direction. When a very small field is applied to this system, the excess electrons readily begin to transfer between the neighboring molecules. The situation corresponds to the conducting state instead of the nonlinear polarization state. The above abnormally large γ_{yyyy} values are thought to be reflected in this conducting state. Therefore, mixed-valence segregated stacks would be inappropriate as nonlinear optical system. In ionic segregated stacks, the excess electrons on each molecule do not behave as conducting electrons by virtue of the mutual Coulomb repulsions, but can cause large nonlinear polarization. In neutral segregated stacks, on the other hand, no excess electrons exist, so that large nonlinear polarization cannot be expected.

4. Discussion and concluding remarks

The present calculations show that several models of CT complexes exhibit large γ values. The nonlinear polarizations in these systems are caused by the intermolecular CT effects. These systems have been proposed as the high conducting systems constructed of D and A molecules, and many species of D and A molecules have been synthesized [16]. Both the mixed and neutral/ionic segregated stacks are found to possess large γ values in the column direction. In the mixed-valence segregated stack, the γ value diverges due to the lower CT energy. For both the mixed and neutral segregated stacks, the γ values in the column direction seem to be determined by the interactions between the nearest neighboring molecules. As a result, the γ values increase linearly with the increase in cluster size. By contrast, in the ionic segregated stack, the γ value is effected by the non-local polarization effects between molecules lying more distant than at the nearest intermolecular distance. However, the

contributions with opposite phase to the top and bottom molecules develop near the stack ends, so that the nonlinear increase of the $\gamma_{yyyy} / (N\text{-}1)$ values come to be saturated. In general, the γ values in the column direction for the CT complexes except for the mixed-valence stack tend to increase linearly with the size of the cluster.

Previously, we investigated polymeric systems involving the intramolecular CT effects (through-bond interactions [19]) through main chain [17]. In this paper, complexes involving the intermolecular CT effects (through-space interactions [19]) enhancing the γ in the chain direction have been investigated. For large polymeric systems, it was found that the γ values per unit bond come to saturate. Similarly, the γ values in the column direction for medium-size CT complexes seem to increase linearly with the increasing cluster size. In order to judge the utility of the CT complex-type nonlinear optical systems, the variation behavior of the γ values in the case of the large-size cluster have to be investigated. Further, from the view point of the mechanism involving the CT effects as mentioned above, new nonlinear optical systems which will have both the through-bond and through-space CT interactions can be suggested. We have proposed such new polymeric systems with polar side chains that are expected to possess large CT effects between the neighboring side chains [20]. These systems are expected to involve both the through-bond CT effects in the main chain and the through-space CT effects between the neighboring polar side chains to enhance the γ in the chain direction.

The results for the mixed stack of tetracyanoquinodimethane (TCNQ) and perylene investigated by Gotoh et al. [15] are in good agreement with our theoretical predictions. Clearly, large CT effects from D to A molecules seem to contribute to the enhancement of the γ values in the column direction. However, it is noteworthy that there are other important factors exhibiting enormously large γ values. The most important factor among them is the dispersion effect induced by the close approach between the energy of an external electric field and the CT excitation energy. Since the CT bands of the CT complexes are generally located at rather low

energy levels, the practical dynamic hyperpolarizabilities seem to be rather enhanced by the dispersion effects. Theoretical calculations based on the time-dependent Hartree-Fock (TDHF) and time-dependent perturbation theory (TDPT) are now in progress in order to investigate the dispersion effects.

References

[1] *Nonlinear Optical Properties of Polymers*, edited by A. J. Heeger, J. Orenstein and D. R. Ulrich, Vol. **109** (Material Research Society Publication, Pittsburgh, 1988).

[2] *Nonlinear Optical Properties of Organic and Polymeric Materials*, edited by D. J. Williams (Am. Chem. Soc., Washington, D. C. , 1983).

[3] M. Nakano, M. Okumura, K. Yamaguchi and T. Fueno, Mol. Cryst. Liq. Cryst. **182A** (1990) 1.

[4] M. Nakano, K. Yamaguchi and T. Fueno, in *Nonlinear Optics of Organics and Semiconductors*, edited by T. Kobayashi, Springer Proceedings in Physics **36** (1989) 98 ; 103.

[5] R. J. Bartlett and G. D. Purvis III, Phys. Rev. **A20** (1979) 1313.

[6] E. F. McIntyre and H. F. Hameka, J. Chem. Phys. **68** (1978) 3481 ; 5534 ; **69** (1978) 4814 ; **70** (1979) 2215.

[7] O. Zamani-Khamiri, E. F. McIntyre and H. F. Hameka, J. Chem. Phys. **71** (1979) 1607 ; **72** (1980) 1280 ; **72** (1980) 5906.

[8] J. R. Heflin, K. Y. Wong, O. Zamani-Khamiri and A. F. Garito, Phys. Rev. **B38** (1988) 1573.

[9] A. F. Garito and J. R. Heflin, K. Y. Wong and O. Zamani-Khamiri, in *Organic Materials for Nonlinear Optics*, edited by D. J. Andre and D. Bloor (1988).

[10] G. J. B. Hurst, M. Dupuis and E. Clementi, J. Chem. Phys. **89** (1988) 385.

[11] P. Chopra, L. Carlacci, H. F. King and P. N. Prasad, J. Phys. Chem. **93** (1989) 7120.

[12] E. Perrin, P. N. Prasad, P. Mougenot and M. Dupuis, J. Chem. Phys. **91** (1989) 4728 .

[13] B. M. Pierce, J. Chem. Phys. **91** (1989) 791.

[14] B. F. Levine and C. G. Bethea, J. Chem. Phys. **65** 2439 (1976) ; **66** (1977) 1070.

[15] T. Gotoh, T. Kondoh and K. Egawa, J. Opt. Soc. Am.**B.6** (1990) 703

[16] J. B. Torrance, Acc. Chem. Res. **12** (1979) 79.

[18] J. A. Pople and D. L. Beveridge, *Approximate Molecular Orbital Theory* (McGraw-Hill, New York, 1970).

[17] M. Nakano, K. Yamaguchi and T. Fueno, submitted.

[19] R. Hoffmann, A. Imamura and W. J. Hehre, J. Am. Chem. Soc. **90** (1968) 1499.

[20] M. Nakano, K. Yamaguchi and T. Fueno, Synthetic Metal to appear.

Table 1. γ_{yyyy} values [a.u.] for the CT clusters.[a)]
N is the number of monomers.

N	(a)	$(b)^0$	$(b)^{N-}$
2	1229	42	154
4	3611	189	733
6	6078	366	1406
8	8443	514	2027

a) (a) ; Mixed clusters
$(b)^0$; Neutral segregated clusters
$(b)^{N-}$; Ionic segregated clusters

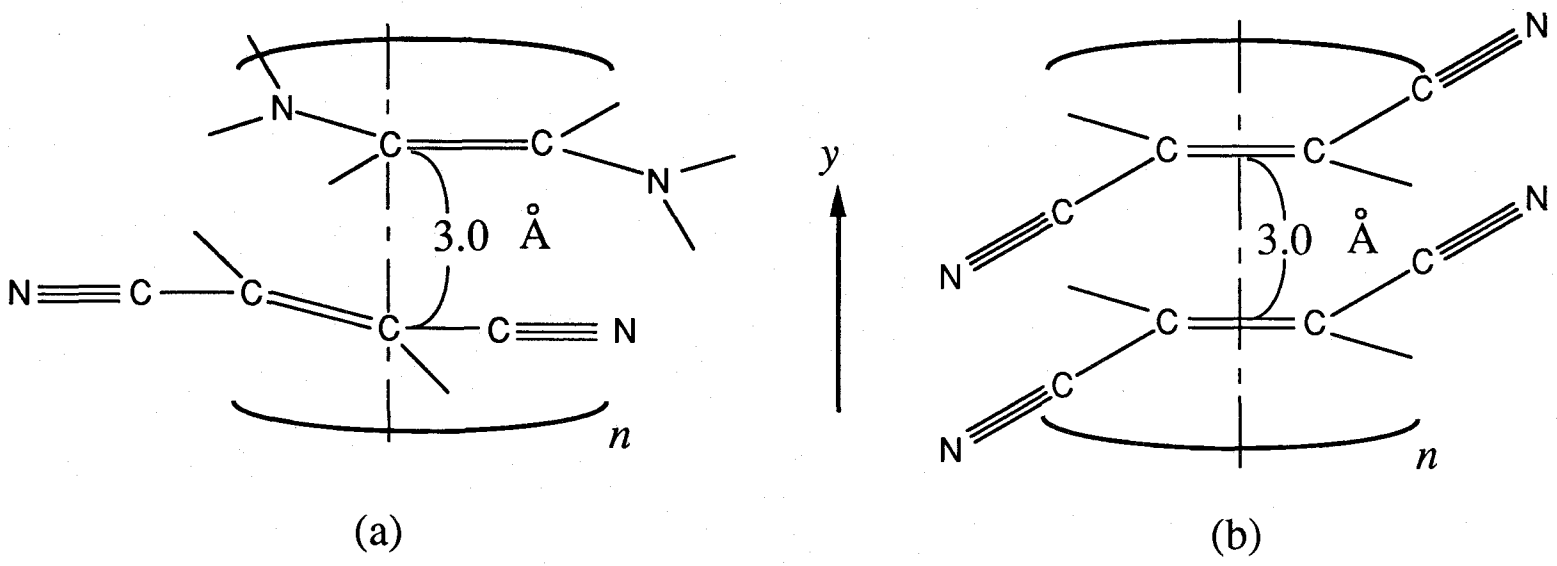

Fig.1. Charge-transfer (CT) clusters studied.
(a) ; Mixed clusters
(b) ; Segregated clusters

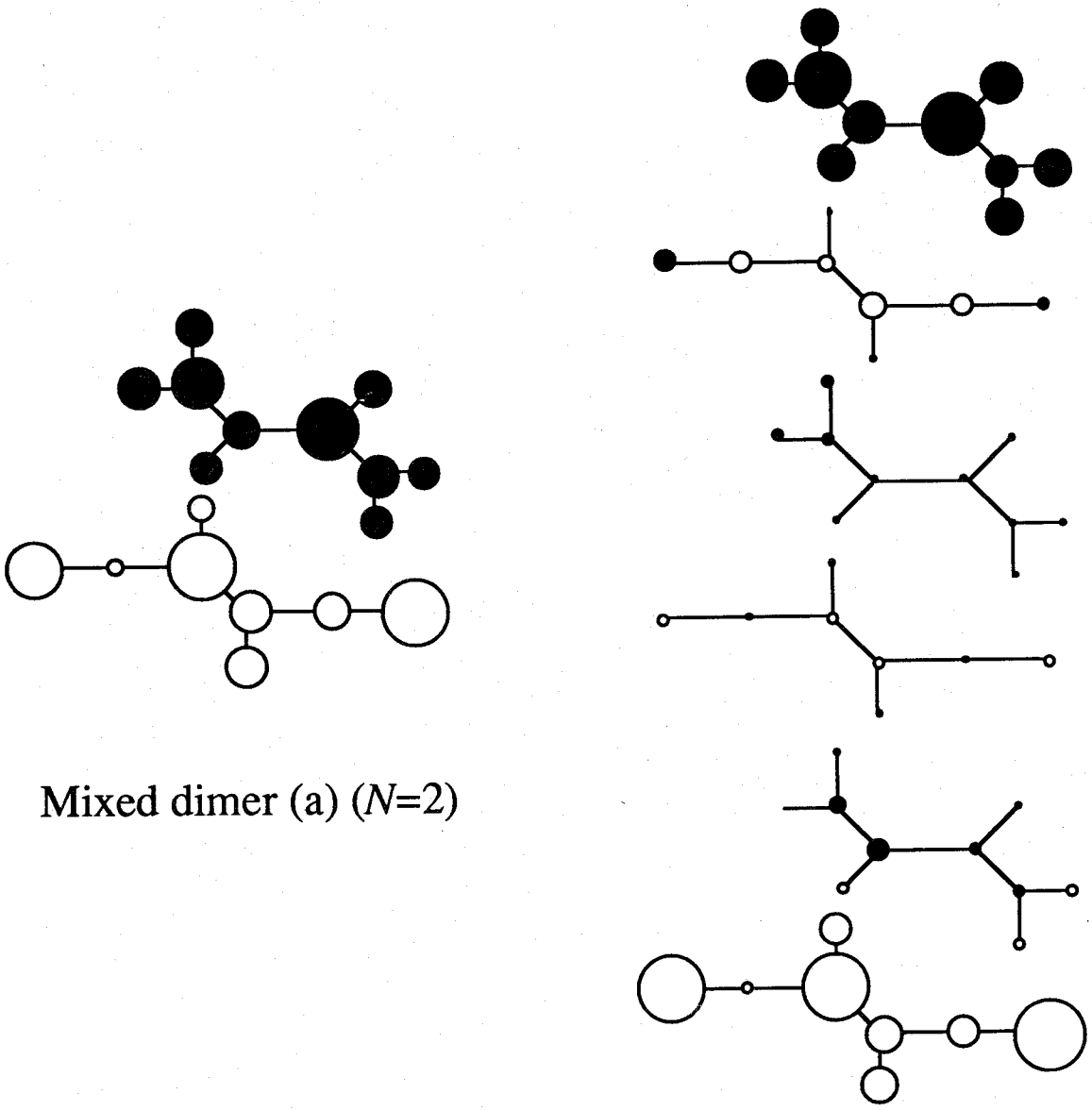

Mixed dimer (a) (N=2)

Mixed hexamer (a) (N=6)

Fig.2. γ_{yyyy} densities for the dimers and the hexamers of the mixed clusters.

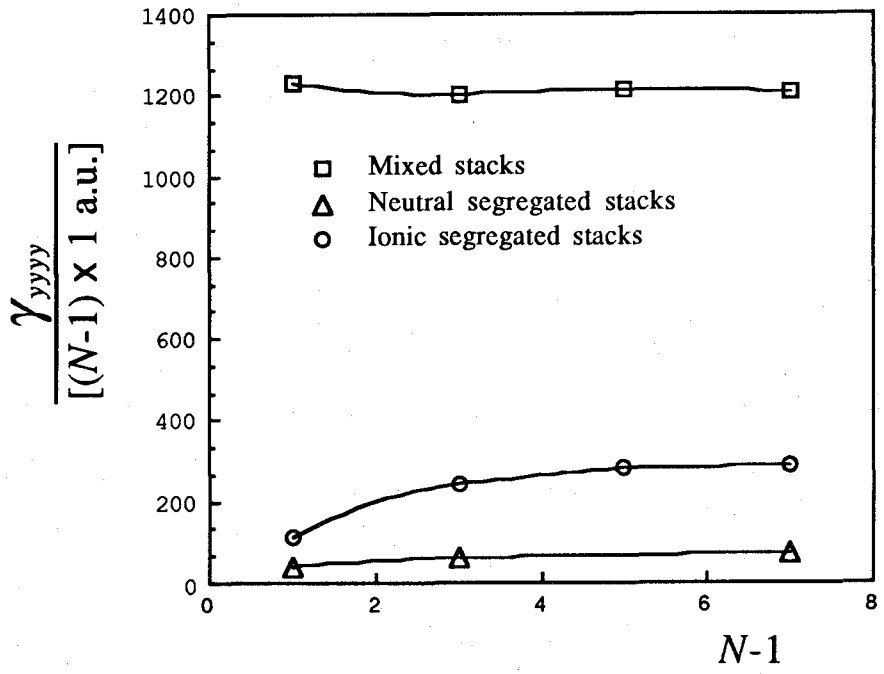

Fig.3. γ_{yyyy} / (N-1) [a.u.] values calculated for three types of the CT clusters by the INDO CHF method. N is the number of monomers.

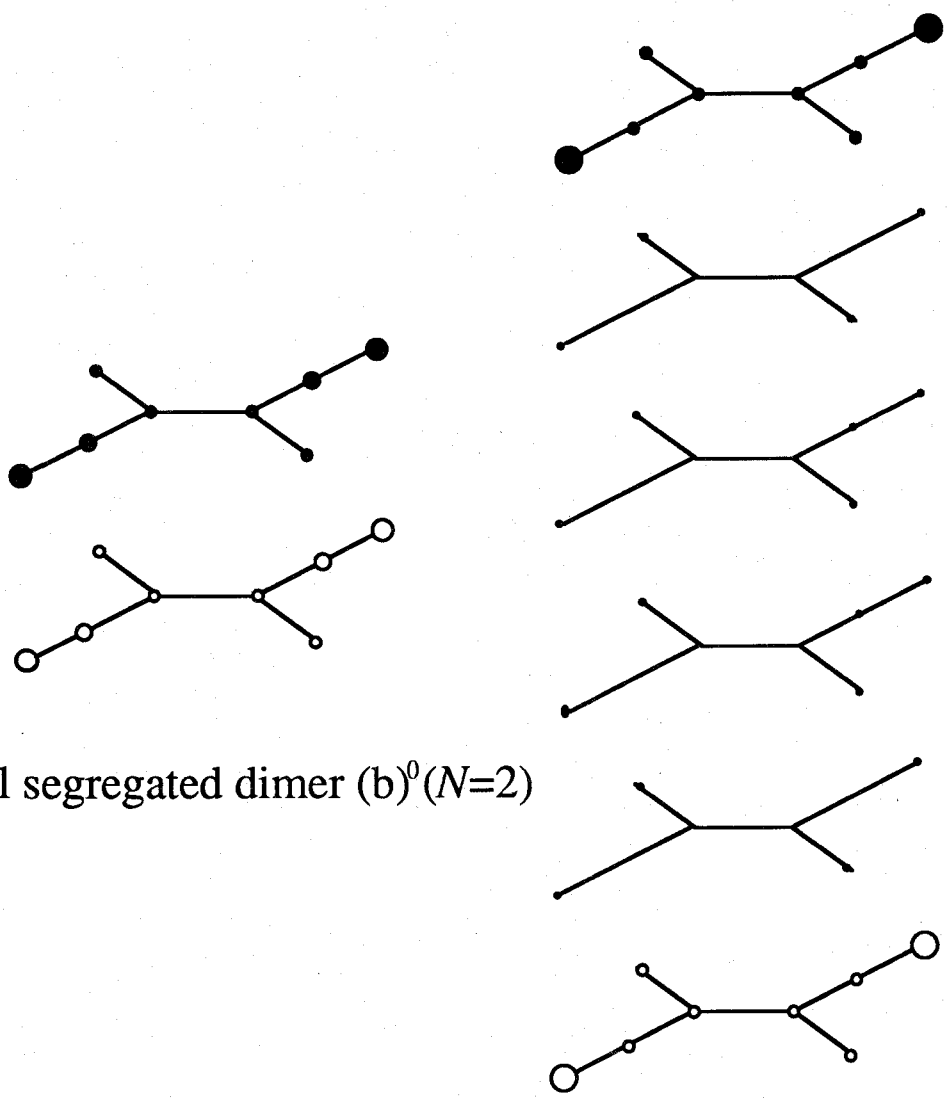

Neutral segregated dimer $(b)^0(N=2)$

Neutral segregated hexamer (b^0) $(N=6)$

Fig.4. γ_{yyyy} densities for the dimers and the hexamers of the neutral segregated clusters.

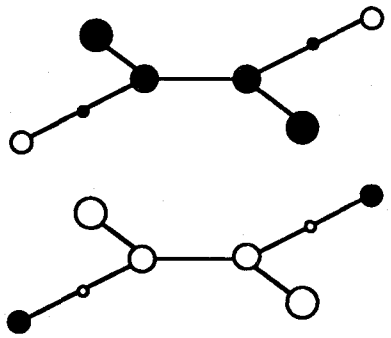

α - γ_{yyyy} densities

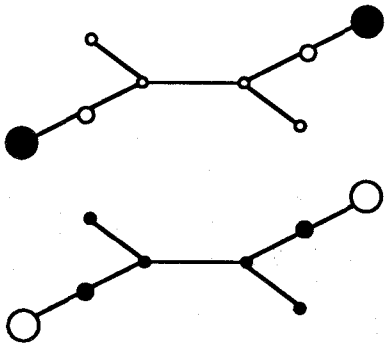

β - γ_{yyyy} densities

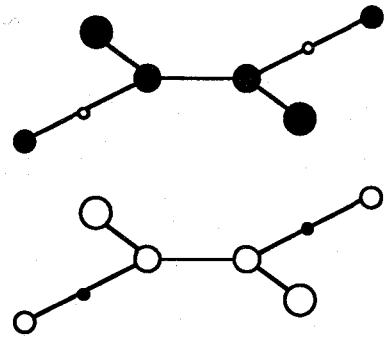

Total γ_{yyyy} densities

Ionic segregated dimer $(b)^{2-}$ (N=2)

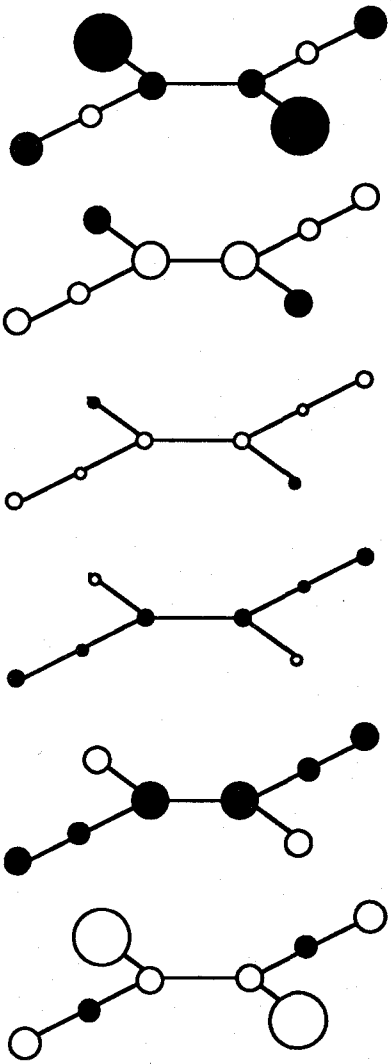

Ionic segregated hexamer $(b)^{6-}$ (N=6)

Fig.5. γ_{yyyy} densities for the dimers and the hexamers of the ionic segregated clusters.

Chapter 6

A Classification of the Third-order Organic Nonlinear Optical Systems and Proposal of New-type Nonlinear Optical Systems

In this work, we classify the third-order organic nonlinear optical systems based on the mechanism inducing the third-order nonlinear effects and discuss several appropriate calculation methods of their third-order hyperpolarizabilities (γ). The criteria of the classification are the symmetry of charge distributions (centro- and noncentro-symmetric charge distributions) and the types of the interactions which induce the charge-transfer (CT) effects (through-bond and through-space interactions). From the viewpoint of the mechanism of the CT interactions, most conventional third-order organic nonlinear systems involve the through-bond interactions. In the previous paper, as the new models of the third-order nonlinear systems, we proposed some CT complexes which involve the intermolecular interactions. In this paper, another new-type polymeric systems with polar side chains which involve both the through-bond and through-space interactions are proposed. For the calculation methods, the time-independent perturbational and variational approaches which are appropriate for each classified system are discussed.

1. Introduction

It is well known that the organic nonlinear optical systems exhibit the large nonlinear optical effects by the delocalized π electrons [1,2]. The second-order hyperpolarizability (β) for the centrosymmetric systems disappears, so that the intramolecular charge-transfer (CT) systems with donor (D) and acceptor (A) substituent groups have been investigated [3]. By contrast, the third-order hyperpolarizabilities (γ) exists for centro- and noncentro-symmetric systems. Many conventional third-order nonlinear systems with large γ values are either the noncentrosymmetric systems with strong CT effects or the centrosymmetric polymeric systems with large delocalization of π electrons in the chain direction [1,2]. However, the explicit criteria designing the third-order nonlinear systems with large γ values are still not completely elucidated.

Previously, we proposed the three-type approximation [4] based on the time-dependent perturbation theory (TDPT) [4-7]. This approximation divides the expression of γ value into three-type approximate virtual excitation processes [4-7]. These virtual excitation processes are shown in Fig.1. The γ values for the types (I) and (III)' are positive, while the value of type (II)' is negative in sign. Therefore, the magnitude and sign of γ values are determined by the balance among three-type contributions. The type (I) contributions mainly relate to the differences of the ground and excited dipole moments and the types (II)' and (III)' to the transition moments between the states. That is to say, the contributions of type (I) mainly determine the tendency of the γ values for noncentrosymmetric systems, while for the centrosymmetric systems, the detailed balance between types (II)' and (III)' determines the magnitude and sign of γ values. Therefore, we adopt the symmetry of the charge distributions as one of the criteria of the classification.

Another criterion of the classification is the mechanism inducing the CT effects. One is the system which involves the through-bond interactions [8], and the other is the system which

involves the through-space interactions [8]. In the previous paper [9], we proposed some types of the CT complexes which involve the intermolecular CT effects. It was found that both the mixed and the neutral/ionic segregated stacks indicate the large γ values in the column direction.

Further, using the classification proposed here, we propose the polymeric systems with polar side chains which involve both the CT interactions through space between the neighboring side chains and intramolecular CT interactions through the main chain.

The calculation methods of third-order hyperpolarizability are divided into the time-dependent [4-7] and time-independent methods [9-17]. These methods possess the perturbational [4,10,11,13,14] and variational approaches [10-12,15-17]. In this work, for the time-independent methods, the relationships between the perturbational and the variational methods and the electron correlation effects for the γ values are discussed.

2. A Classification of the Organic Third-order Nonlinear Optical Systems

2.1. A Classification based on the Three-type Virtual Excitation Process

Figure 1 shows the three-type virtual excitation processes in the TDPT three-type approximation. The type (I) process (0,*n*-*n*,*n*-*n*,*n*-*n*,0) relates to the transition moments between the ground and the *n*th excited states ($\mu_{0,n}$), the excitation energies of the *n*th excited states ($E_{0,n}$) and the differences of the dipole moments between the ground and the *n*th excited states ($\Delta\mu_{0,n}$). The type (II)' process (0,*n*-*n*,0-0,*n*-*n*,0) relates to the transition moments between the ground and the *n*th excited states ($\mu_{0,n}$) and the excitation energies of the *n*th excited states ($E_{0,n}$). The type (III)' process (0,*n*-*n*,*m*-*m*,*n*-*n*,0) relates to the transition moments between the ground and the *n*th excited state ($\mu_{0,n}$), the excitation energies of the *n*th excited states ($E_{0,n}$), the transition moments between the *n*th and the *m*th excited states

($\mu_{n,m}$) and the excitation energies between the nth and the mth excited states ($E_{n,m}$). The static γ values are expressed as [4]

$$\gamma_{iiii}^{(I)} = \sum_{n=1} \frac{(\mu_{n0}^{i})^2 (\Delta\mu_{n0}^{i})^2}{E_{n0}^{3}}, \tag{1}$$

$$\gamma_{iiii}^{(II)'} = -\sum_{n=1} \frac{(\mu_{n0}^{i})^4}{E_{n0}^{3}}, \tag{2}$$

$$\gamma_{iiii}^{(III)'} = \sum_{\substack{m,n=1 \\ m\neq n}} \frac{(\mu_{n0}^{i})^2 (\mu_{mn}^{i})^2}{E_{n0}^{2} E_{m0}}. \tag{3}$$

As can be seen from Eqs.(1)-(3), $\gamma^{(I)}$ and $\gamma^{(III)'}$ values are positive, whereas the $\gamma^{(II)'}$ values are negative in sign.

For the centrosymmetric systems, the contributions of the type (I) disappear because the differences of the dipole moments between the ground and the nth excited states ($\Delta\mu_{0,n}$) equal to 0. Therefore, the detailed balance between the types (II)' and (III)' determine the magnitude and sign of the total γ values for the centrosymmetric systems. The relative magnitude of types (II)' and (III)' are found to be mainly determined by the balance between the transition moments between the ground and the nth excited states ($\mu_{0,n}$) and those between the nth and the mth excited states ($\mu_{n,m}$). If $|\mu_{0,n}|$ are smaller than $|\mu_{n,m}|$, then |type (III)'| tend to be larger than |type(II)'| and the total γ values are expected to be positive in sign. On the contrary, if $|\mu_{0,n}|$ are larger than $|\mu_{n,m}|$, then |type (III)'| tend to be smaller than |type(II)'| and the total γ values are expected to be negative in sign.

On the other hand, the γ values for the noncentrosymmetric systems with strong CT effects are mainly determined by the type (I) contributions since the |type (I)| values are much larger than |types (II)' and (III)'| values and the sign of type (II)' values are opposite to the type

(III)' values. Large type (I) contributions suggest that the large dipole moment differences between the ground and the CT excited states ($\Delta\mu_{0,n}$) determine the tendency of the total γ values for the noncentrosymmetric systems.

2.2. A Classification by the Mechanism Inducing the CT Interaction

The next criterion of the classification is the mechanism of the CT interactions induced by the external electric field. That is to say, there are the systems involving the through-bond and through-space interactions. Though most conventional nonlinear systems involve the intramolecular (through-bond) CT effects, the new models of third-order nonlinear systems proposed previously [9] involve intermolecular (through-space) CT effects. These systems are the CT complexes which are inherently presented as the conducting molecular crystals [18]. More recently, it is reported that Perylene-TCNQ mixed stacking CT complexes come to exhibit enormously large γ values [19]. This tendency is in good agreement with our predictions [9].

2.3. A Classification of the Existing Organic Systems

The systems classified into four categories are listed in Table 1. The noncentrosymmetric and centrosymmetric systems are given in the symbols (NS) and (CS), respectively. The through-bond and through-space interaction systems are given in the symbols (TB) and (TS), respectively. The representative systems which belong to each category are shown in Fig.2. These systems are also divided into the monomolecular (M), the polymeric (P) and the CT complex (C) systems.

Detailed descriptions of each system shown in Fig.2 are given as follows.

Monomolecular systems (M)

(M-1) ; Polyaromatic systems which possess no D or A substituent groups.

(M-2) ; Aromatic systems with D or A substituent groups which exhibit large noncentrosymmetric charge distributions.

(M-3) ; Aromatic systems which are substituted centrosymmetrically by D or A substituent groups.

Polymeric systems (P)

(P-1) ; Nonsubstituted polymeric systems.

(P-2) ; Polymeric systems which are substituted centrosymmetrically by D or A substituent groups.

(P-3) ; Polymeric systems with D and A substituent groups. Noncentrosymmetric charge distributions are developed in the acetylenic, diacetylenic and aromatic main chain.

(P-4) ; Centrosymmetric systems which possess defects.
ex. Charged soliton-like polyenes, Neutral soliton-like polyenes

(P-5) ; Noncentrosymmetric polymeric systems which possess the defects.

(P-6) ; Centrosymmetric polymeric systems with polar side chains. The polar side chains are arranged as face-to-face stacking. The CT effects between the neighboring side chains contributes to enhance the total γ values. The main chain does not only control the arrangement of the side chains, but also contribute to enhance the total γ values by the CT effects in the main chain.

(P-7) ; Noncentrosymmetric polymeric systems which utilize the CT effects between side polar chains. The main chain does not only control the arrangement of the side chains, but also contribute to enhance the total γ values by the CT effects in the main chain.

CT complex systems (C)

(C-1) ; CT complex which is constructed of the alternatively stacking D and A

molecules.

D molecule ; Aromatic systems, TTF, TMTSF, etc.

A molecule ; TCNE, TCNQ, DCNQI, etc.

(C-2) ; Segregated CT complexes which are constructed of segregate D and A stacks. Neutral segregated stacks (D or A column). The charge-transfer from D to A column are not induced.

(C-3) ; Mixed-valence segregated stacks (D or A column). The incomplete charge-transfer from D to A column are induced. This system is appropriate to the conducting systems, but are not appropriate to the third-order nonlinear systems because the γ values diverge.

(C-4) ; Ionic segregated stacks (D or A column). The complete charge-transfer from D to A column are induced.

The γ values in the column direction for these CT complexes are large. The γ values in the column direction per unit interaction become nearly constant for the medium-size cluster constructed of about ten monomers.

Details of the four categories listed in Table 1 are explained below.

(CS-TB)

Centrosymmetric charge distributions. Through-bond interactions.

Contributions of type (I) disappear. The balance between types (II)' and (III)' determines the tendency of the total γ values.

(NS-TB)

Noncentrosymmetric charge distributions. Through-bond interactions.

Large $\Delta\mu_{0,n}$ values. Type (I) determines the tendency of the total γ values.

(CS-TS)

Centrosymmetric charge distributions. Through-space interactions.

Contributions of type (I) disappear. The balance between types (II)' and (III)' determines the tendency of the total γ values.

(NS-TS)

Noncentrosymmetric charge distributions. Through-space interactions. Type (I) determines the tendency of the total γ values.

3. New Models of the Third-order Nonlinear Optical System

New models of the nonlinear optical systems proposed previously [9,10] are the conducting systems which do not exhibit good conducting properties. These systems are polymeric systems with defects ((P-4,5)) and the molecular crystals involving the through-space interactions ((C-1-4)).

In this work, we propose another new polymeric systems with polar side chains which are expected to involve both the through-space CT interactions between the neighboring side chains and intramolecular CT interactions through the main chain. Characteristics of the main- and side-chain contributions are investigated by the γ density analysis [9-11] based on the coupled-Hartree-Fock (CHF) calculations [9-12,15-17].

3.1. Calculations

The energy of a molecule in the presence of an static, uniform electric field can be expressed as the power series of an electric field. The fourth-order coefficients represent the third-order hyperpolarizability tensors. These tensor components can be determined from the differentiations of the energies with respect to the electric fields. In this work, the finite-field (FF) method based on the INDO [20] CHF approximation. The minimum field strength in the FF method is 0.002 a.u. This value is appropriate to assess the calculated results.

In the previous paper [9-11], we proposed the method using the γ density analysis which can reveal the characteristics of the spatial contributions of the γ values. The approximate γ_{iiii} value by the γ density analysis is expressed as follows.

$$\gamma_{iiii} \approx -\frac{1}{3!}\sum_{s}(\boldsymbol{PS})^{(3)}_{ss} q^{i}_{s}. \qquad (1)$$

Here, the $(\boldsymbol{PS})_{ss}$ is the Mulliken charge density. The q^{i}_{s} represents the i component of the coordinate of the atom located at the center of the atomic orbital s. This approximation implies that the charge densities are concentrated to the center of the atomic orbitals s. We call the third-derivative of $(\boldsymbol{PS})_{ss}$ the γ density [9-11]. The spatial characteristics of the γ value can be obtained by the use of the plots of the magnitude and sign of the γ densities on each atom. The plus sign of the γ density implies that the second-derivative of the charge density increases with the increase in the field, while the minus sign implies the inverse effect.

Figure 3 shows an example of the new polymeric systems with polar side chains. These systems correspond to (P-6,7) shown in Fig.2. The main chain is the polyacetylenic chain. The polar side groups are perpendicular to the plane of the main chain. Therefore the side donor (D) and acceptor (A) groups are aligned as the face-to-face stacking in order to induce the CT interactions through the neighboring substituents. Four types of the polymeric systems; (i) CCCC, (ii)DDAA, (iii) DAAD and (iv) AAAA, are examined. The number of carbon atomic sites is eight. The donor (D) and acceptor (A) groups are amino and nitro groups, respectively.

3.2. Results and Discussion

The γ_{zzzz} values (chain direction component) calculated by INDO CHF are listed in Table 2. The approximate γ_{zzzz} values obtained from γ density analysis are found to be in good

agreement with the CHF γ_{zzzz} values. The approximate γ_{zzzz} values are separated to the contributions of the main- and side-chain regions as shown in Fig.4. Large differences in the contributions of γ density with the arrangement of the substituent groups are not observed. It is found that for the regular polyene (i) CCCC, the ratio of contributions of the side-chain region is about 20% of the total γ_{zzzz} value, whereas for the polyenes with polar side chains, those reach about 40%. Compared with the results for the same-size regular polyene (i) CCCC, the main-chain contributions for (ii) DDAA, (iii) DAAD and (iv) AAAA are found to be about 1.26 times that of (i) CCCC, whereas the side-chain contributions for (ii) DDAA, (iii) DAAD and (iv) AAAA are found to be about 3.82, 2.70 and 2.95 times respectively. Large contributions of type (I) in the TDPT three type approximation [4] seem to be responsible for the larger enhancement of the γ values of the side-chain regions for (ii) DDAA, since the type (I) contributions only exist in the noncentrosymmetric systems. These results also suggest that the polar side chains do not only significantly increase the contribution of the side-chain region, but also slightly increase the contribution of the main-chain region. We are at present applying the CHF method to investigate the contributions of the other substituent groups and the other main chains.

4. Appropriate Calculation Methods of the γ for the Classified Systems

The calculation methods of the γ values are separated to the time-dependent methods which can describe the dependence of γ value on the oscillations of the external electric field and the time-independent methods which can describe the static γ value. In this paper, the time-independent methods are discussed. Figure 5 shows the several procedures. These procedures are classified by two criteria. One is the number of the Slater determinants used to describe each state (single- and multi- references) and the other is the approximated methods (variational and perturbational methods).

For the perturbational approaches, the Rayleigh-Schrödinger perturbation theory (RSPT) is employed [10,13,14]. In general, this approach is based on the double perturbation theory [10] in which the potentials of the external field and the electron correlations are considered to be two perturbations. In this approach, the analytic formula of γ_{ijkl} value is obtained from the fourth-order energy term respect to the external field. In this paper, the RSPT method with the nth order electron correlation effects is referred to as the RSPTn method [10]. This method can include the higher correlation effects systematically. However, the explicit formula including higher correlation effects is not practically used to calculate the γ values because of the complication of its formula. In order to include correlation effects, the variational approach is employed as the starting point.

For the variational approaches, the coupled-Hartree-Fock (CHF) method is generally used at the Hartree-Fock (HF) level. The total energy in the presence of the external electric field is calculated variationally. The total energy is differentiated by the external fields and the fourth-order derivatives represent the γ values. There are some numerical [16,17] and analytical differentiation methods [15]. When the numerical differentiation is performed carefully, the results of the numerical differentiation are found to be equal to those of the analytical differentiation [16]. The approximate level of the CHF methods is equal to that of the RSPT method including the first order correlation effects (RSPT1) [12]. In order to include the higher electron correlation effects, the Møller-Plesset (MP) perturbation theory [21] and coupled-cluster (CC) theory [22] are employed. In this case, the conventional sophisticated programs can be utilized.

For the systems which cannot be represented by the single determinant, or the systems which possess strong electron correlation effects, the multi-configurational coupled-Hartree-Fock (MCCHF) [23] and multi-reference coupled-cluster (MRCC) methods [24] have to be applied.

We discuss the appropriate procedures for the calculation of the γ values for the systems listed in Table 1. For the noncentrosymmetric closed-shell systems without defects ((M-2),(P-3,7),(C-1)) and the centrosymmetric closed-shell systems without defects ((M-1,3),(P-1,2,6),(C-2)), the RSPT0, CHF and CHF+MP2 methods are considered to be adequate for the calculations of the qualitative γ values at least. For the large-size systems, the CHF method seem to be practically appropriate since the inclusions of the correlation effects are fairly difficult. For the rest of the systems listed in Table 1, which are open-shell systems except the charged soliton-like molecules, at least the calculations including correlation effects have to be needed. Particularly for the systems with excess electrons or holes which can transfer easily, the methods including higher electron correlations or the multi-reference based methods will be expected.

In this paper, only the time-independent methods which exhibit the static hyperpolarizability were mentioned. However, in order to gain the practical γ values which are useful for the designs of the optical electric devices, the time-dependent approaches have to be employed. Particularly for the CT complexes and the conducting polymers with low excitation energies, when the differences between the energies of the external field and those of the low excited states for the systems are small, the dispersion effects of the γ values must be considered.

Some differences between the results of ab initio and semiempirical molecular orbital (MO) methods also exist [11]. For the ab initio approach, it is well-known that the augmentations of the standard basis set are mandatory for the calculation of the semiquantitative γ values [15,16]. For the semiempirical approaches, the calculated γ values tend to be smaller than those by the ab initio method because of the inadequacy of the basis sets [11]. In this case, in order to estimate the γ values at the ab initio level, the scaling

procedure of the γ values at the semiempirical level seems to be useful for most medium and large-size systems [11].

5. Concluding Remarks

The conclusions are listed as follows.

(1) By the criteria of the TDPT three type virtual excitation processes and the types of the CT interactions, the third-order nonlinear optical systems are classified into four categories given in Table 1. As the new models of the third-order nonlinear systems, the centrosymmetric systems with defects, the CT complexes with strong intermolecular CT effects and the polymers with polar side chains involving both the through-bond and through-space interactions are proposed.

(2) For the centrosymmetric, when the |type (III)'| < |type (II)'|, the total γ values come to be negative. This case seems to correspond to the case : $|\mu_{0,n}| > |\mu_{0,m}|$.

(3) For the CT complexes, the D-A mixed stacks and the neutral/ionic segregated stacks are expected to exhibit large γ values in the column direction. The mixed-valence segregated stacks which are good for the conducting system seem to be inappropriate for the third-order nonlinear optical systems.

(4) For the polymeric systems involving the CT effects between the neighboring polar side chains, the main chain is used to arrange the side polar substituents and to enhance the chain length component of γ value. Therefore, these systems utilize both the through-bond and through-space CT interactions.

(5) The open-shell systems with defects are expected to exhibit large γ values than those of the closed-shell systems owing to the mobility of the electrons or holes. However, the theoretical evaluation of the γ values for the open-shell systems is fairly difficult and available

experimental γ values for the open-shell systems don't exist yet. Further experimental and theoretical studies for the open-shell systems have to be performed.

(6) As the time-independent calculation methods, the CHF method is appropriate to evaluate the qualitative γ values for the closed-shell systems. For the open-shell systems, the multi-reference based methods and the methods which can estimate higher-order correlation effects have to be carried out.

(7) For the systems with low excitation energies, in order to evaluate the dispersion effects of γ values, the time-dependent methods must be employed.

References

[1] *Nonlinear Optical Properties of Polymers*, edited by A. J. Heeger, J. Orenstein and D. R. Ulrich, Vol. **109** (Material Research Society Publication, Pittsburgh, 1988).

[2] *Nonlinear Optical Properties of Organic and Polymeric Materials*, edited by D. J. Williams (Am. Chem. Soc., Washington, D. C. , 1983).

[3] M. Nakano, K. Yamaguchi and T. Fueno, in *Nonlinear Optics of Organics and Semiconductors*, edited by T. Kobayashi, Springer Proceedings in Physics **36** (1989) 98 ; 103.

[4] M. Nakano, M. Okumura, K. Yamaguchi and T. Fueno, Mol. Cryst. Liq. Cryst. **182A** (1990) 1.

[5] J. R. Heflin, K. Y. Wong, O. Zamani-Khamiri and A. F. Garito, Phys. Rev. **B38** (1988) 1573.

[6] A. F. Garito and J. R. Heflin, K. Y. Wong and O. Zamani-Khamiri, in *Organic Materials for Nonlinear Optics*, edited by D. J. Andre and D. Bloor (1988).

[7] B. M. Pierce, J. Chem. Phys. **91** (1989) 791.

[8] R. Hoffmann, A. Imamura and W. J. Hehre, J. Am. Chem. Soc. **90** (1968) 1499.

[9] M. Nakano, K. Yamaguchi and T. Fueno, submitted.

[10] M. Nakano, K. Yamaguchi and T. Fueno, submitted.

[11] M. Nakano, K. Yamaguchi and T. Fueno, unpublished.

[12] R. J. Bartlett and G. D. Purvis III, Phys. Rev. **A20** (1979) 1313.

[13] E. F. McIntyre and H. F. Hameka, J. Chem. Phys. **68** (1978) 3481 ; 5534 ; **69** (1978) 4814 ; **70** (1979) 2215.

[14] O. Zamani-Khamiri, E. F. McIntyre and H. F. Hameka, J. Chem. Phys. **71** (1979) 1607 ; **72** (1980) 1280 ; **72** (1980) 5906.

[15] G. J. B. Hurst, M. Dupuis and E. Clementi, J. Chem. Phys. **89** (1988) 385.

[16] P. Chopra, L. Carlacci, H. F. King and P. N. Prasad, J. Phys. Chem. **93** (1989) 7120.

[17] E. Perrin, P. N. Prasad, P. Mougenot and M. Dupuis, J. Chem. Phys. **91** (1989) 4728 .

[18] J. B. Torrance, Acc. Chem. Res. **12** (1979) 79.

[19] T. Gotoh, T. Kondoh and K. Egawa, J. Opt. Soc. Am.**B.6** (1990) 703

[20] J. A. Pople and D. L. Beveridge, *Approximate Molecular Orbital Theory* (McGraw-Hill, New York, 1970).

[21] C. Møller and M. S. Plesset, Phys. Rev. **46** (1934) 618 .

[22] H. J. Monkhorst, Int. J. Quant. Chem. **S11** (1977) 421.

[23] E. Dalgaard and P. Jørgensen, J. Chem. Phys. **69** (1978) 3833.

[24] S. Pal, M. Rittby, R. J. Bartlett, D. Sinha and D. Mukherjee, J. Chem. Phys. **88** (1988) 4357.

Table 1. Classification of third-order nonlinear optical systems based on the symmetry of the charge ditributions (centrosymmetric and noncentrosymmetric systems) and the types of interactions (through-bond and through-space interactions). The symbols M, P and C indicate the monomolecular, the polymeric and the CT complex systems, respectively.

	Through-bond (TB) interactions	Through-space (TS) interactions
Centrosymmetric systems (CS) Main contributions : Type (II)',(III)' $\gamma > 0$ ($\|\mu_{0,n}\| < \|\mu_{n,m}\|, E_{n,m} \lesssim E_{0,n}$) [a] $\gamma < 0$ ($\|\mu_{0,n}\| > \|\mu_{n,m}\|, E_{n,m} \gtrsim E_{0,n}$) [a]	(M-1),(M-3), (P-1),(P-2),(P-4),(P-6)	(P-6), (C-2),(C-3),(C-4)
Noncentrosymmetric systems (NS) Main contributions : Type (I)' $\gamma > 0$ (large $\Delta\mu_{0,n}$) [a]	(M-2), (P-3),(P-5),(P-7)	(P-7),(C-1)

a) $\Delta\mu_{0,n}$ is the differences of the dipole moment between ground and the nth excited states. $\mu_{n,m}$ is the the transition moment between the nth and the mth states. $E_{n,m}$ is the the transition energy between the nth and the mth states.

Table 2. Approximate γ_{zzzz} values[a] and CHF γ_{zzzz} values for regular polyene (i) and polyenes with polar side chains (ii)-(iv).

System		Approximate values[a.u.]	CHF values[a.u.]
(i) CCCC	Main	9098.8(76.6%)	
	Side	2773.2(23.4%)	
	Total	11872	12785
(ii) DDAA	Main	11423.3(51.9%)	
	Side	10587.5(48.1%)	
	Total	22010.8	23335
(iii) DAAD	Main	11490.0(60.6%)	
	Side	7483.3(39.4%)	
	Total	18973.3	20270
(iv) AAAA	Main	11488.1(58.4%)	
	Side	8185.3(41.6%)	
	Total	19673.4	21041

a) The percentage of the contributions from main and side chains is shown in parentheses.

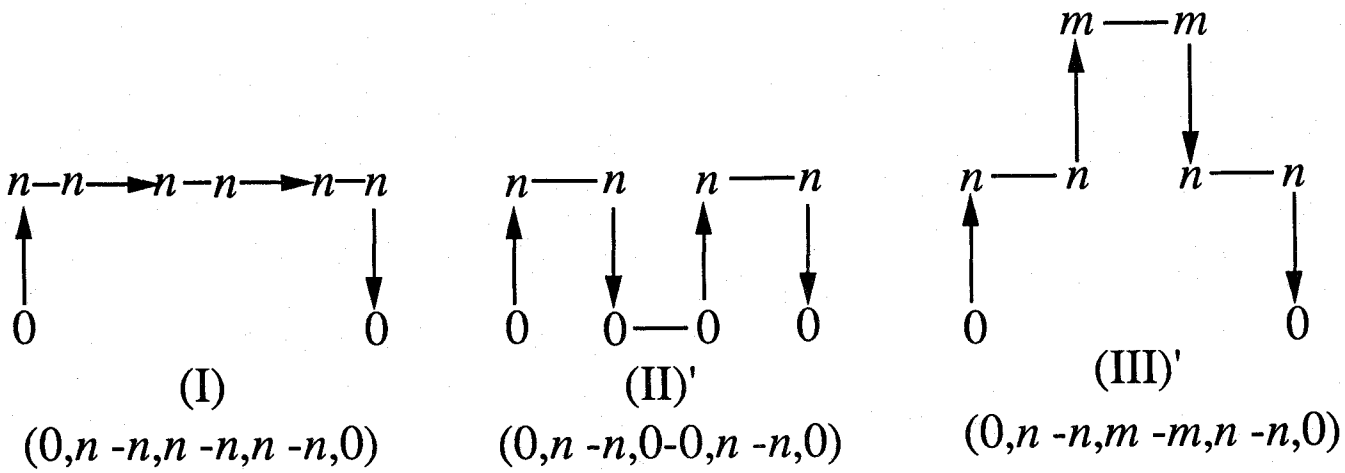

Fig.1. TDPT three-type virtual excitation processes. The symbol 0, *n* and *m* indicate the each state which is included in the virtual excitation processes.

Monomolecular systems (M)

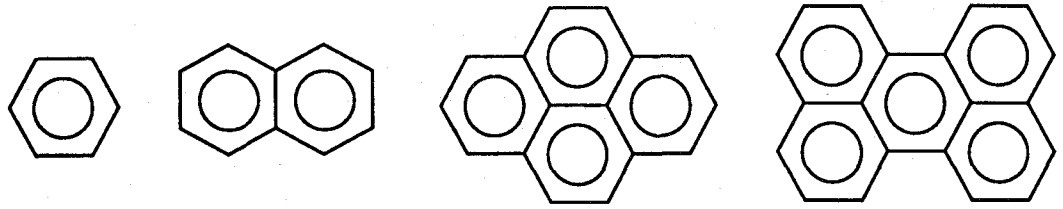

(M-1-1) (M-1-2) (M-1-3) (M-1-4)

(M-1) Centrosymmetric aromatic systems

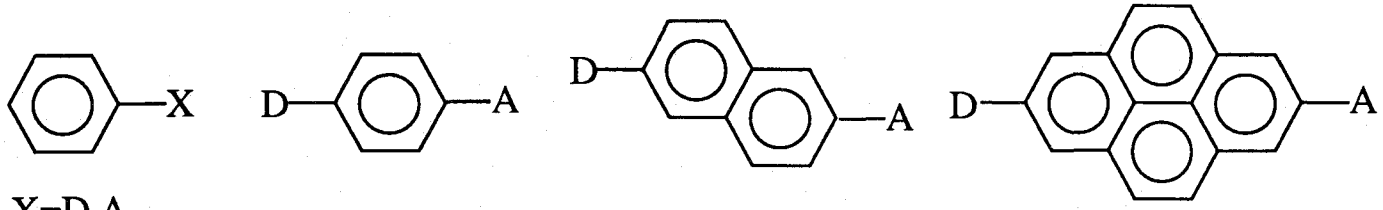

X=D,A
(M-2-1)

(M-2-2) (M-2-3) (M-2-4)

(M-2) Noncentrosymmetric D-A substituted aromatic systems

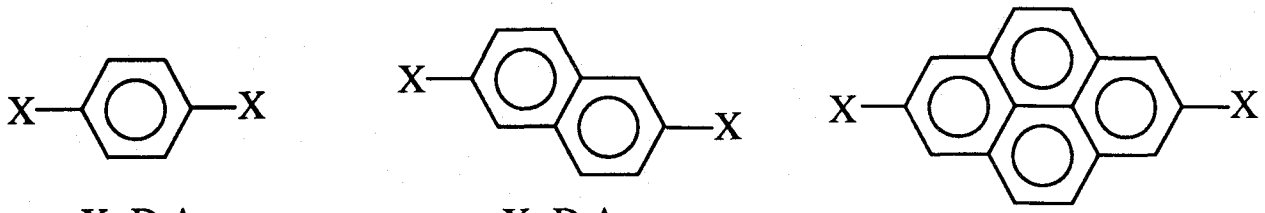

X=D,A
(M-3-1)

X=D,A
(M-3-2)

X=D,A
(M-3-3)

(M-3) Centrosymmetric monomolecular systems
with D or A substituents

Polymeric systems (P)

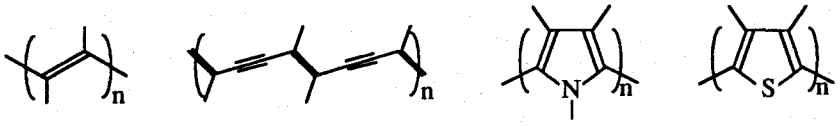

(P-1-1) (P-1-2) (P-1-3) (P-1-4)

(P-1) Centrosymmetric regular polymeric systems

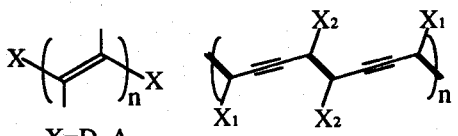

X=D, A (P-2-1)

X_1, X_2 = D, A (P-2-2)

(P-2) Centrosymmetric polymeric systems with D or A substituents

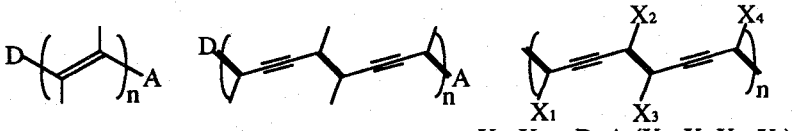

(P-3-1) (P-3-2)

$X_1 \sim X_4$ = D, A ($X_1 \neq X_4, X_2 \neq X_3$) (P-3-2)

(P-3) Noncentrosymmetric D-A substituted polymeric systems

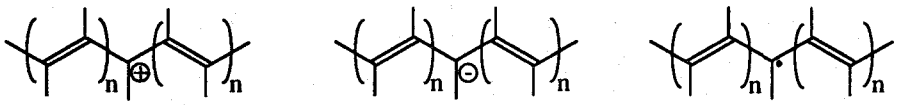

(P-4-1) (P-4-2) (P-4-3)

(P-4) Centrosymmetric polymeric systems with defects

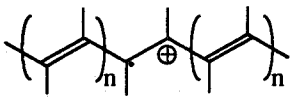

(P-5-1)

(P-5) Noncentrosymmetric polymeric systems with defects

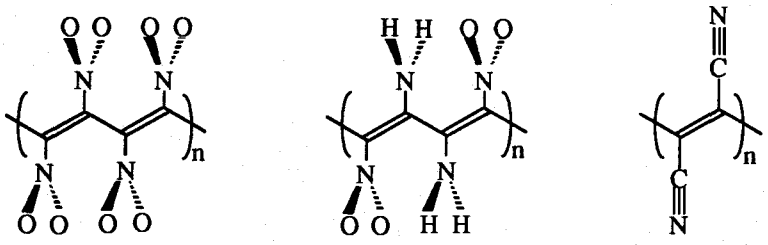

(P-6-1) (P-6-2) (P-6-3)

(P-6) Centrosymmetric polymeric systems with polar side chains

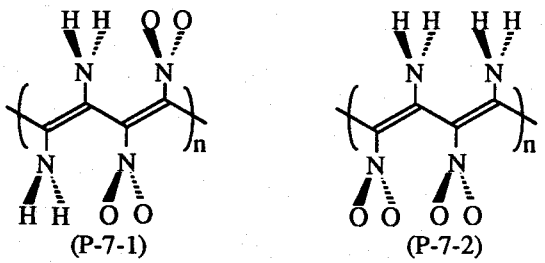

(P-7-1) (P-7-2)

(P-7) Noncentrosymmetric polymeric systems with polar side chains

CT complex systems (C)

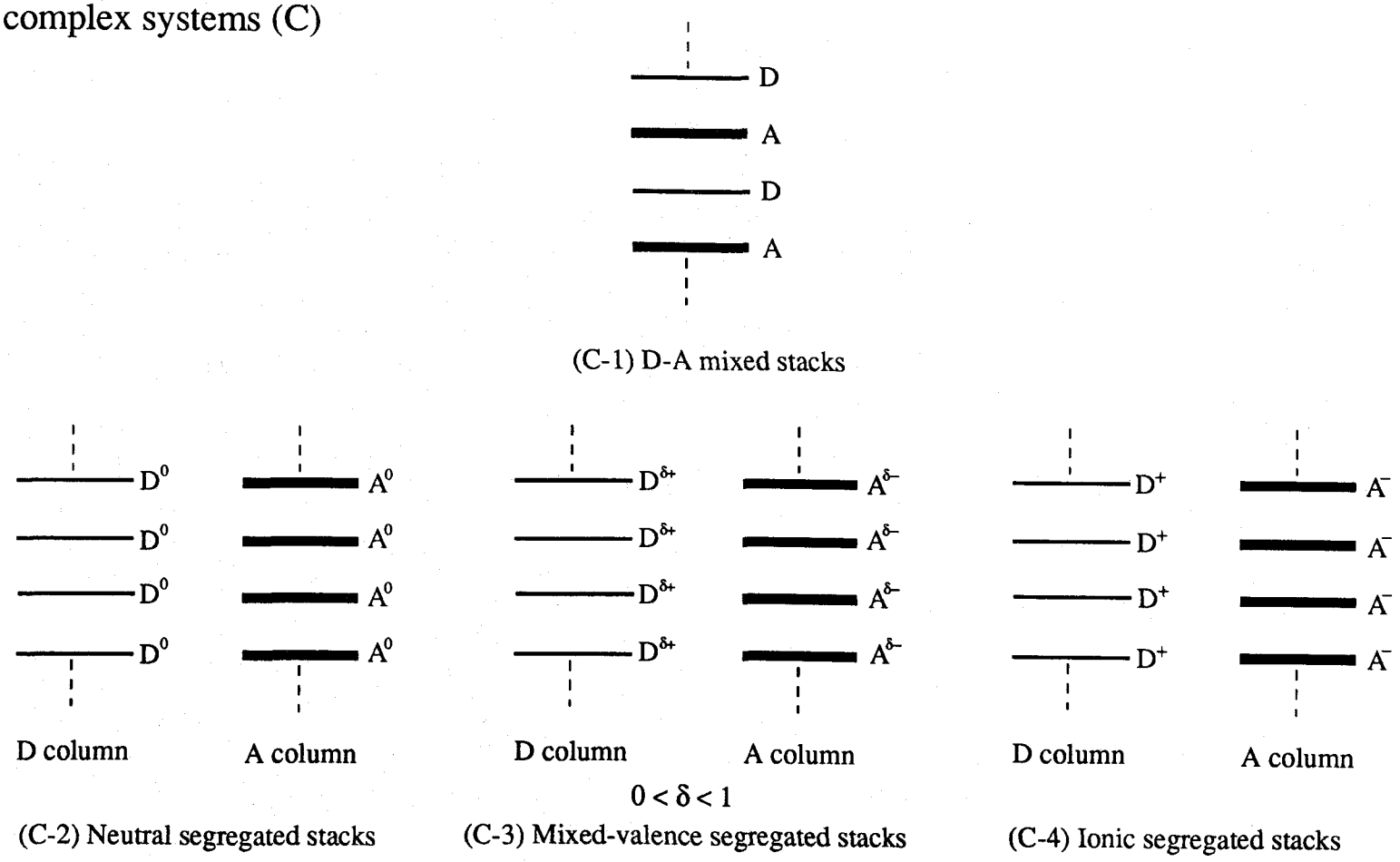

Fig.2. Representative organic systems which belong to the each category classified in Table 1. The symbols M, P and C indicate the monomolecular, polymeric and CT complex systems, respectively.

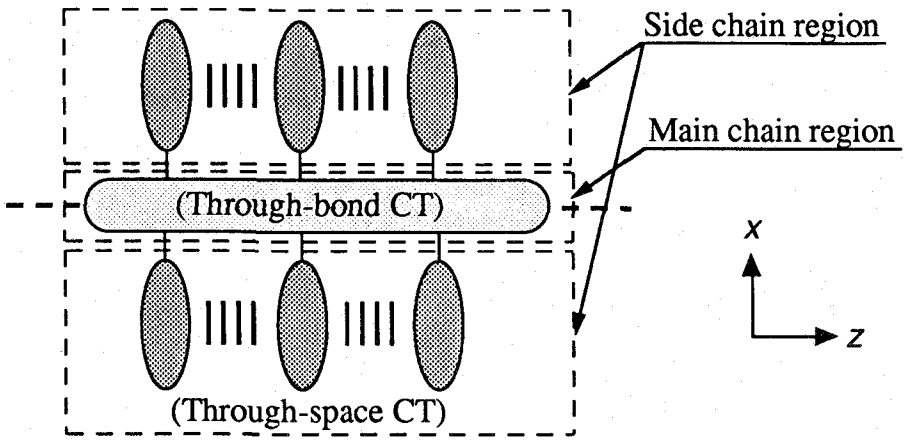

(a) New polymeric systems with polar side chains

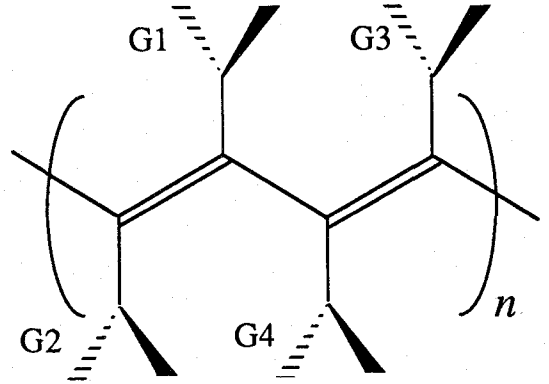

G1-G4 ; donor(D) and acceptor(A) groups.
D=NH_2, A=NO_2

(b) Polacetylenic systems with donor and acceptor groups (G1G2G3G4)

Fig.3. Schematic diagrams of the new polymeric systems with polar side chains (a). An example of the new system (a) is the polyacetylenic systems with donor(D) and acceptor(A) groups. ((ii) DDAA, (iii) DAAD, (iv) AAAA).

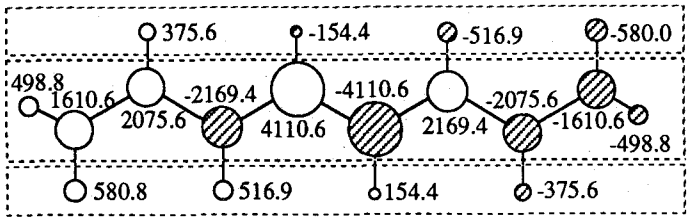

(i) CCCC (Main chain 9098.8 a.u.(76.6%), Side chain 2773.2 a.u.(23.4%))

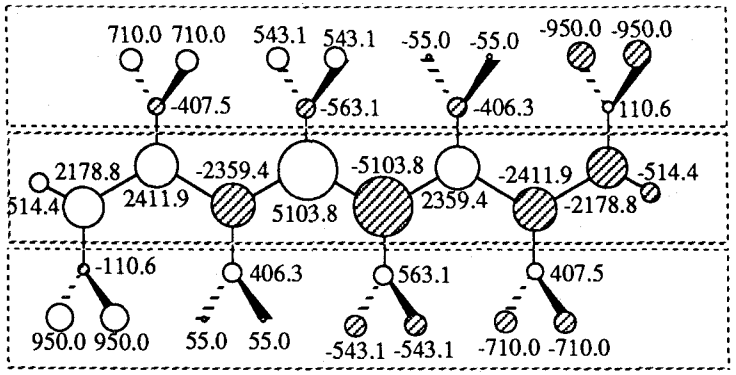

(iii) DAAD (Main chain 11490.0 a.u.(60.6%), Side chain 7483.3 a.u.(39.4%))

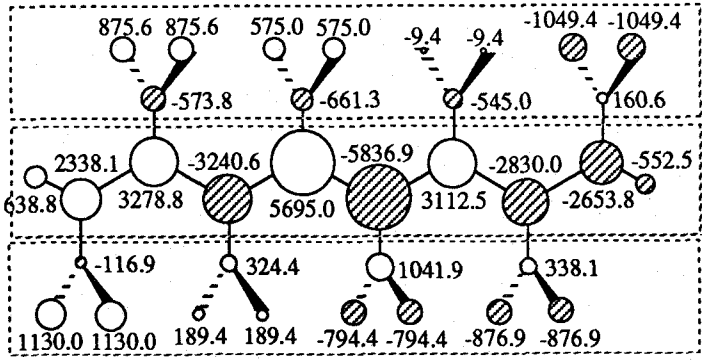

(ii) DDAA (Main chain 11423.3 a.u.(51.9%), Side chain 10587.5 a.u.(48.1%))

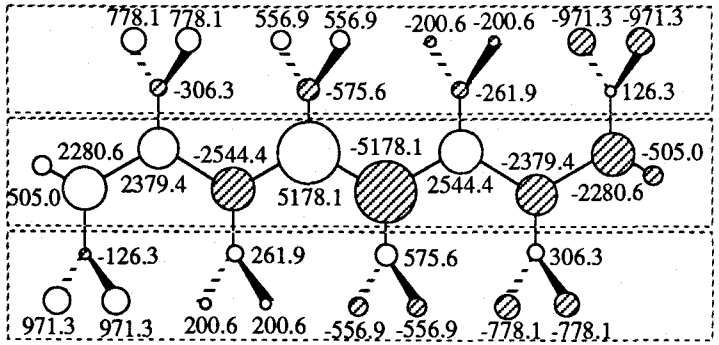

(iv) AAAA (Main chain 11488.1 a.u.(58.4%), Side chain 8185.3 a.u.(41.6%))

Fig.4. Plots of the γ_{zzz} densities for the polymeric systems (i)-(iv).

Time-independent methods

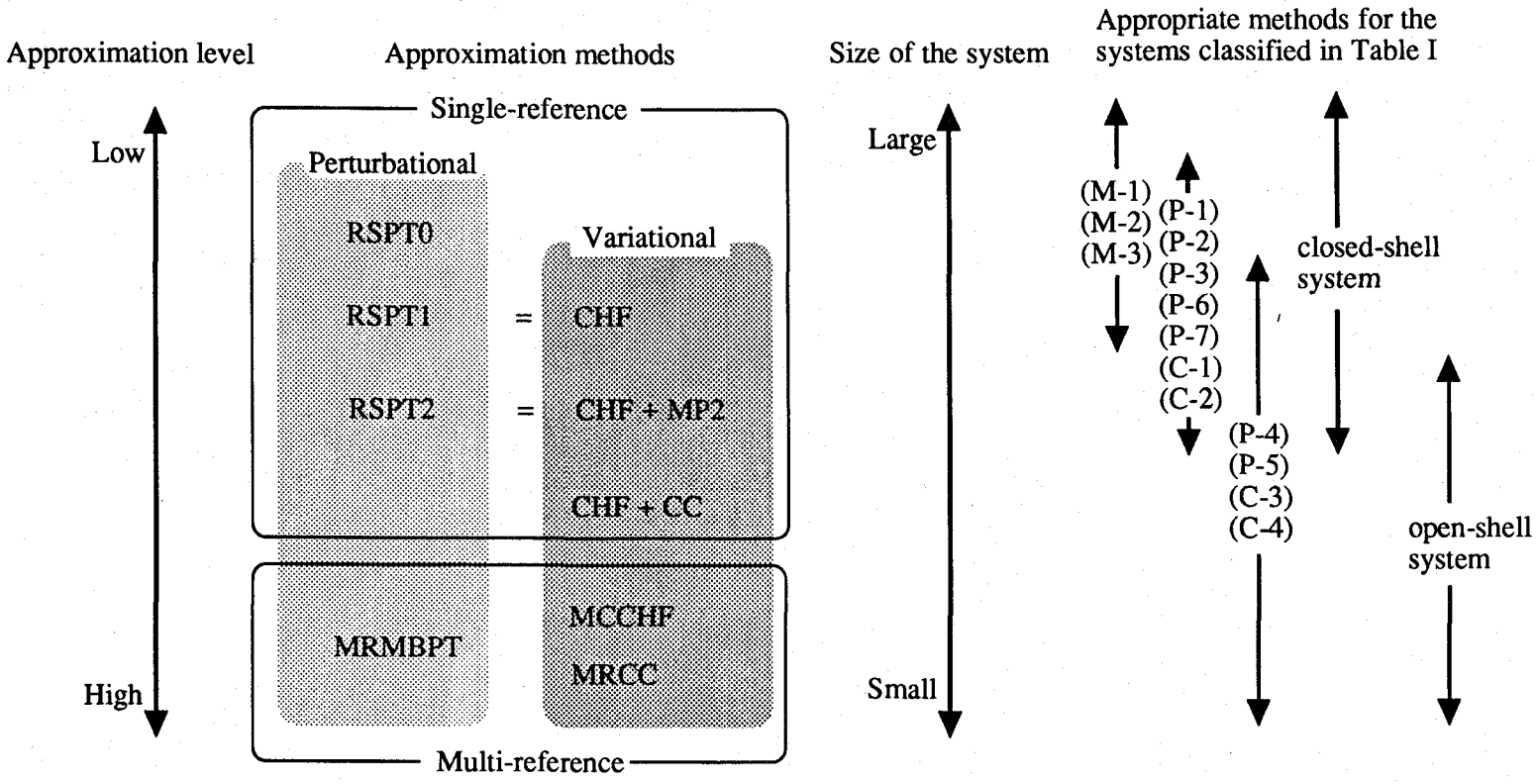

Fig.5. Classification of the time-independent calculation methods for the third-order hyperpolarizability and the appropriate methods for each claasified system listed in Table 1.